UNIVERSIDADE ESTADUAL PAULISTA
"JÚLIO DE MESQUITA FILHO"
Campus de Botucatu

Instituto de Biociências
Unesp Botucatu

ESTUDOS SOBRE O EFEITO DO NOCAUTE E DA SUPEREXPRESSÃO DO COMPONENTE RNA DA TELOMERASE (*Leish*TER) NOS TELÔMEROS, NO DESENVOLVIMENTO E NA SOBREVIDA DE *Leishmania major*

BEATRIZ CRISTINA DIAS DE OLIVEIRA

BOTUCATU, SP
2024

UNIVERSIDADE ESTADUAL PAULISTA
"Julio de Mesquita Filho"
INSTITUTO DE BIOCIÊNCIAS DE BOTUCATU

ESTUDOS SOBRE O EFEITO DO NOCAUTE E DA SUPEREXPRESSÃO DO COMPONENTE RNA DA TELOMERASE (*Leish*TER) NOS TELÔMEROS, NO DESENVOLVIMENTO E NA SOBREVIDA DE *Leishmania major*

NOME DO CANDIDATO: BEATRIZ CRISTINA DIAS DE OLIVEIRA

ORIENTADOR: MARIA ISABEL NOGUEIRA CANO

Tese apresentada ao Instituto de Biociências, Câmpus de Botucatu, UNESP, para obtenção do título de Doutora no Programa de Pós-graduação em Ciências Biológicas (Genética).

BOTUCATU, SP
2024

FICHA CATALOGRÁFICA ELABORADA PELA SEÇÃO TÉC. AQUIS. TRATAMENTO DA INFORM.DIVISÃO TÉCNICA DE BIBLIOTECA E DOCUMENTAÇÃO - CÂMPUS DE BOTUCATU - UNESP

BIBLIOTECÁRIA RESPONSÁVEL: MARIA CAROLINA A. CRUZ E SANTOS-CRB 8/10188

Oliveira, Beatriz Cristina Dias de.
Estudos sobre o efeito do nocaute e da superexpressão do componente RNA da telomerase (*Leish*TER) nos telômeros, no desenvolvimento e na sobrevida de *Leishmania major* / Beatriz Cristina Dias de Oliveira. - Botucatu, 2024

Tese (doutorado) - Universidade Estadual Paulista "Júlio de Mesquita Filho", Instituto de Biociências de Botucatu
Orientador: Maria Isabel Nogueira Cano
Capes: 20202008

1. Telomerase. 2. Telômero. 3. Autofagia. 4. Fatores de virulência. 5. *Leishmania major*.

Palavras-chave: Autofagia; Baixo índice de infectividade; Encurtamento dos telômeros; L. major TER nocaute; SHAPE-MaP.

UNIVERSIDADE ESTADUAL PAULISTA

Câmpus de Botucatu

ATA DA DEFESA PÚBLICA DA TESE DE DOUTORADO DE BEATRIZ CRISTINA DIAS DE OLIVEIRA, DISCENTE DO PROGRAMA DE PÓS-GRADUAÇÃO EM CIÊNCIAS BIOLÓGICAS (GENÉTICA), DO INSTITUTO DE BIOCIÊNCIAS - CÂMPUS DE BOTUCATU.

Aos 25 dias do mês de janeiro do ano de 2024, às 09:00 horas, no(a) Sala de Pós-Graduação do Instituto de Biociências, realizou-se a defesa de TESE DE DOUTORADO de BEATRIZ CRISTINA DIAS DE OLIVEIRA, intitulada **Estudos sobre o efeito do nocaute e da superexpressão do componente RNA da telomerase (*Leish*TER) nos telômeros, no desenvolvimento e na sobrevida de *Leishmania major*.** A Comissão Examinadora foi constituida pelos seguintes membros: Profa. Dra. MARIA ISABEL NOGUEIRA CANO (Orientador(a) - Participação Presencial) do(a) Departamento de Ciências Químicas e Biológicas / Instituto de Biociências UNESP Câmpus de Botucatu, Assistant Professor NOELIA MARINA LANDER MANFREDI (Participação por Parecer Circunstanciado) do(a) Biological Sciences / University of Cincinnati, Senior Bioinformatics Research Officer ELTON JOSE ROSAS DE VASCONCELOS (Participação Virtual) do(a) LeedsOmics – Faculty of Biological Sciences / University of Leeds, Profª. Drª. CAROLINA BORSOI MORAES HOLANDA DE FREITAS (Participação Virtual) do(a) Departamento de Análises Clínicas e Toxicológicas / Faculdade de Ciências Farmacêuticas – Universidade de São Paulo, Prof. Dr. GUILHERME TARGINO VALENTE (Participação Presencial) do(a) Laboratório de Biotecnologia Aplicada / Faculdade de Medicina de Botucatu - Unesp. Após a exposição pela doutoranda e arguição pelos membros da Comissão Examinadora que participaram do ato, de forma presencial e/ou virtual, a discente recebeu o conceito final: __APROVADO . Nada mais havendo, foi lavrada a presente ata, que após lida e aprovada, foi assinada pelo(a) Presidente(a) da Comissão Examinadora.

Profa. Dra. MARIA ISABEL NOGUEIRA CANO

gov.br Documento assinado digitalmente
MARIA ISABEL NOGUEIRA CANO
Data: 25/01/2024 17:25:54-0300
Verifique em https://validar.iti.gov.br

Dedicatória

Dedico este trabalho ao meu avô, José Chrispim da Silva, que plantou a sementinha da pós-graduação em minha cabeça com um de seus poemas. À minha mãe que sempre enfatizou que a coisa mais valiosa que ela poderia proporcionar a mim e a minha irmã era o estudo, pois isso ninguém tira de nós. E aos meus sobrinhos, Carolina, Eduardo e Gael que representam o futuro e a esperança em minha vida.

Eu amo vocês.

Agradecimentos

Durante todo esse período de pós-graduação tive a sorte de ter ao meu lado pessoas que de alguma forma deixaram essa caminhada mais leve. Dessa forma não poderia deixar de destacar meus mais profundos agradecimentos:

À Deus, por guiar meus passos e por me abençoar durante todo meu caminho.

À minha família, por todo apoio e incentivo aos estudos, pelos ensinamentos e pelo amor. Em especial agradeço minha mãe Sol, meu pai Cláudio, minha irmã Aline, meus sobrinhos Carolina e Eduardo, meu cunhado Ricardo e meu vô Zé. Essas pessoas tiveram um papel muito importante na minha formação, seja na vida pessoal como na profissional. Estiveram sempre me apoiando e torcendo por mim. Minha conquista também é de vocês. E aos meus doguinhos, Floquinho e Belinha, que me alegravam toda vez que eu chegava em casa cansada e estressada.

Ao meu esposo, Victor de Oliveira Esteves por me apoiar desde o início e por sempre ter acreditado em mim quando nem eu mesma acreditava. Obrigada por sempre me falar o quanto tinha orgulho de mim, pelas massagens nos meus ombros e braços cansados do trabalho, e por entender que em muitos dias o que eu queria era apenas dormir e comer. Você é um dos pilares da minha vida e seu apoio foi fundamental.

À minha segunda família, Oliveira e Esteves, que me acolheram de braços abertos. Uma grande, alegre e amorosa família.

Aos meus amigos, que ao longo da jornada escutaram minhas reclamações e vibraram com minhas vitórias. Em especial aos meus amigos do LabTelo, com os quais compartilhei minhas frustações, alegrias, bancada, soluções e experimentos.

À minha orientadora, Dra. Maria Isabel Nogueira Cano, que me acolheu em seu laboratório de braços abertos, e que durante todos esses anos sempre me incentivou a voar alto, a dar o meu melhor e a não desistir. Posso dizer que tive muita sorte de ter a Bel como orientadora, pois ela realmente me orientou, me desafiou, me ajudou, confiou em meu trabalho e sempre se fez presente. Tenho uma profunda admiração pela profissional que ela é, pelo coração gigante que possui e pelo senso de justiça.

À UNESP e ao Instituto de Biociências de Botucatu. Sempre foi meu sonho fazer parte dessa instituição, e esse sonho se tornou realidade na pós-graduação. Foram anos incríveis, com profissionais excelentes que contribuíram para minha formação.

Ao Chakrabarti's lab da University of North Carolina at Charlotte (UNCC) por me receberem durante seis meses de estágio. Em especial ao Dr. Kausik Chakrabarti pelos muitos ensinamentos.

Às agências de fomento que tornaram possível minha jornada acadêmica: ao CNPq (Conselho Nacional de Desenvolvimento Científico e Tecnológico), processo n° 143311/2019-0 - GM/GD-Cotas do Programa de Pós-Graduação, pelo apoio durante os 4 meses de mestrado, que antecedeu a transição para o doutorado direto; à CAPES (Coordenação de Aperfeiçoamento de Pessoal de Nível Superior) – Código de Financiamento 001, processo n° 88887.470062/2019-00, pelo suporte nos dois primeiros meses de doutorado; e à FAPESP (Fundação de Amparo à Pesquisa do Estado de São Paulo), processo n° 2019/25985-6, pela concessão de bolsa no país, e processo n° 2022/05039-1, pela concessão de bolsa de estágio no exterior (BEPE). Expresso minha sincera gratidão e reconhecimento a essas agências, cujo apoio é fundamental para o avanço científico do nosso país. Que continuem sendo reconhecidas e valorizadas por seu papel essencial na promoção da pesquisa e do desenvolvimento científico.

Epígrafe

“Um pouco de ciência nos afasta de Deus. Muito, nos aproxima.”

Louis Pasteur

Resumo

Parasitos do gênero *Leishmania* causam leishmaniose, uma doença tropical negligenciada que afeta pessoas em todo o mundo. A doença apresenta diferentes manifestações clínicas, alta taxa de incidência e vai desde lesões auto curáveis até a forma letal, conhecida como leishmaniose visceral. Apesar de muitos esforços, até agora não existem vacinas e protocolos de tratamento eficientes disponíveis e, portanto, encontrar novos alvos terapêuticos é crucial. Os telômeros, extremidades físicas dos cromossomos de eucariotos, são essenciais para manter a estabilidade do genoma e têm sido considerados alvos potenciais contra parasitos. Em *Leishmania* spp. os telômeros são compostos por repetições conservadas do tipo TTAGGG, mantidas pela telomerase, uma ribonucleoproteína minimamente composta pelos componentes TERT (transcriptase reversa da telomerase) e TER (RNA da telomerase). Na maioria dos eucariotos o TER é uma molécula única e contém a sequência molde copiada pela TERT durante a elongação dos telômeros. Sua estrutura secundária contém domínios com funções de controle da inserção de nucleotídeos pela TERT, reconhecimento da sequência telomérica e de ligação com proteínas acessórias. Em 2014 nosso grupo identificou e caracterizou parcialmente o componente TER da telomerase de *Leishmania* (*Leish*TER). O presente trabalho visa desvendar os papéis biológicos desempenhados pelo componente TER de *Leishmania major* (*Leish*TER) na homeostase do parasito. Para isso obtivemos uma linhagem celular knockout (*Lm*TER$^{-/-}$) que apresentou alterações no perfil de proliferação do parasito, divisão celular e replicação do DNA, principalmente nas primeiras passagens in vitro. Durante o crescimento contínuo, *Lm*TER$^{-/-}$ apresentou *arrest* parcial do ciclo celular G0/G1, encurtamento progressivo dos telômeros e maior porcentagem de fosforilação da histona γH2A. Além disso, alterações ultraestruturais características da autofagia foram detectadas sem que as células apresentassem danos no DNA ou fenótipos de apoptose. *Lm*TER$^{-/-}$ promastigotas diferenciam-se em metacíclicos apresentando índice de infectividade *in vitro* menor que o controle *Lm*007. Curiosamente, o addback de *Leish*TER não retornou o comprimento dos telômeros aos níveis do tipo selvagem, corroborando resultados preliminares que mostram que a expressão episssomal de TER, semelhante à sua ablação, tem um efeito negativo dominante na vida do parasito, o que pode ser um potencial alvo terapêutico contra a leishmaniose. Além disso, resultados preliminares que visam acessar a estrutura secundária de *Leish*TER através da acilação seletiva de 2'-hidroxila analisada por extensão de primer e perfil mutacional (SHAPE MaP) com o uso de 2-metilnicotínico imidazolide (NAI) confirmaram algumas estruturas já descritas pelo nosso grupo, incluindo a Hélice II (TBE), o molde e a hélice proximal ao modelo (TPH). A estrutura inicial de ~100 nt de *Leish*TER se assemelhou à de TbTR (TER de *Trypanosoma brucei*), com um motivo 5' CCGUCA 3' na extremidade 3' proximal a TBE, similar a TBE de *Tetrahymena thermophila*. Nucleotídeos na base de TPH mostraram baixa reatividade, indicando rigidez, enquanto o ápice apresentou reatividade. O molde de *Leish*TER compreende principalmente elementos de cadeia simples, exceto por alguns nucleotídeos que sugerem envolvimento em interações de longo alcance ou transitórias. Entretanto, experimentos adicionais são necessários para confirmação e uma compreensão completa da estrutura de *Leish*TER.

Palavras-chave: *L. major* TER nocaute; alteração da proliferação; encurtamento dos telômeros; sinalização de danos ao DNA; autofagia; baixo índice de infectividade; CRISPR/Cas9; SHAPE-MaP.

Abstract

Parasites of the genus *Leishmania* cause leishmaniasis, a neglected tropical disease that affects people worldwide. The disease has different clinical manifestations, a high incidence rate and ranges from self-healing lesions to the lethal form known as visceral leishmaniasis. Despite many efforts, until now there are no vaccines and efficient treatment protocols available and therefore finding new therapeutic targets is crucial. Telomeres, the physical ends of eukaryotic chromosomes, are essential for maintaining genome stability and have been considered potential targets against parasites. In *Leishmania* spp. telomeres are composed of conserved TTAGGG-like repeats maintained by telomerase, a ribonucleoprotein minimally composed of TERT (telomerase reverse transcriptase) and TER (telomerase RNA) components. In most eukaryotes, TER is a single molecule and contains the template sequence copied by TERT during telomere elongation. Its secondary structure contains domains with functions to control the insertion of nucleotides by TERT, recognition of the telomeric sequence and binding with accessory proteins. In 2014 our group identified and partially characterized the TER component of *Leishmania* telomerase (*Leish*TER). The present work aims to unravel the biological roles played by the TER component of *Leishmania major* (*Leish*TER) in the parasite's homeostasis. For this, we obtained a knockout cell line (*Lm*TER$^{-/-}$) that showed alterations in the profile of parasite proliferation, cell division and DNA replication, mainly in the first passages in vitro. During continuous growth, *Lm*TER$^{-/-}$ showed partial arrest of the G0/G1 cell cycle, progressive telomere shortening and a higher percentage of histone γH2A phosphorylation. Furthermore, ultrastructural alterations characteristic of autophagy were detected without the cells showing DNA damage or apoptosis phenotypes. *Lm*TER$^{-/-}$ promastigotes differentiate into metacyclics with an *in vitro* infectivity index lower than the *Lm*007 control. Interestingly, the *Leish*TER addback did not return telomere length to wild-type levels, corroborating preliminary results showing that episomal TER expression, similar to its ablation, has a dominant negative effect on parasite lifespan, which may be a potential therapeutic target against leishmaniasis. Additionally, preliminary results aiming to access the secondary structure of *Leish*TER through selective 2'-hydroxyl acylation analyzed by primer extension and mutational profiling (SHAPE MaP) using 2-methyl nicotinic imidazolide (NAI) confirmed some structures previously described by our group, including Helix II (TBE), the template, and the template proximal helix (TPH). The initial structure of ~100 nt of *Leish*TER closely resembled that of *Tb*TR (*Trypanosoma brucei* TER), with a 5' CCGUCA 3' motif at the 3' end proximal to TBE, similar to TBE in *Tetrahymena thermophila*. Nucleotides at the TPH base showed low reactivity, indicating rigidity, while the apex exhibited reactivity. The *Leish*TER template mainly comprised single-stranded elements, except for a few nucleotides suggesting involvement in long-range or transient interactions. However, additional experiments are needed for confirmation and a comprehensive understanding of the *Leish*TER structure.

Keywords: *L. major* TER knockout; alteration of proliferation; telomere shortening; DNA damage signaling; autophagy; low infectivity rate; CRISPR/Cas9; SHAPE-MaP.

Resumo para a sociedade

Vocês já ouviram falar das leishmanioses? Elas são doenças causadas por um ser vivo bem pequeno impossível de observar a olho nu, chamado *Leishmania*. Esses organismos são parasits e são transmitidos através da picada do mosquito palha infectado. Existem vários tipos de leishmanioses, como por exemplo: leishmaniose cutânea, caracterizada por feridas na pele; e a leishmaniose visceral que ataca órgãos muito importantes para nossa sobrevivência, como o fígado e o baço, podendo levar a morte. O tipo de leishmaniose que a pessoa infectada pode desenvolver depende de como está seu sistema imunológico e qual tipo de *Leishmania* a infectou. Além disso, a leishmaniose é considerada uma zoonose que afeta principalmente cães domésticos, os quais atuam como reservatórios da doença. A Organização Mundial da Saúde declarou as leishmanioses como doenças de grande impacto e importância, porém elas ainda são negligenciadas, ou seja, mesmo afetando milhões de pessoas no mundo, incluindo o Brasil, ainda não há vacinas nem tratamentos eficazes para combatê-las.

Dessa forma, é importante estudar esses parasitos para tentar encontrar um de seus pontos fracos que possam ser utilizados para lutar contra eles. Apesar da *Leishmania* ser um organismo unicelular e diferente de nós humanos em muitos aspectos, nós compartilhamos muitas coisas em comum. Então, para criar um medicamento ou uma vacina eficaz, precisamos tomar cuidado para encontrar algo que ataque apenas a *Leishmania* e que não faça mal aos seres humanos.

Pensando nisso, nós no Laboratório de Telômeros estudamos os telômeros e a telomerase de *Leishmania* como potenciais alvos terapêuticos. Mas o que são telômeros e telomerase?

Você já deve ter ouvido falar do DNA, nosso material genético. O DNA é como um livro de receitas. Nele há todas as informações necessárias para fazer você ser você. Ele é o centro de informações das nossas células (pequenos "blocos" que constroem nosso corpo). O DNA em nossas células, assim como na *Leishmania* estão organizados em moléculas lineares denominadas cromossomos. E assim como um livro possui capa, nosso DNA também tem uma "capa" para protegê-lo, chamada de "Telômeros". Esses telômeros ficam nas pontas dos cromossomos protegendo todas as informações contidas nele. Porém, assim como as capas dos livros vão se desgastando ao longo do tempo, os telômeros também vão, e nesse caso seu desgaste causa seu encurtamento. Se esses telômeros ficarem bem curtinhos, isso pode ser um problema para a célula, já que seu centro de informações, o DNA, ficará desprotegido, com possibilidade de perdê-las. Para tentar resolver essa situação, temos a participação de uma personagem muito importante, a telomerase. Ela funciona como uma máquina de elongar telômeros e consegue produzir mais telômeros nas pontas do DNA, ajudando-o a recuperar o que estava sendo perdido/desgastado.

Essa telomerase é composta por algumas peças: uma peça se chama TERT e a outra se chama TER. A TERT é quem coloca a "mão na massa" e produz mais telômeros, enquanto o TER tem um molde que a TERT utiliza para essa produção. É como se a TERT fosse a boleira e o TER a forma do bolo. E da mesma forma que há várias formas de bolo, essa peça chamada de TER também varia muito, sendo exclusiva em cada ser vivo. Ou seja, TER de *Leishmania* é diferente do TER de humanos, apesar de terem a mesma função. E com isso, ele pode ser o "ponto fraco" que procuramos para combater a *Leishmania* e consequentemente as leishmanioses.

Sabendo disso, o meu projeto de doutorado busca estudar:

- Os efeitos que a retirada e a produção em excesso do TER causa nos telômeros de *Leishmania*, e como isso afeta o desenvolvimento e o seu poder de infecção;
- Analisar a estrutura do TER de *Leishmania*.

Para tentar responder essas perguntas, muitos experimentos foram realizados, e chegamos aos seguintes resultados: a ausência do TER influencia no tamanho dos telômeros de forma negativa, ou seja, ao longo do tempo os telômeros das *Leishmanias* que não tem o TER vão encurtando, e isso prejudica seu crescimento populacional. Além disso, identificamos mudanças nas estruturas interiores da célula de *Leishmania*, mas sem afetar o material genético. As *Leishmanias* com telômeros curtos também apresentaram um baixo poder de infecção quando comparada com as *Leishmanias* controles (aquelas que ainda possuem o TER e telômeros intactos). Também verificamos que a superprodução do TER nas *Leishmanias* acaba tendo um efeito dominante negativo, o que significa que sua superprodução atrapalha o funcionamento normal da *Leishmania*, fazendo com que ela apresente características similares as *Leishmania* que não possuem o TER.

Ainda temos resultados preliminares, porém ao analisarmos uma parte da estrutura do TER vimos que ele se parece com o TER de outro parasito chamado *Trypanosoma brucei*, causador da doença do sono. Porém, mais pesquisas estão em andamento para desvendar a estrutura completa do TER de *Leishmania.*

Assim, esses achados indicam que o componente TER se destaca como um alvo promissor na busca por medicamentos inovadores contra a leishmaniose

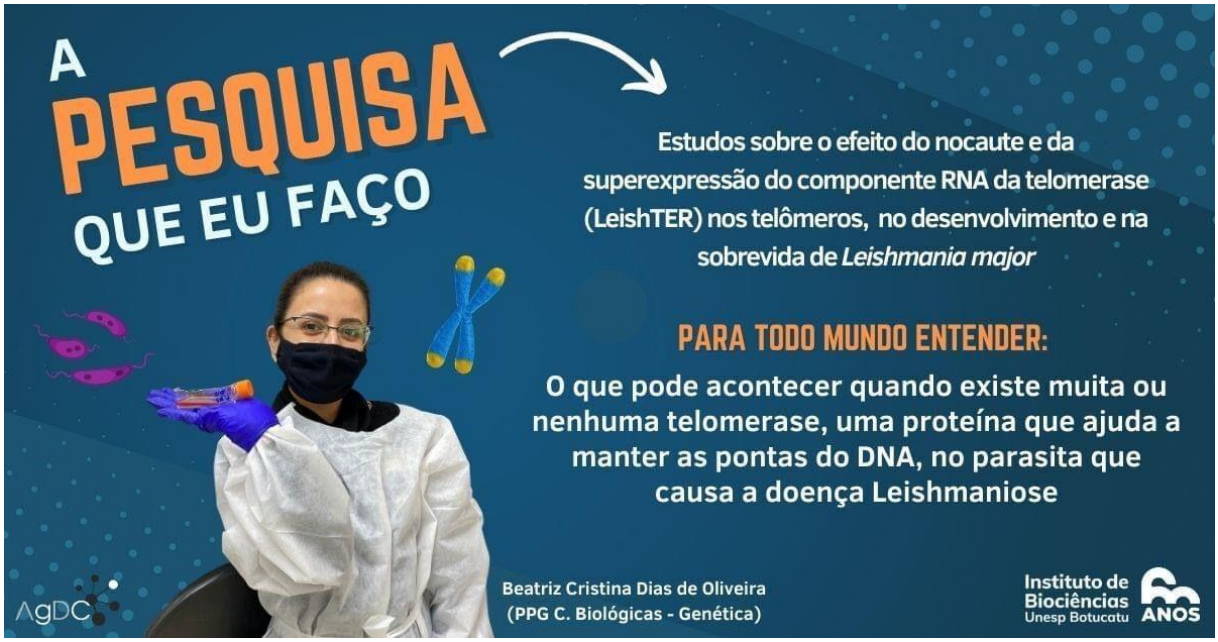

Card gerado na disciplina de "Divulgação Científica"

Lista de figuras

1 Introdução

3.1 Capítulo 1 - *The impact of knocking out the Leishmania major telomerase RNA (LeishTER): from altered cell proliferation to decreased parasite infectivity*

3.2 Capítulo 2 - *Structural assessment of the core domains of Leishmania major telomerase RNA (LeishTER)*

3.3 Capítulo 3 - *Geração de linhagem de Leishmania major duplo nocaute para o TER e para a TERT*

Lista de tabelas

3.1 Capítulo 1 - *The impact of knocking out the Leishmania major telomerase RNA (LeishTER): from altered cell proliferation to decreased parasite infectivity*

3.2 Capítulo 2 - *Structural assessment of the core domains of Leishmania major telomerase RNA (LeishTER)*

3.3 Capítulo 3 - *Geração de linhagem de Leishmania major duplo nocaute para o TER e para a TERT*

Sumário

1 Introdução

1.1 O parasito *Leishmania* spp. e as leishmanioses

O gênero *Leishmania* recebe esse nome em homenagem a Major William Leishman, que em 1903 descreveu detalhadamente características de corpúsculos ovais, os quais ele acreditava se tratar de resíduos de tripanossomas, encontrados no baço *post-mortem* pertencente a um soldado que havia morrido em decorrência da "kala-zar", uma febre negra popularmente conhecida na Índia. A descoberta de uma nova espécie e um novo gênero se concretizou após os estudos de Leishman serem analisados juntamente aos estudos do Capitão Charles Donavan por Major Ross que após observar as amostras, chegou à conclusão que não se tratava de fragmentos de tripanossomas e sim de uma nova espécie de organismo, o qual nomeou de *Leishmania donovani*, criando assim o gênero *Leishmania* (Cupolillo et al., 2014; Ross, 1903).

Desde então mais de 50 espécies de *Leishmania* foram descritas e classificadas. As espécies que infectam o ser humano são divididas em dois subgêneros: *Viannia* e *Leishmania* (Pacheco e Carvalho-Costa, 2014), sendo o subgênero *Viannia* restrito ao Novo Mundo, e o subgênero *Leishmania* presente tanto no Velho Mundo como no Novo Mundo (Akhoundi et al. 2016; Kerr, 2000; Lainson e Shaw, 1987).

Os parasitos do gênero *Leishmania* pertencem a família Trypanosomatidae e ordem Kinetoplastida (Silva et al., 2014) que também engloba outros parasitos de importância médica como *Trypanosoma cruzi* e *Trypanosoma brucei*, causadores das doenças de Chagas e do sono, respectivamente. Organismos pertencentes a ordem Kinetoplastida se diferenciam dos demais eucariotos pela presença de cinetoplasto, o qual está localizado dentro da única mitocôndria do parasito, que contém DNA mitocondrial em alto número de cópias (kDNA) (Neves, 2005; Silva et al., 2014).

As *Leishmanias* são parasitos digenéticos, os quais necessitam de um hospedeiro invertebrado e um vertebrado para completar seu ciclo de desenvolvimento (Cupolillo et al., 2014; Silva et al., 2014). Durante o ciclo, os parasitos passam por três principais estágios de desenvolvimento morfologicamente distintos, sendo eles:

- Promastigota procíclica: possui alta capacidade proliferativa, é alongada, extracelular, possui um flagelo para auxiliar na mobilidade e encontra-se no trato digestório do hospedeiro invertebrado (insetos das espécies *Lutzomya* ou *Phlebotomus*), popularmente conhecido como mosquito-palha (Fig. 1) (Neves, 2005; Silva et al., 2014).

- Promastigota metacíclica: é a forma infectante do parasito sendo transmitida aos hospedeiros vertebrados durante o repasto sanguíneo da fêmea do inseto. Embora possua características similares à promastigota procíclica, seu corpo é menos alongado e seu flagelo mais longo, além de não serem proliferativas, ou seja, não se dividem. As metacíclicas podem ser encontradas no trato digestivo anterior do inseto (Fig. 1) (da Silva e Sacks, 1987; Lainson e Shaw, 1987; Neves, 2005).
- Amastigota: encontrada no meio intracelular do hospedeiro vertebrado, é altamente proliferativa, arredondada e seu flagelo é inaparente, pois não se exterioriza (Fig. 1) (Neves, 2005; Silva et al., 2014).

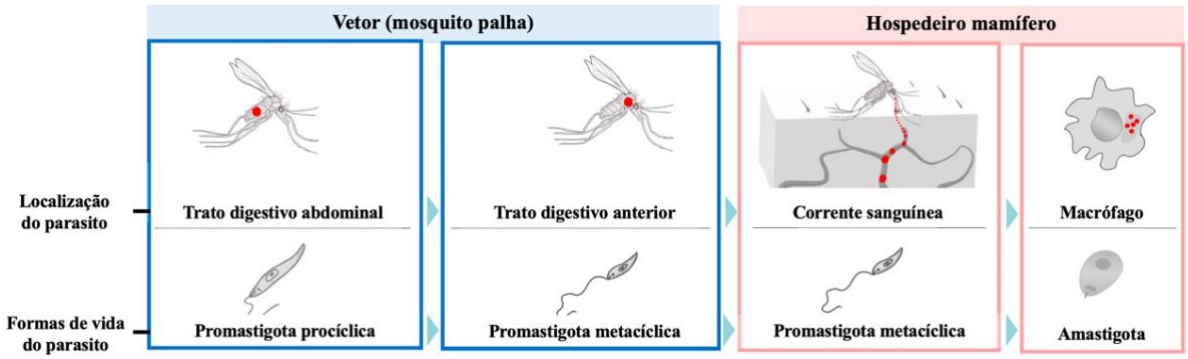

Figura 5. Principais formas do parasito do gênero *Leishmania* nos diferentes ambientes durante o ciclo de desenvolvimento. Imagem extraída e traduzida de Karamysheva et al. (2020).

A capacidade que o parasito possui de se diferenciar, deve-se principalmente a alterações da expressão gênica ocasionada devido ao estresse causado por mudanças como diferença de temperatura, pH e nutrientes, no meio onde se encontra o parasito (Karamysheva et al. 2020).

1.2 Ciclo biológico dos parasitos do gênero *Leishmania*

Durante a hematofagia do inseto (flebotomíneo) infectado, o parasito na sua forma metacíclica penetra na pele do hospedeiro mamífero sendo fagocitado por neutrófilos e depois por macrófagos periféricos recrutados no local da lesão. Uma vez dentro do macrófago, o parasito se diferencia na forma amastigota, e começa a se multiplicar por fissões binárias sucessivas, os quais após causarem o rompimento da membrana do macrófago, são liberados na corrente sanguínea, podendo infectar novas células, ou serem sugados por uma nova fêmea do flebotomíneo durante o repasto sanguíneo (Chappuis et al., 2007). Dentro do inseto, os parasitos na forma amastigota se agrupam, e após aproximadamente 12 horas, eles começam a

se diferenciar em promastigotas procíclicas (Morea et al., 2021), os quais migram para o epitélio do trato digestório e começam a se multiplicar sucessivamente por divisão binária, aderindo ao epitélio pelo flagelo. Alguns parasitos podem ser eliminados com as fezes do mosquito, e os demais migram para a região anterior do intestino até a válvula estomodeal, onde se concentram e passam pela diferenciação celular denominada metaciclogênese, em que o tamanho do corpo celular diminui e o flagelo aumenta. As formas promastigotas metacíclicas resultantes dessa transformação, são extremamente móveis e infectivas e migram para a probóscide do inseto sendo regurgitadas e transmitidas ao hospedeiro vertebrado através da picada, reiniciando um novo ciclo de transmissão (Fig. 2) (Neves, 2005). Todo o ciclo de desenvolvimento do parasito pode ser replicado *in vitro* em culturas axênicas (Bates, 1994), facilitando a manipulação e estudos sobre a biologia, desenvolvimento e interações do parasito com o meio e seus hospedeiros.

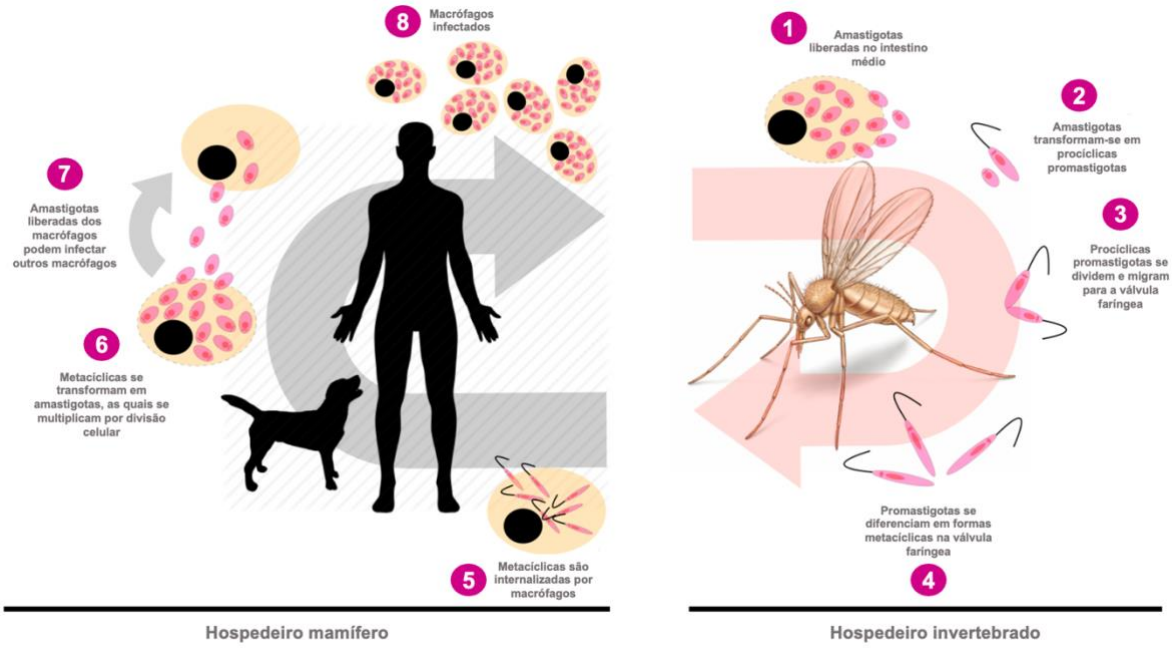

Figura 6. Ciclo de vida de *Leishmania* spp. Durante o repasto sanguíneo, insetos fêmeas das espécies *Lutzomya* (Velho Mundo) ou *Phlebotominae* (Novo Mundo), infectados com parasitos do gênero *Leishmania*, regurgitam as formas promastigotas metacíclicas no hospedeiro mamífero. Estas são fagocitadas por macrófagos e dentro da célula se diferenciam em amastigotas. As amastigotas se multiplicam e causam a *lise* celular podendo infectar outras células do hospedeiro ou ser absorvidas durante a hematofagia por outros insetos. Uma vez dentro do inseto, as amastigotas se diferenciam em promastigotas procíclicas, as quais se dividem e se diferenciam em metacíclicas, migrando para a probóscide do mosquito, sendo regurgitadas durante o repasto sanguíneo e assim, reiniciando o ciclo. Imagem extraída e traduzida de Assis et al. (2021).

1.3 As leishmanioses

As *Leishmanias* têm uma grande importância médica, uma vez que causam leishmanioses, endêmicas em mais de 80 países (Fig. 3A e 3B) e caracterizadas pela sua complexidade e diversidade (Desjeux, 1992; WHO, 2021; Pace, 2014). Embora seja considerada pela Organização Mundial da Saúde doenças tropicais de grande impacto em países subdesenvolvidos, elas também podem ser encontradas em países desenvolvidos como França, Grécia e Itália (Chappuis et al., 2007; Nascimento e Santos, 2020; Pace, 2014).

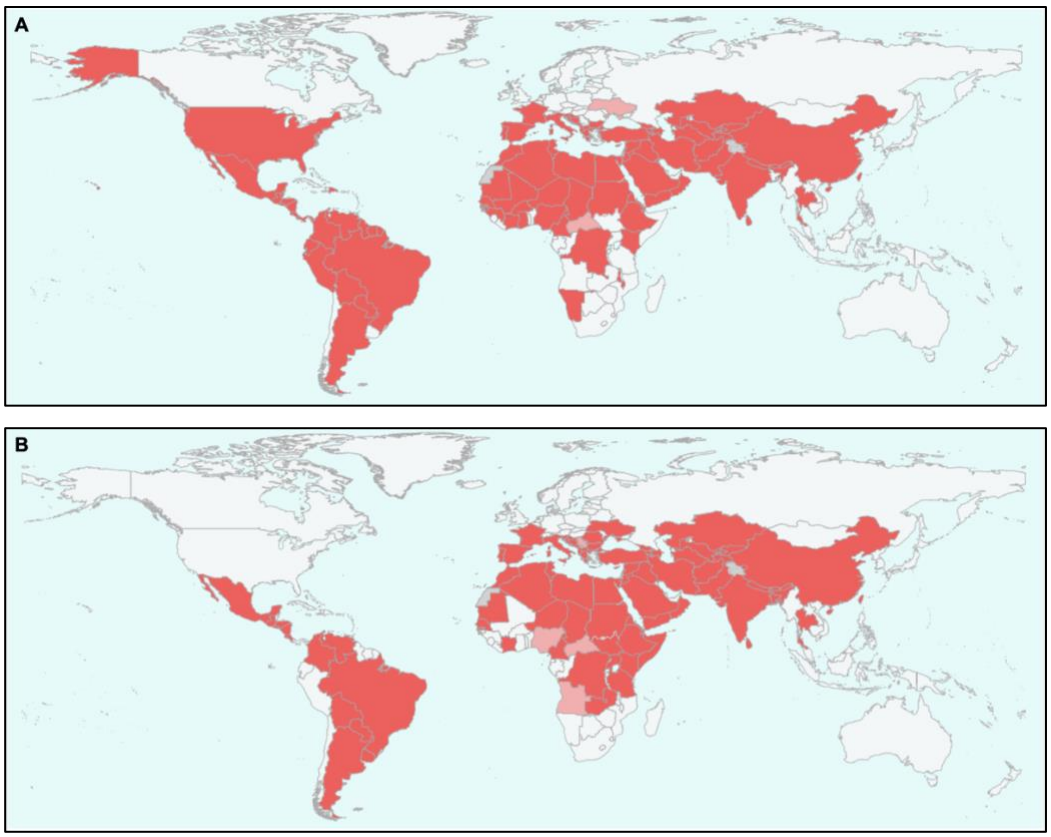

Figura 7. Mapa mundial contendo dados reportados de países e territórios sobre o estado de endemicidade das leishmanioses. a) Endemicidade da leishmaniose cutânea em 2021; b) Endemicidade da leishmaniose visceral em 2021. Em vermelho: países endêmicos; em rosa: casos previamente reportados; em branco: não há casos autóctones relatados; em cinza: não aplicável. (Fonte: http://apps.who.int/neglected_diseases/ntddata/leishmaniasis/leishmaniasis.html).

Atualmente sabe-se que aproximadamente 20 espécies de protozoários flagelados do gênero *Leishmania* são patogênicas para o ser humano (Chappuis et al., 2007; Desjeux, 1992; Nascimento e Santos, 2020), cuja transmissão ocorre por aproximadamente 30 espécies de insetos do gênero *Phlebotomus* (Velho Mundo) e *Lutzomyia* (Novo Mundo) (Desjeux, 1992; Steck, 1974). Além do ser humano, animais domésticos e silvestres também podem ser

infectados, tornando-se reservatórios da doença, o que destaca sua importância veterinária (Desjeux, 1992).

As diversas manifestações clínicas das leishmanioses podem variar de acordo com a interação entre a espécie infectante e o sistema imune do organismo infectado (Pace, 2014; Reithinger et al., 2007), podendo ficar restritas ao local da picada ou induzir metástase via sistema linfoide do hospedeiro (Steck, 1974). Os tipos de leishmanioses são diferenciados pelas suas características clínicas e epidemiológicas, onde podemos destacar cinco grupos principais:

- Leishmaniose cutânea (LC): caracterizada por lesões pontuais na pele onde ocorreu a picada. Elas podem variar no grau de severidade e duração, e em muitos casos a cura pode ocorrer sem a necessidade de tratamento (Fig. 4A) (Chappuis et al., 2007; Desjeux, 1992; Galvis-Ovallos et al., 2020).
- Leishmaniose cutânea difusa (LCD): manifesta-se através de lesões espalhadas pela pele cuja severidade depende da condição imunológica do paciente (Fig. 4B) (Carregal et al., 2019).
- Leishmaniose mucocutânea (LMC): caracteriza-se pelas lesões nas mucosas do nariz, boca, faringe e laringe, o que pode levar a destruição do septo nasal, e outras estruturas da nasofaringe (Fig. 4C) (Chappuis et al., 2007; Desjeux, 1992; Pace, 2014).
- Leishmaniose visceral (LV): também conhecida como leishmaniose calazar, é a manifestação mais severa da doença e foi descrita pela primeira vez na Índia. Entre os sintomas dessa doença podemos destacar a febre prolongada, hepatomegalia e esplenomegalia (aumento do fígado e do baço, respectivamente), pancitopenia, anemia, perda de peso e quando não tratada pode levar a morte (Fig. 4D) (Chappuis et al., 2007; Desjeux, 1992; Galvis-Ovallos et al., 2020; Nascimento e Santos, 2020).
- Leishmaniose dérmica pós-calazar (LDPC): considerada uma complicação da leishmaniose visceral, ela pode se manifestar meses ou até anos após o término do tratamento da LV, sendo caracterizada por erupções cutânea, pápulas ou nódulos na pele. Esse tipo de manifestação é mais comumente observado em regiões da África e Ásia (Fig. 4E) (OP, 2020; Pace, 2014).

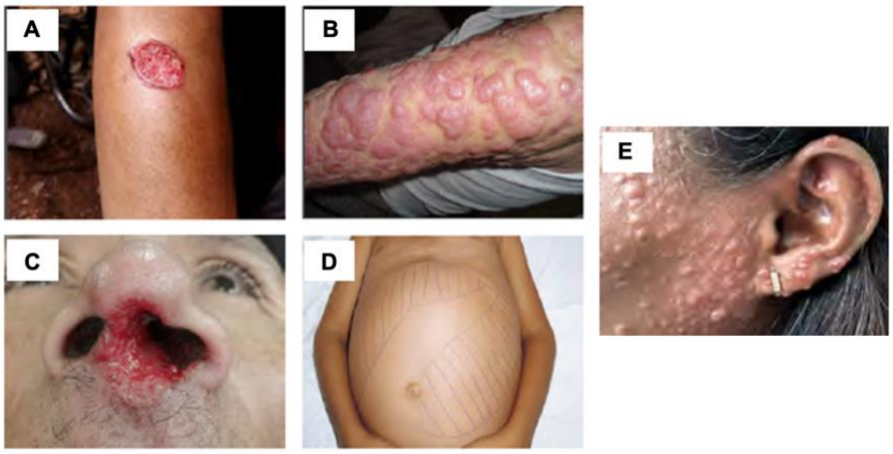

Figura 8. Manifestações clínicas da leishmaniose. a) Leishmaniose cutânea; b) Leishmaniose cutânea difusa; c) Leishmaniose mucocutânea; d) Leishmaniose calazar, e) Leishmaniose dérmica pós-calazar. Fonte: Atlas interactivo de leishmaniasis en las Américas: aspectos clínicos y diagnósticos diferenciales.

Segundo a Organização Pan-Americana de Saúde (OPAs), 90% dos casos de leishmaniose visceral estão concentrados no Brasil, Índia, Sudão, Sudão do Sul, Etiópia e Quênia; e 75% dos novos casos de leishmanioses cutâneas no mundo ocorrem em cinco países: Afeganistão, Brasil, Iran, Iraque e Síria. Já as leishmanioses mucocutâneas ocorrem majoritariamente na América, se destacando Brasil, Bolívia e Peru (Reithinger et al., 2007). Aproximadamente 30 mil novos casos de leishmaniose visceral e um milhão de casos de leishmaniose cutânea são registrados anualmente e entre 20.000 a 30.000 mortes ocorrem por ano (OPAs, 2020).

Os tratamentos disponíveis para leishmanioses baseiam-se principalmente no uso de antimoniais pentavalentes (Carregal et al., 2019; Nascimento e Santos, 2020), embora apresentem alta toxicidade causando efeitos colaterais indesejados, e além de desenvolver resistência do parasito ao fármaco, eles vêm sendo utilizados há mais de 60 anos como tratamentos de primeira linha (Reis-Cunha et al., 2016). Outros medicamentos alternativos para tratar as leishmanioses incluem a anfotericina B e a miltefosina, sendo o primeiro um medicamento de alto custo o que o torna inviável em muitos países, e o segundo possui ação teratogênica, o que restringe seu uso (Nascimento e Santos, 2020; Reis-Cunha et al., 2016). Como não há protocolos eficazes de tratamento e profilaxia disponíveis, torna-se crucial encontrar novos alvos terapêuticos para combater a doença (Carregal et al., 2019).

1.4 Telômeros e telomerase

1.4.1 Telômeros

Telômeros, do grego “telos” que significa fim e “meros” parte, são estruturas nucleoproteicas presentes nas extremidades de cromossomos lineares (Xu, 2011), formadas por sequências curtas de DNA não codificante repetidas em *tandem*, as quais possuem uma alta conservação entre os eucariotos (Blackburn, 1991; Griffiths et al., 2016). Sequências do tipo 5' TTAGGG 3' compõem os telômeros de vertebrados e protozoários tripanosomatídeos, incluindo *Leishmania* (Cano, 2001). Os telômeros caracterizam-se pela presença de uma fita rica em G, que se estende além da sua fita complementar rica em C, formando assim uma protusão conhecida como 3' G – *overhang* (Blackburn et al., 2015).

Nos terminais cromossômicos há sítios específicos de interação com proteínas teloméricas, tanto no DNA simples-fita como no dupla-fita, formando uma estrutura nucleoproteica dinâmica (Dmitriev et al., 2003). Essas proteínas, que podem interagir diretamente com o DNA ou se associarem a outras proteínas teloméricas, aparentemente influenciam no tamanho, estabilidade e proteção dos telômeros (Dmitriev et al., 2003; Fernandes et al., 2020). Em humanos, essas proteínas formam o complexo *shelterin*, composto por: TRF1 e TRF2, *Protection of telomeres* 1 (POT1), TRF1-e TRF2-*Interacting Nuclear protein* 2 (TIN2), *Repressor / Activator Protein* 1 (RAP1) e TIN2 e POT1 *interacting Protein* 1 (TPP1). Já em *Leishmania amazonensis*, tripanosomatídeo com complexo telomérico melhor caracterizado, podemos destacar algumas proteínas que interagem com a telomerase e com a fita simples de DNA rica em G: proteína de ligação de RNA 38 (LaRBP38), as proteínas de replicação A1 (LaRPA-1) e “calmodulin-like protein” (LCaLA) (Lira et al., 2007; Morea et al., 2017; Neto et al., 2007) e as proteínas que se associam com a dupla fita de DNA telomérico: proteína de ligação de telômeros 1 (LaTBP1) (Lira et al., 2007) e a proteína fator de ligação a repetição telomérica (LaTRF) (da Silva et al., 2010) (Fig. 5).

Além das proteínas do complexo telomérico, RNAs longos não codificantes conhecidos como TERRA (*Telomere Repeat containing RNA*) (Fig.5) foram caracterizados em diversos organimos modelos como humanos, camundongos e leveduras de brotamento (*S. cerevisiae*) (Azzalin et al., 2007; Schoeftner & Blasco, 2008; Luke et al., 2008). A transcrição desses RNAs se inicia nas regiões subteloméricas e continua até as extremidades dos cromossomos, resultando em variabilidade na porção 5’ da molécula e conservação na região 3’, composta por repetições teloméricas (Rivosecchi et al., 2024). Entre as funções atribuídas aos TERRAs, podemos destacar sua importância na regulação telomérica e estabilidade auxiliando na regulação da estrutura da cromatina telomérica, na replicação do DNA nos telômeros, no

processamento das extremidades cromossômicas e na atividade da telomerase (Rivosecchi et al., 2024). Ademais, os TERRAs podem formam híbridos de DNA:RNA denominados R-loops e assumir a estrutura de RNA G4 (rG4), os quais facilitam interações com proteínas associadas ao TERRA. Já os R-loops também podem facilitar a recombinação homóloga nos telômeros, contribuindo para a estabilidade telomérica por meio de mecanismos alternativos de alongamento telomérico (ALT) (Rivosecchi et al., 2024). Transcritos TERRA também foram caracterizados em *T. brucei* e *Leishmania* spp. e em ambos os casos eles parecem também estar envolvidos com a manutenção dos telômeros (Damasceno et al., 2017; Morea et al., 2021).

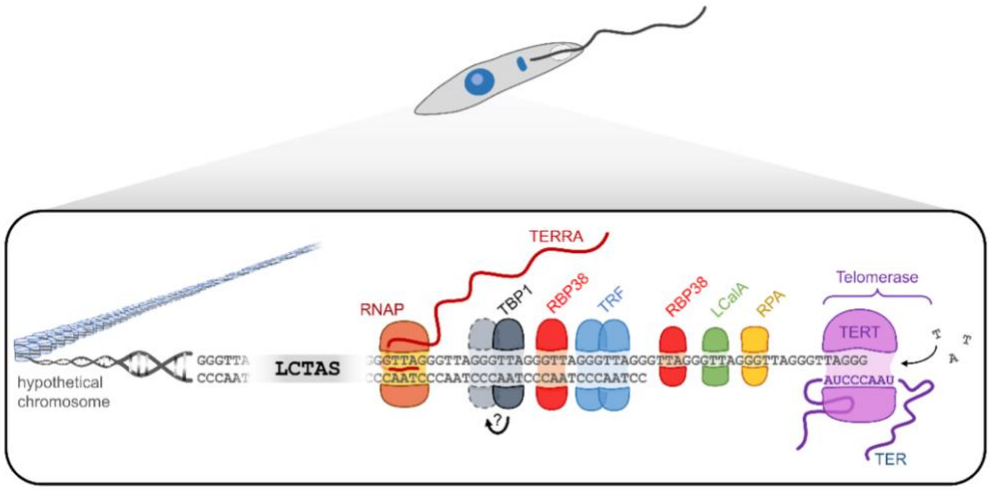

Figura 5. Representação dos telômeros de *Leishmania* spp. Os telômeros de *Leishmania* são formados por regiões subteloméricas (LCTAS), DNA dupla fita e simples fita, formando o último uma protusão conhecida como 3' G *overhang* e proteínas associadas (TBP1, RBP38, TRF, LCalA, RPA). RNAs longos não codificantes TERRA são transcritos a partir dos telômeros e estão envolvidos com a regulação do tamanho dos telômeros, os quais podem ser elongados através da ação da enzima telomerase, composta principalmente pelo componente TERT e TER. Imagem extraída de Assis et al. (2021).

O complexo telomérico possui funções fundamentais na estabilidade do genoma, prevenindo que as extremidades cromossômicas sejam reconhecidas como quebra de DNA em dupla fita, impedindo assim, que ocorra degradação do material genético, recombinação e fusão dos terminais cromossômicos. Danos na estrutura telomérica ou a depleção de proteínas que compõe esta maquinaria, podem levar a célula ao estado de senescência ou apoptose (Blackburn et al., 2015; Eisenberg, 2011). Fenômeno semelhante é observado normalmente em células somáticas humanas que apresentam perda gradual dos telômeros após sucessivas duplicações (Barbé-Tuana et al., 2021; Giardini et al., 2014).

Estas perdas ocorrem devido a uma inabilidade da DNA polimerase em completar a síntese de moléculas lineares (Ohki e Ishikawa, 2004). Este fenômeno é conhecido como "*end*

replication problem", em português "problema do final da replicação" (Fig. 6) (Chan e Blackburn, 2004; Eisenberg, 2011; Olovnikov, 1973; Watson, 1972), na qual a DNA polimerase, que apresenta síntese de modo direcional (5' – 3'), não consegue realizar uma síntese regular na fita descontínua do DNA, a qual é orientada no sentido 3' – 5'. Dessa forma, faz-se necessário a síntese repetida de iniciadores RNA na região 5' do local de iniciação, de modo que a DNA polimerase consiga sintetizar novas sequências (fragmentos de Okazaki), de forma descontínua (Griffiths et al., 2016; Martínez e Blasco, 2015). Neste caso, o último iniciador envolvido na replicação da fita descontínua, próximo da extremidade 3', ao ser removido, não é reposto pela DNA polimerase deixando um intervalo na fita complementar (Griffiths et al., 2016; Martínez e Blasco, 2015). Isto gera uma protrusão simples fita na extremidade telomérica conhecida como 3' G-*overhang* (fita rica em G) (Martínez e Blasco, 2015). Também é sabido que mesmo as fitas de síntese contínua, ao final da replicação são processadas por nucleases, como Apollo and Exo I, as quais promovem a ressecção do terminal da fita contínua (fita telomérica rica em C) de forma a gerar um terminal 3' G-*overhang* também nessa fita (Fig. 6) (Martínez e Blasco, 2015; Wu et al., 2012). Desta maneira, o encurtamento dos telômeros pode ocorrer nos terminais 3' das duas fitas do DNA. Assim, quando as células com telômeros curtos atingem o número máximo de divisões celulares, conhecido como "limite de Hayflick", elas entram no estado de senescência replicativa (Chan e Blackburn, 2004; Eisenberg, 2011; Olovnikov, 1973; Watson, 1972). Além da divisão celular, outros fatores endógenos e exógenos podem influenciar o encurtamento dos telômeros tais como estresse oxidativo causado por processos metabólicos, ação de nucleases e agentes físicos ou químicos (Blackburn et al., 2015; Eisenberg, 2011). Por outro lado, sabe-se que eucariotos unicelulares, células germinativas, células tronco embrionárias e células somáticas altamente proliferativas conseguem manter o tamanho dos telômeros por ação de uma enzima especializada em adicionar repetições teloméricas nas extremidades 3' G *overhang*, conhecida como telomerase (Autexier e Lue, 2006).

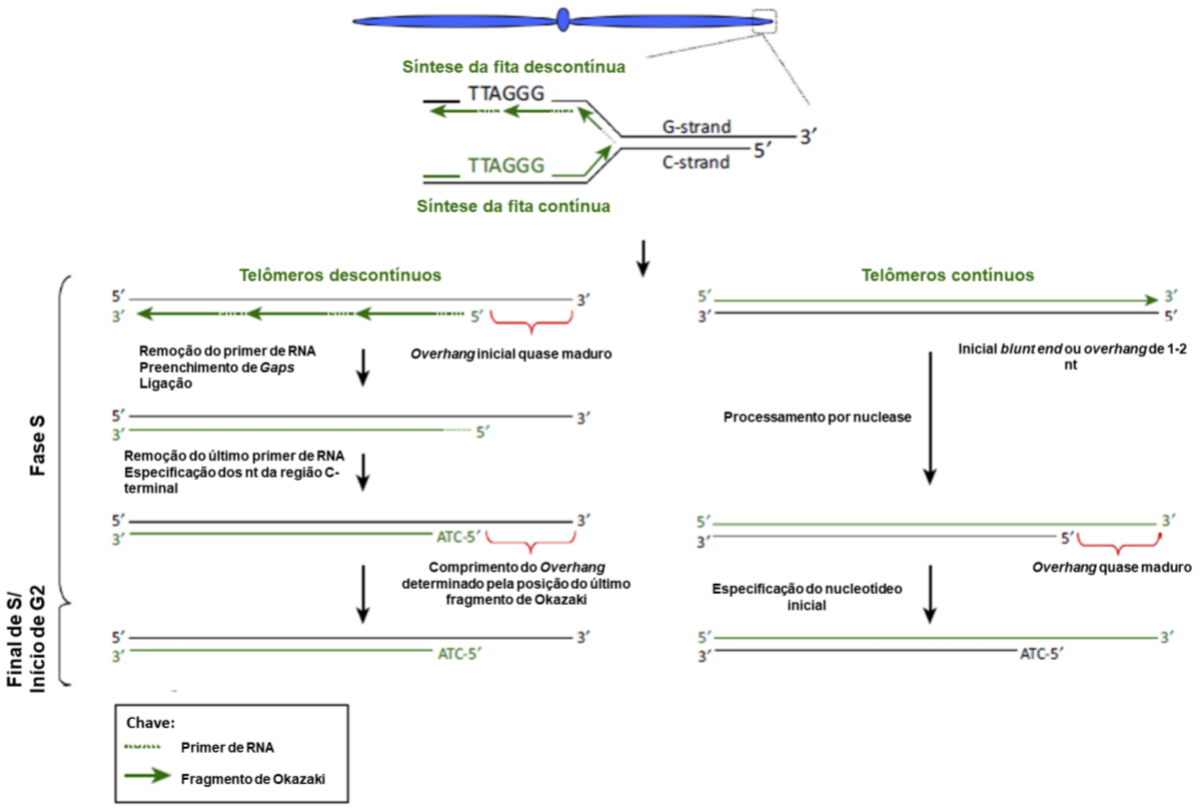

Figura 6. Replicação semiconservativa do DNA telomérico e seu processamento. A replicação semiconservativa do DNA telomérico ocorre por meio da maquinaria de replicação convencional, onde a fita contínua e a fita descontínua são sintetizadas pela DNA polimerase de modo unidirecional (5' – 3'). O início da síntese depende de um primer de RNA (linhas pontilhadas verde), o qual confere um grupo -OH livre na extremidade 3' para que a DNA polimerase possa começar a síntese da nova fita. Devido ao sentido da fita descontínua (3' – 5'), é necessário a síntese de vários primers de RNA durante sua replicação, que servem como iniciadores para a síntese dos fragmentos de Okazaki. Esses primers são degradados e repostos por DNA, exceto o último primer, que não pode ser substituído. O primer final de RNA na fita descontínua não é terminal, mas posicionado aleatoriamente 70-100 nucleotídeos (nt) das extremidades e, portanto, as protusões da fita G já exibem um tamanho quase maduro imediatamente após a replicação, onde fica evidente a especificidade da sequência na extremidade 5' da fita C (ATC 5'). Já a síntese da fita contínua resulta em extremidades cegas (*blunt ends)* ou apresentam uma saliência de 1 ou 2-nt consistentes com o conceito de que a máquina de replicação se esgota e se dissocia dos terminais cromossômicos. A fita gerada durante a síntese contínua é processada por nucleases 1–2 h após a replicação do telômero, para gerar uma protrusão 3' G-overhang e as fitas ricas em C adquirem a especificação ATC 5' no final da fase S / G2. Imagem extraída e traduzida de Martínez e Blasco (2015).

1.4.2 Telomerase

A possibilidade de uma célula resolver o problema do encurtamento dos telômeros através da adição de repetições teloméricas na extremidade 3' rica em G dos cromossomos foi descoberta em 1978 por Elizabeth Blackburn e Joseph Gall, ao estudarem o ciliado unicelular *Tetrahymena thermophila*. Depois foi confirmada em 1985 por Blackburn & Grieder, quando descobriram que esse processo era realizado por uma enzima, nomeada primeiramente de *telomere terminal transferase*, e posteriormente de telomerase.

A telomerase é um complexo ribonucleoproteico (RNP) com função de transcriptase reversa, possuindo um núcleo catalítico composto por uma subunidade proteica conhecida como transcriptase reversa da telomerase (TERT), que possui a função de adicionar as repetições teloméricas na extremidade 3' G–*overhang*, e a subunidade RNA da telomerase (TER), um RNA longo não codificante, que contém o molde utilizado pela TERT para realizar a síntese de novas repetições teloméricas além de auxiliar na processividade da enzima (Fig. 7). Embora esses dois componentes sejam suficientes para a replicação telomérica *in vitro* (Collins, 1999), *in vivo*, a telomerase contém proteínas acessórias espécie-específicas que auxiliam na biogênese e na regulação da atividade da enzima (Lue, 2004; Webb and Zakian, 2016). Como exemplos podemos citar as subunidades da telomerase de leveduras, a Est1p e Est3p, ambas importantes para o funcionamento da enzima *in vivo* (Giardini et al., 2014). Est1p interage com Cdc13 (proteína ligante do terminal 3' G-*overhang*) recrutando a telomerase para elongar os terminais dos cromossomos (Giardini et al., 2014; Yang et al., 2006). Em humanos, a proteína EST1A, ortóloga à Est1p, está relacionada tanto com a proteção das extremidades cromossômicas como pela elongação telomérica (Giardini et al., 2014). Outros exemplos de proteínas acessórias do complexo telomerase estão descritas na seção 1.4.2.2.1.

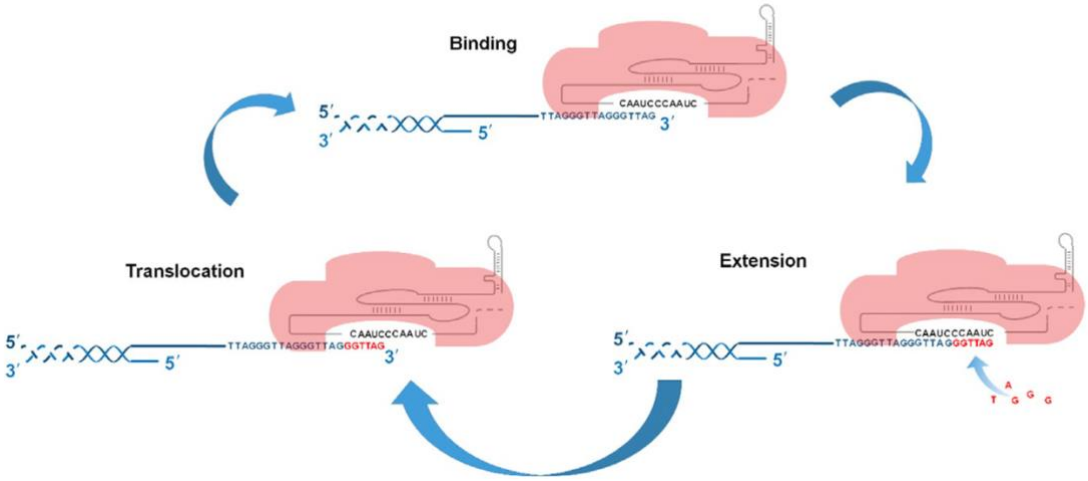

Figura 7. Ação da telomerase nos telômeros. Na etapa de ligação (*binding*), a TERT interage com a repetição telomérica e permite que o componente TER se acople a protusão 3'G. Em seguida, a TERT sintetiza uma cópia de repetição telomérica na extremidade 3'OH do DNA telomérico utilizando o molde contido no TER (*extension* - extensão). Ao término da adição de uma repetição, a TERT se desloca e se reposiciona em relação a repetição telomérica (*translocation* - translocação) para dar início a um novo ciclo de amplificação. Imagem extraída de Giardini et al., 2014).

Além da telomerase, há outros métodos alternativos para elongar telômeros (ALT, *Alternative Lengthening of Telomeres*), os quais utilizam a maquinaria de recombinação homóloga, de forma que uma fita de DNA homólogo é utilizada como molde para o elongamento de outra fita (Autexier e Lue, 2006; Podlevsky e Chen, 2016; Xu, 2011).

1.4.2.1 O componente Transcriptase Reversa da Telomerase (TERT)

O componente TERT é uma DNA polimerase dependente de RNA, com função de transcriptase reversa, a qual utiliza o grupo 3'-OH presente no 3' G-*Overhang* como iniciador da síntese de novas sequências teloméricas (Autexier e Lue, 2006). A TERT é altamente conservada entre os diferentes grupos de organismos, e apresenta quatro domínios estruturais e funcionais e 11 motivos canônicos, onde alguns são únicos das TERTs e outros conservados entre as transcriptases reversas (Fig. 8) (Autexier e Lue, 2006; Zhang et al., 2011). Entre os domínios exclusivos das TERT pode-se citar os domínios funcionais N-Terminal (TEN - *Telomerase Essential N-terminal*) e o domínio de ligação ao RNA da telomerase (TRBD - *Telomerase RNA Binding Domain*), ambos encontrados na região amino-terminal da TERT (Autexier e Lue, 2006), que além de serem exclusivos das telomerases, também são essenciais na interação com ácidos nucleicos (DNA telomérico e o TER) e com proteínas do complexo telomerase (Jacobs et al., 2006).

O domínio transcriptase reversa (RT - *Reverse Transcriptase*), está presente na região mais próxima ao carboxi-terminal, e é similar as transcriptases reversas clássicas em relação a estrutura, estando associado com a catálise enzimática. O domínio RT apresenta alta conservação estrutural contendo todos os motivos específicos das RTs (1, 2 e A-E), compreendidos dentro dos sub-domínios conhecidos como “dedos” (*fingers*) e “palma da mão” (*palm*), no qual o primeiro é responsável pela interação com ácido nucleico e o segundo contém o sítio catalítico da enzima (Hukezalie e Wong, 2013). O domínio CTE (*C-Terminal Extention*) representa o “polegar” (*thumb*) e apesar de ser importante na atividade enzimática, é uma região menos conservada entre os organismos de diferentes espécies, o que sugere que ele possui função espécie-específica (Barbé-Tuana et al., 2021; Hukezalie e Wong, 2013).

A TERT de tripanosomatídeos, apresenta alta similaridade de sequência entre as espécies de *Leishmania* (em torno de 85 a 95%), e quando comparado ao componente TERT de outros organismos pode-se notar que ela apresenta características estruturais conservadas e substituições em resíduos de aminoácidos específicos ao gênero (Giardini et al., 2006). Assim como as TERTs de outros organismos, a de *Leishmania* é capaz de adicionar repetições teloméricas, nesse caso TTAGGG, na extremidade 3' da fita telomérica rica em G (Cano et al., 1999; Giardini et al., 2006; Giardini et al., 2011).

Figura 8. Estrutura primária do componente TERT. Na região amino-terminal estão representados os domínios TEN e TRBD, essenciais na interação da TERT com ácidos nucleicos (DNA e RNA). Na fração carboxi-terminal estão representados os domínios RT e CTE, sendo ambos importantes na atividade enzimática da telomerase. Os motivos conservados presentes em cada domínio (GQ, CP, QFP, T, 1, 2, A, B', C, D E) estão mostrados. Imagem adaptada de Giardini et al. (2014).

1.4.2.2 O componente RNA da telomerase (TER)

1.4.2.2.1 TER em organismos modelos

TER é um RNA longo não codificante que possui a sequência reversa complementar da repetição telomérica utilizada como molde pela TERT durante a síntese de DNA telomérico (Gilson e Géli, 2007). Além de ser importante na montagem do complexo ribonucleoproteico da telomerase, ele também auxilia na processividade da enzima (Sandhu et al., 2013; Zappulla e Cech, 2006). Portanto, mutações no TER podem prejudicar a interação TER-TERT levando ao encurtamento dos telômeros (Lin et al., 2004; Lue, 2004).

Embora os principais elementos da estrutura secundária do TER sejam conservados entre diversas espécies, o tamanho e a composição da sequência variam (Theimer e Feigon, 2006). A sequência primária pode variar de 150 nt em protozoários ciliados, a 450 nt em humanos, 1300 nt em leveduras de brotamento e $\geq$ 2100-2200 nt em *Leishmania* e *Plasmodium* (Blackburn e Collins, 2011; Chen e Greider, 2004; Vasconcelos et al., 2014).

Entre os elementos estruturais conservados pode-se citar o motivo TBE (*Template Boundary Element*) (Fig. 9), presente na porção 5' da molécula (Giardini et al., 2014) que fornece um local com alta afinidade de ligação com o domínio TRBD da TERT (Blackburn e Collins, 2011; Collins, 1999). O TBE também impede que a transcrição reversa pela TERT ocorra além do molde, também presente na porção 5' da molécula, próximo ao motivo TBE (Webb e Zakian, 2016). A região do molde (Fig. 9), na maioria dos organismos, é constituído por uma cópia e meia da sequência reversa da repetição telomérica, complementar a sequência do 3' G-*overhang* usado como substrato pela TERT para a adição de nucleotídeos nos telômeros (Lai et al., 2012). A interação TERT-TER expõe o molde contido no TER, facilitando o pareamento dele com a fita simples rica em G do DNA telomérico (3' G-*overhang*) (Webb e Zakian, 2016). Mutações ou deleções na sequência molde podem afetar a ação da telomerase causando encurtamento dos telômeros, conforme observado em *Saccharomyces cerevisiae* (Singer e Gottschling, 1994).

Outras regiões importantes para a interação TERT-TER são o *pseudoknot* e o STE (*Stem Terminus Element*) (Fig. 9). O *pseudoknot*, caracterizado como tripla hélice dentro do complexo RNP, forma o domínio central envolvido na interação com a TERT, juntamente com o motivo TBE e o molde, estando envolvidos, na montagem do complexo telomerase e sua atividade (Webb e Zakian, 2016; Wu et al., 2017). O STE, também denominado de CR4/CR5 em humanos e TWJ (*three-way junction*) em *S. cerevisiae*, também está relacionado com a interação TERT-TER (Webb e Zakian, 2016).

Ademais, dependendo do organismo, o TER pode se ligar a outras proteínas acessórias importantes para o funcionamento da telomerase *in vivo*, como é o caso da interação do TER (TLC1) com subunidades do heterodímero KU em *Saccharomyces cerevisiae*, que promove a síntese *de novo* de repetições teloméricas nos terminais cromossômicos (Giardini et al., 2014). Em *Tetrahymena thermophila*, a proteína p65, membro da *LARP7 family*, se liga no *stem IV* do componente TER (Fig. 9) auxiliando na sua biogênese, tornando-se fundamental para a montagem do complexo telomerase *in vivo* (Jiang et al., 2013).

Já em seres humanos, o componente TER possui um domínio adicional, o domínio H/ACA box, presente na porção 3' do TER (Fig. 9), o qual contém o motivo CAB que interage com as proteínas acessórias DKC1, GAR1, NOP10 e NHP2 (Barbé-Tuana et al., 2021; Giardini et al., 2014), que auxiliam na montagem do complexo *in vivo*, o qual é então recrutado para os telômeros pela proteína TPP1 (*POT1 interacting protein 1*), integrante do complexo *shelterin*, sendo transportado pela proteína TCAB1 (*Telomere Cajal Body protein 1*) até os telômeros (Barbé-Tuana et al., 2021). Vale ressaltar que o domínio H/ACA box além de estar relacionado com a interação de proteínas acessórias, ele também é importante para a biogênese e estabilidade do TER, além de auxiliar na atividade da telomerase (Barbé-Tuana et al., 2021).

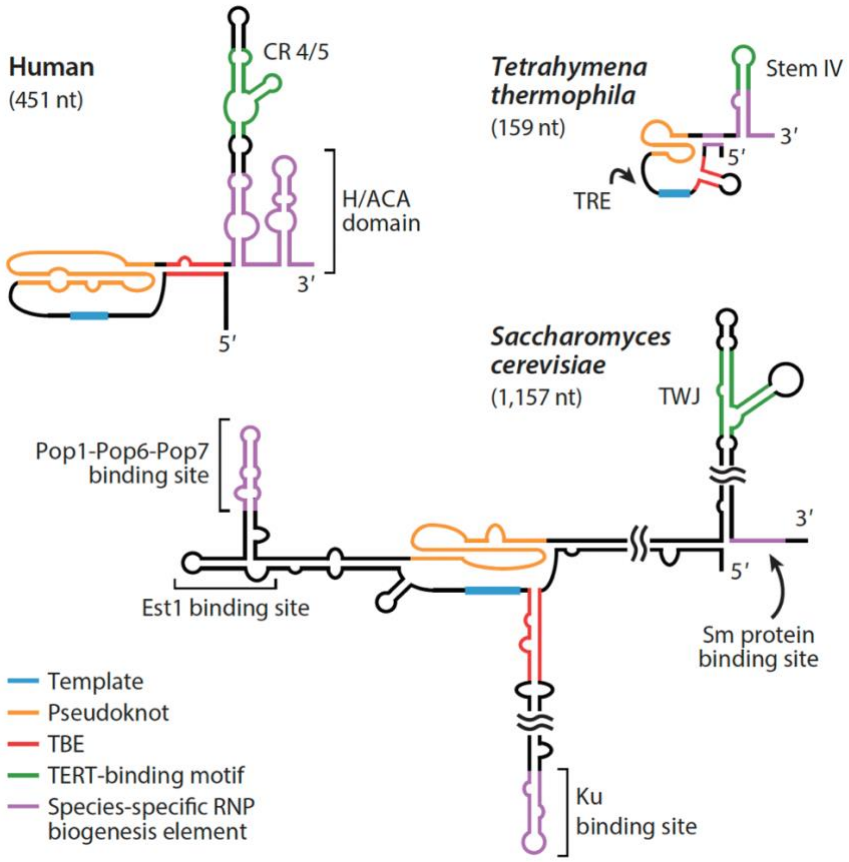

Figura 9. Esquema da estrutura secundaria do TER de humanos, *S. cerevisiae* e *T. thermophila*. Os TERs compartilham estruturas funcionais conservadas como o molde (azul), pseudoknot (laranja), motivo TBE (vermelho) e domínio de ligação à TERT (correspondente a CR 4/5 em *H. sapiens*, Stem IV em *T. thermophila*, e TWJ em *S. cerevisiae*) (verde). Em roxo, pode-se observar os sítios de ligação do TER às proteínas envolvidas na biogênese da telomerase. Imagem extraída de Wu. et al. (2017).

1.4.2.2.2 TER de protozoários

Em *Tetrahymena* o componente TER (159 nt) é transcrito pela RNA polimerase III e possui dois domínios principais: molde/*pseudoknot* e *stem loop* 4 (atuando como STE de ciliados) (Cash e Feigon, 2017; Greider e Blackburn, 1989). A sequência do molde é caracterizada como 5' CAACCCCAA 3' (Greider e Blackburn, 1989). Além disso, os ciliados também possuem o *Template recognition element* (TRE), o qual está localizado na porção 3' do molde, e é utilizado pela TERT para direcionar corretamente a transcrição reversa (Fig. 9) (Cash e Feigon, 2017).

Já no protozoário flagelado *T. brucei*, TER possui ~900 nt (Fig. 9), é processado por *trans-splicing* e poliadenilado. *Tb*TER interage com proteínas centrais do BOX C/D snoRNA e se associa à *methyltransferase-associated protein* (MTAP) (Gupta et al., 2013). O silenciamento ou mesmo nocaute de *Tb*TER, levam ao encurtamento progressivo dos telômeros indicando que o TER é fundamental para o funcionamento da telomerase e consequentemente na manutenção dos telômeros em *T. brucei* (Gupta et al., 2013; Sandhu et al., 2013).

Em *Leishmania major* o componente TER caracterizado pelo nosso grupo de pesquisa (Fig. 10) (Vasconcelos et al., 2014), é codificado por um gene de cópia única, localizado no cromossomo 25. O gene também é transcrito pela RNA polimerase II o que difere dos TERs de ciliados, os quais são transcritos pela RNA polimerase III, como descrito acima (Greider e Blackburn, 1989). Em *Leishmania*, o transcrito gerado tem aproximadamente ~2100 nt, o qual é processado por *trans-splicing*, o que confere a molécula madura um 5' *spliced leader* (SL) *cap*, e uma cauda 3' poli-A comum a maioria dos TER de eucariotos (Barbé-Tuana et al., 2021; Vasconcelos et al., 2014). Segundo análises realizadas por Vasconcelos et al. (2014), a sequência do molde em *Leish*TER é 5' ACCUAACCCUA 3' localizada próximo ao motivo TBE que é altamente conservado entre os eucariotos (Podlevsky e Chen, 2016; Sandhu et al., 2013). Além desses elementos, *Leish*TER também apresenta um BOX C/D snoRNA compartilhado com o TER de outros organismos que indica que a biogênese desse RNA pode ser conservada (Gupta et al., 2013; Vasconcelos et al., 2014). Ademais, em *Leishmania major*, evidenciou-se que *Leish*TER imunoprecipita com a TERT, co-localizando-se tanto com a TERT quanto com os telômeros no núcleo do parasito. (Vasconcelos et al., 2014).

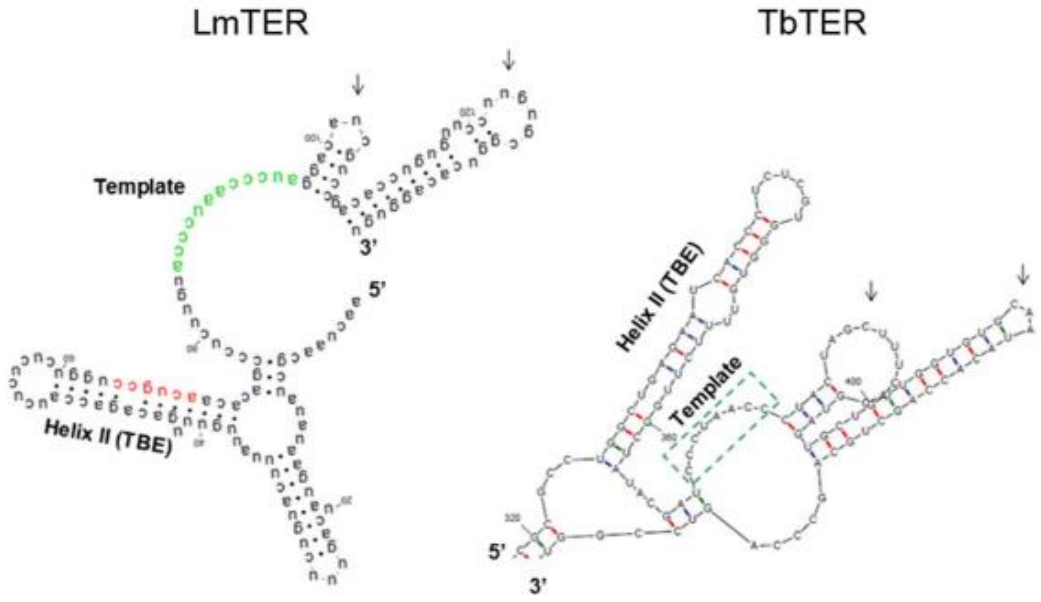

Figura 10. Modelo da estrutura predita para o TER de *L. major* (*Leish*TER) e TER de *T. brucei* (*Tb*TER). Presença da Helix II (TBE) e a sequência do molde (*template*) utilizado pela TERT. As setas indicam as semelhanças entre as estruturas em forma de gancho imediatamente a jusante do modelo em ambos os TERs. Imagem extraída de Vasconcelos et al. (2014).

1.4.2.2.3 Comprometimento da ação do componente RNA da telomerase causa o encurtamento progressivo dos telômeros

Para compreender melhor o funcionamento da telomerase vários estudos foram realizados. Dentre esses estudos, podemos ressaltar aqueles envolvendo o componente RNA da telomerase, como forma de melhor caracterizar sua importância no complexo RNP. Estudos com organismos modelos (*Saccharomyces cerevisiae*, células imortalizadas HeLa e camundongos) e organismos mais próximos evolutivamente de *Leishmania* spp. (*Trypanosoma brucei*) mostraram que a remoção, superexpressão ou o comprometimento da ação do TER causa o encurtamento progressivo dos telômeros. Estes estudos evidenciam que apesar da divergência em sequência e tamanho, TER possui função conservada entre os eucariotos, no que diz respeito à sua importância na formação do complexo telomerase e manutenção dos telômeros (Blasco, 2001; Feng et al., 1995; Sandhu et al., 2013; Singer e Gottschling, 1994).

Além disso, sabe-se que muitas telomeropatias humanas podem estar associadas com mutações no TER, tais como: a) disceratose congênita autossômica dominante que causa leucoplasia em mucosas, pigmentação reticulada da pele e distrofia ungueal; b) anemia aplástica, caracterizada pela supressão da produção de células sanguíneas devido a destruição de células tronco hematopoética e c) fibrose pulmonar idiopática, que causa rigidez dos tecidos pulmonares podendo levar à morte (Armanios e Blackburn, 2012; Barbé-Tuana et al., 2021).

1.5 Caracterização da estrutura secundária de *Leish*TER através de SHAPE-MaP

Uma abordagem para investigar a estrutura secundária de uma molécula de RNA é a técnica denominada SHAPE-MaP (Acilação Seletiva de 2'-Hidroxila analisada por Extensão de Primer e Perfil Mutacional). Essa metodologia fornece esclarecimentos sobre a flexibilidade e reatividade de nucleotídeos individuais na cadeia de RNA, pois as sondas químicas utilizadas reagem com o RNA, induzindo modificações mapeáveis na molécula (STROBEL et al., 2018). Dentre as sondas químicas disponíveis, destaca-se o 2-metilnicotínico imidazolide (NAI), que atua de forma generalista, modificando a espinha dorsal do RNA por meio da acilação do grupo 2'-hidroxila da ribose de nucleotídeos flexíveis (STROBEL et al., 2018).

Considerando que a maior parte dos dados sobre a estrutura de *Leish*TER foi obtida predominantemente por meio de predições de modelagem estrutural *in silico*, torna-se imperativo buscar alternativas para esclarecer as estruturas do domínio central de *Leish*TER e, posteriormente, compará-las com os resultados previamente obtidos. Essas informações não apenas aprimoram nossa compreensão da estrutura molecular, mas também têm o potencial de contribuir para o estudo do complexo telomerase, identificando regiões de interação com outras proteínas do complexo além da TERT.

1.6 Justificativa para a investigação do RNA da Telomerase em *Leishmania*

Apesar da significativa relevância da leishmaniose em âmbito global, ela continua sendo uma doença tropical negligenciada, carecendo de profilaxia e tratamentos eficazes, conforme ressaltado anteriormente (Carregal et al., 2019). Diante desse cenário, torna-se imperativo aprofundar a compreensão da biologia molecular do parasito, visando identificar novos alvos terapêuticos.

A investigação do RNA da telomerase de *Leishmania* é essencial para desvendar os mecanismos moleculares pelos quais o parasito assegura a integridade dos telômeros, sendo esta capacidade importante para a estabilidade genômica. Uma característica do RNA da telomerase é que apesar de possuir uma função conservada, sua sequência e tamanho variam entre as espécies (Theimer e Feigon, 2006), sendo este componente considerado espécie-específico, o que o torna um interessante alvo terapêutico. Desta forma, ao compreender melhor sua função e estrutura, podemos obter percepções valiosas para o desenvolvimento de estratégias terapêuticas específicas contra a leishmaniose.

Em suma, o conhecimento adquirido sobre o RNA da telomerase de *Leishmania* auxiliará na compreensão dos mecanismos moleculares envolvidos na sua biogênese e do complexo ribonucleoproteico da telomerase e no enriquecimento do conhecimento sobre a importância dos telômeros na sobrevida do parasito.

2 Objetivos

2.1 Geral:

- Entender o papel do lncRNA *Leish*TER na maquinaria telomérica, no desenvolvimento e na sobrevida de *L. major*.

2.2 Específicos:

- Os efeitos do nocaute de *Leish*TER serão avaliados realizando-se os seguintes ensaios:

a) Teste de proliferação celular;

b) Análise do perfil do ciclo celular;

c) Teste da capacidade de transformação de formas promastigotas procíclicas em promastigotas metacíclicas e sua capacidade de infecção;

d) Análise de alterações no tamanho dos telômeros e de danos no DNA;

e) Análise ultraestrutural através de microscopia eletrônica de varredura e transmissão;

f) Comparação dos efeitos do nocaute e da superexpressão de *Leish*TER.

2.3 Suplementares:

- Acessar a estrutura secundária de *Leish*TER através da técnica SHAPE-MaP;

- Gerar uma linhagem de *Leishmania major* duplo nocaute para o componente TER e TERT.

3 Materiais, métodos, resultados e discussão: introdução aos capítulos

Materiais, métodos, resultados e discussão estão organizados em capítulos (capítulos 1, 2 e 3).

O capítulo 1, intitulado "The impact of knocking out the *Leishmania major* telomerase RNA (*Leish*TER): from altered cell proliferation to decreased parasite infectivity" descreve os resultados da pesquisa sobre o nocaute e superexpressão de *Leish*TER em *Leishmania major*. O pré-print deste artigo foi publicado no BIORXIV (doi: 10.1101/2023.11.10.566567v1.full) e no momento encontra-se em revisão em jornal com seletiva política editorial.

O capítulo 2, intitulado "Structural assessment of the core domains of *Leishmania major* telomerase RNA (*Leish*TER)", reúne resultados preliminares obtidos da estrutura secundária de *Leish*TER acessada pela técnica SHAPE-MaP, durante estágio BEPE no laboratório do Dr. Kausik Chakrabarti, UNCC, Charlotte, EUA.

O capítulo 3, intitulado "Geração de linhagem de *Leishmania major* duplo nocaute para o TER e para a TERT" detalha a obtenção de uma linhagem duplo nocaute para os genes do TER e da TERT a partir da linhagem nocaute do TER.

Ao final de cada capítulo encontram-se os arquivos suplementares.

As referências citadas ao longo dos capítulos estão presentes no final de cada capítulo, enquanto as referências da seção de Introdução estão apresentadas na seção 5, ao final dessa tese.

3.1 Capítulo 1

The impact of knocking out the *Leishmania major* telomerase RNA (*Leish*TER): from altered cell proliferation to decreased parasite infectivity

Beatriz Cristina Dias de Oliveira[1], Mark Ewusi Shiburah[1], Luiz Henrique de Castro Assis[1], Veronica Silva Fontes[1], Pedro Henrique Gallo-Francisco[2], Selma Giorgio[2], Marcos Meuser Batista[3], Maria Nazaré Correia Soeiro[3], Rubem Figueiredo Sadok Menna-Barreto[3], Juliana Ide Aoki[2], Adriano Cappellazzo Coelho[2], Maria Isabel Nogueira Cano[1,*]

[1]Department of Chemical and Biological Sciences, Biosciences Institute, São Paulo State University (UNESP), Botucatu, SP, Brazil

[2]Department of Animal Biology, Biology Institute, University of Campinas (UNICAMP), Campinas, SP, Brazil

[3]Cellular Biology Laboratory, Oswaldo Cruz Institute, Oswaldo Cruz Foundation, Rio de Janeiro, RJ, Brazil

[*] Corresponding author

E-mail: maria.in.cano@unesp.br (MINC)

Abstract

The telomerase RNA, TER, is an intrinsic component of the telomerase ribonucleoprotein complex. It contains the telomere template sequence copied by the enzyme during telomere elongation. This unique molecule shows divergent nucleotide sequences but a more conserved secondary structure containing domains involved with telomerase assembly and biogenesis. The present work aims to characterize the biological roles played by the *Leishmania* TER component (*Leish*TER) in parasite homeostasis. We generated double knockout (*Lm*TER$^{-/-}$) parasites, which showed a distinct growth pattern at early passages, characterized by lower density and an extended stationary phase compared to the control. Although this pattern normalized after multiple in vitro passages, ablation of *Leish*TER affected cell division and proliferation, with cells arrested at the G0/G1 phase. Progressive telomere shortening was also observed during continuous passages, along with a reduction in the expression of TERRA29. Complementation with the episomal expression of *Leish*TER did not restore telomere length to the control levels, corroborating preliminary results showing that the overexpression of TER has a dominant negative effect on parasite lifespan. *Lm*TER$^{-/-}$ also presented a higher percentage of gamma-H2A phosphorylation, likely due to stalled replication forks since no DNA damage was observed. Also, no plasma membrane modifications were detected, but pro-survival autophagic signals were present. Intriguingly, *Lm*TER$^{-/-}$ retained the ability to transform into metacyclic forms, although its in vitro infectivity and growth inside the host cell were compromised. Together, these results highlight the importance of TER in parasite lifespan and open a discussion about its potential as a therapeutic target against *Leishmania*.

Author summary

In our study we investigate the telomerase RNA (TER), a key component in the complex responsible for extending telomeres, the protective ends of our DNA. The research focuses on disrupting TER from *Leishmania major* (*Leish*TER), a parasite responsible for causing diseases known as leishmaniases, for which there is currently no effective treatment or prophylaxis available. The modified parasites absent for *Leish*TER (*Lm*TER$^{-/-}$) initially exhibited slower growth compared to control, but this profile eventually reversed after multiple generations. *Leish*TER's absence disrupted cell division, causing cells to get stuck in a particular growth phase. Moreover, *Lm*TER$^{-/-}$ parasites experienced telomere shortening during continued growth and decreased expression of TERRA29. Attempts to reintroduce *Leish*TER failed to completely restore telomere length, suggesting that an excess of TER may have an adverse effect. Notably,

although *Lm*TER$^{-/-}$ parasites exhibited signs of replication stress, no DNA damage was detected, and the cell membrane remained unaltered. Intriguingly, they retained the capacity to transform into the infective form but demonstrated reduced infectivity and growth in host cells. This highlights the crucial role of TER in the lifespan of the parasite and raises discussions regarding its potential as a promising therapeutic target against *Leishmania*.

Introduction

Leishmania spp. are unicellular eukaryotic organisms classified within the Kinetoplastida class and Trypanosomatidae family [1,2]. They present three main morphologically distinct stages of development. The procyclic promastigotes reside extracellularly in the digestive tract of insect vectors (Lutzomya or Phlebotomus species). They are highly proliferative, featuring elongated bodies and flagella that help them migrate in the insect digestive tract. At the proboscis, they transform into metacyclic promastigotes, the infective forms transmitted to mammalian hosts during the insect's blood meal [2,3]. Metacyclic promastigotes have slender bodies with elongated flagella but are non-proliferative. After inoculating into the mammalian host, they are phagocytosed by neutrophils or macrophages. Inside the parasitophorous vacuoles, they further transform into amastigotes, characterized by rounded, highly proliferative cells with no apparent flagella [1,2,3,4]. The parasite's ability to differentiate is primarily due to alterations in gene expression determined by environmental changes, such as pH and temperature [5].

Several *Leishmania* species cause various forms of leishmaniases [6], characterized by diverse clinical manifestations (cutaneous, diffuse cutaneous, mucocutaneous, and visceral) with varying severity and epidemiological characteristics [6,7]. Despite their global distribution, these diseases are neglected, lacking effective treatments, human vaccines, and robust transmission control methods [8]. Understanding the molecular biology of these parasites is crucial for identifying new therapeutic targets to combat the diseases they cause.

Telomeres, important for genome stability and integrity, are potential candidates for drug development [9]. They are nucleoprotein structures located at the ends of linear chromosomes in eukaryotes [10]. They avoid chromosome end degradation, recombination, and fusion and a local DNA damage response that would recognize them as DNA double-strand breaks [11]. Telomeres consist of tandemly repeated DNA sequences and exhibit a G-rich strand that extends beyond the complementary C-rich strand, forming a 3' G-overhang [11,12].

In vertebrates and trypanosomatids, including *Leishmania*, the telomeres comprise 5' TTAGGG 3' repeated sequences [13,14,15].

In most eukaryotes, telomeres are maintained by telomerase, a ribonucleoprotein complex comprising two essential subunits: telomerase reverse transcriptase (TERT), which adds telomeric repeats at the 3' G-overhangs, and Telomerase RNA (TER), a non-coding RNA that contains a template sequence used by TERT during *de novo* telomere synthesis [16,17]. TERT is highly conserved among different organisms, whereas TER is organism-specific, playing a crucial role in assembling the telomerase ribonucleoprotein complex [16,18,19,20].

TER has conserved regions, including the template sequence used by TERT and the Template Boundary Element (TBE), which prevents reverse transcription beyond the template. TBE also interacts with the TERT RNA Binding domain [21,22,23,24,25,26]. The 3' portion of TER acts in telomerase assembly and repeat addition processivity [18,21]. In addition, it contains the pseudoknot and the Stem Terminus Element (STE) (called CR4/CR5 in humans and Helix IV in trypanosomatids) [27,28]. In some organisms, TER may contain additional domains, such as the H/ACA box in mammals and the C/D box in flagellates like trypanosomatids [13,29,30].

While the secondary structure of TER is conserved across species, the primary sequence's size and composition vary. Despite these differences, TER has a conserved function in forming the telomerase complex and maintaining telomeres. Studies in model organisms and organisms closely related to *Leishmania* have shown that the removal or depletion of TER can lead to progressive telomere shortening, which is detrimental to cell homeostasis [25,31,32,33].

Here, we show that the knockout of both *Leish*TER alleles (*Lm*TER$^{-/-}$) induced alterations in cell proliferation, partial G0/G1 cell cycle arrest, phosphorylation of histone γH2A, progressive telomeres shortening, and reduced expression of TERRA29. No significant morphological changes were observed in *Lm*TER$^{-/-}$ cells, although they showed signals of an autophagic process with neither DNA fragmentation nor plasma membrane modifications. Despite presenting these molecular and cellular defects, *Lm*TER$^{-/-}$ cells could still differentiate into metacyclic promastigotes, although impairment in infectivity compared to the parental strain was found. In addition, the overexpression of *Leish*TER also caused a dominant negative effect in *L. major*, arguing in favor of TER being important for the parasite’s homeostasis and survival.

Results

Generation of *Leish*TER double knockout (*Lm*TER$^{-/-}$) was successfully achieved

Given the importance of telomerase in telomere elongation, our objective was to establish a lineage of *L. major* knockout for the TER component to investigate its impact on parasite survival. Initially, we generated a *L. major* cell lineage that episomally expresses the pTB007 plasmid (*Lm*007), encompassing the Cas9 endonuclease, T7 RNA polymerase, and the hygromycin resistance gene [34]. The *Lm*007 population was cloned by plating selection, and one clone was chosen based on Cas9 expression by Western blot (S1A Fig) and a thorough assessment of its growth pattern and cell cycle progression when compared to the wild-type parasites (*Lm*WT) (S1B-C Figs). Then, *Lm*007 was used as the genetic background lineage to proceed with the experiments to obtain the knockout of the two *Leish*TER alleles (*Lm*TER$^{-/-}$) and as a control for comparative analysis with *Lm*TER$^{-/-}$.

In the *Lm*TER$^{-/-}$ lineages, both alleles of *Leish*TER were deleted and replaced by a donor template encoding the neomycin resistance gene, as detailed in S1E Fig.

PCR, RT-PCR, Southern blot, and Sanger sequencing were performed and confirmed the successful deletion of the two alleles of the *LeishTER* gene and its replacement by the neomycin resistance gene in the *LeishTER*-specific locus, showing that *Leish*TER knockout is not lethal to the parasites (S1D-E and S2A-D Figs, S1 Table).

Knockout of *Leish*TER induces growth defects and arrest in the G0/G1 phase, mainly at early passages

Growth curves and proliferation assays were conducted to check if the ablation of *Leish*TER could affect the parasite development. At early passage (P5), *Lm*TER$^{-/-}$ showed a different growth pattern than *Lm*007 in both exponential and stationary phases. At the exponential phase, the density of parasites per mL was lower than the control (Fig 1A – left panel). Despite *Lm*TER$^{-/-}$ entering the stationary phase simultaneously with *Lm*007 (day 4), it remained longer than *Lm*007. The number of parasites was unaltered until day 12 but progressively declined (Fig 1A – left panel). Interestingly, during the continuous *in vitro* passages, *Lm*TER$^{-/-}$ growth returned to a profile similar to *Lm*007. Growth curves of parasites at P50 (Fig 1A – right panel) showed that *Lm*TER$^{-/-}$ promastigotes presented a similar growth profile to the parental strain *Lm*007 in exponential and stationary phases. Only on day six a significant difference at P50 was observed, and the density of control parasites decayed faster than the *Lm*TER$^{-/-}$ (Fig 1A – right panel).

To explain the above results, we conducted a more sensitive proliferation assay employing Carboxyfluorescein succinimidyl ester (CFSE), which is a permeable fluorescent dye incorporated by cells and subsequently distributed among daughter cells [35], serving as a valuable tool for tracking and monitoring cell division [36]. As shown, *Lm*TER$^{-/-}$ presented a significant reduction in CFSE fluorescence emission compared to *Lm*007, independent of which passage (P5 and P50) the parasites were analyzed. This result indicates that *Lm*TER$^{-/-}$ had a decrease in proliferation compared to the control (Fig 1B). Briefly, *Lm*TER$^{-/-}$ parasites from P5 were collected 7 h after adding CFSE in the culture, exhibiting a fluorescence emission of approximately 75 %, whereas *Lm*007 showed ~45 % fluorescence under the same conditions. After 14 h, *Lm*TER$^{-/-}$ displayed roughly 45 % fluorescence, compared to approximately 35 % in *Lm*007. This discrepancy normalized after 21-28 h (Fig 1B – left panel). At P50, *Lm*TER$^{-/-}$ continued exhibiting higher fluorescence emission than *Lm*007 after 14 h. However, despite the statistically significant difference (p<0.05), the fluorescence emissions of both *Lm*TER$^{-/-}$ and *Lm*007 became more similar, ranging from ~40 % (*Lm*TER$^{-/-}$) to around 36% (*Lm*007) at 14 h, 28% (*Lm*TER$^{-/-}$) to 23% (*Lm*007) at 21 h, and approximately 18% (*Lm*TER$^{-/-}$) to about 12% (*Lm*007) at 28 h (Fig 1B – right panel). These results suggest that the absence of *Leish*TER impacts *L. major* promastigote cell division, with the disparity being most noticeable in *Lm*TER$^{-/-}$ of early passages.

Further, we analyzed the cell cycle progression of non-synchronized *Lm*TER$^{-/-}$ and *Lm*007 cultures in the exponential and stationary growth phases at P5 and P50. Independently of the passage analyzed, *Lm*TER$^{-/-}$ and *Lm*007 in the exponential phase showed a similar cell cycle profile (Fig 1C – left panel). However, in the stationary phase, a statistically significant arrest at the G0/G1 phase was observed in *Lm*TER$^{-/-}$ at both passages (Fig 1C – right panel). Likely, more *Lm*TER$^{-/-}$ cells were not committed to divide compared to *Lm*007. Similar results are shown in Figs 1A-B (left panels), where *Lm*007 exhibited a higher proliferation rate than *Lm*TER$^{-/-}$.

Cells were further incubated with EdU (5-ethynyl-2'-deoxyuridine) to monitor DNA replication. The results depicted in Fig 1D reveal that EdU incorporation is approximately 8% lower in *Lm*TER$^{-/-}$ cells at P5 (exponential phase) compared to *Lm*007. However, this difference was not statistically significant (p=0.07), aligning with the outcomes of the cell cycle analysis, indicating no disparity between *Lm*TER$^{-/-}$ and *Lm*007 in the S phase at both P5 and P50 (Fig 1C).

Altogether, the results suggest that the absence of *Leish*TER has a mild impact on promastigotes growth and cell cycle progression.

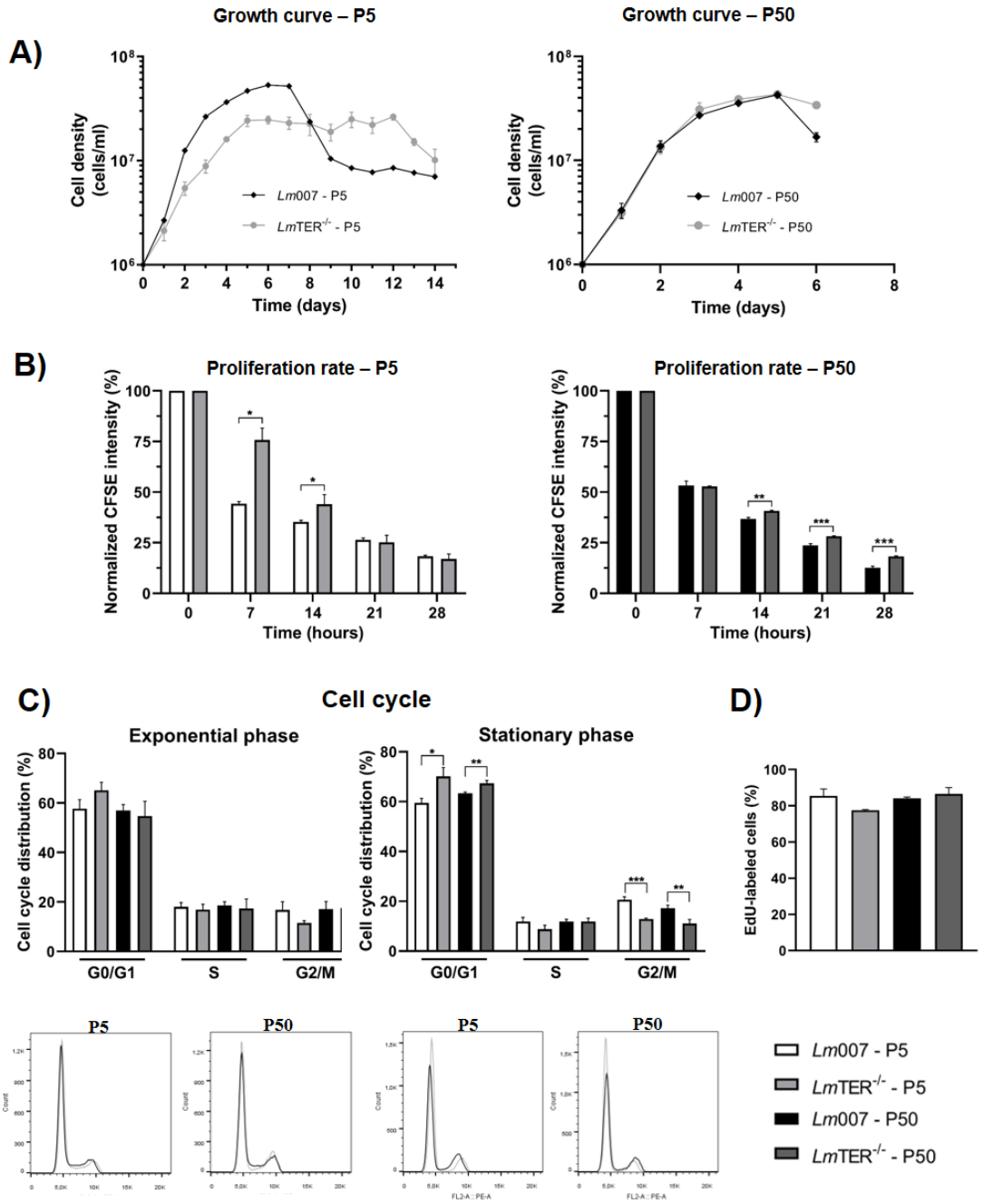

Fig 1. Knockout of *Leish*TER induces growth defects and arrest in the G0/G1 phase, mainly at early passages. A) Growth curves of *Lm*TER$^{-/-}$ and *Lm*007 procyclic promastigotes at P5 (left panel) and 50 (right panel). B) CFSE labeling was used to assess the proliferation rate of *Lm*TER$^{-/-}$ and *Lm*007 at P5 (left panel) and P50 (right panel). C) Cell cycle analysis of *Lm*TER$^{-/-}$ and *Lm*007 in the exponential growth phase (bar graph and histograms - left panel) and stationary growth phase (bar graph and histograms - right panel) collected at P5 and P50 are depicted. D) EdU labeling was performed with *Lm*TER$^{-/-}$ and *Lm*007 in the exponential growth phase collected at P5 and P50. All data are presented as mean ± standard deviation (S.D.) of three replicates. Statistical analysis was conducted using the student t-test with Welch's correction when necessary. *$p \leq 0.05$, **$p \leq 0.01$, ***$p \leq 0.001$.

Ablation of *Leish*TER causes progressive telomere shortening in *Lm*TER$^{-/-}$ during continuous in vitro passages

Telomeres play a crucial role in maintaining genome stability, and it is well-established that in numerous organisms devoid of telomerase activity, telomeres tend to undergo shortening. Therefore, we initially performed a Southern blot analysis using genomic DNA from *Lm*TER$^{-/-}$ and *Lm*007 digested with *Rsa*I and hybridized with a DIG-labeled TelC probe. It is worth reminding that in a regular telomeric Southern blot, *L. major* terminal restriction fragments appear as hybridized bands greater than 3,000 bp due to the presence of high levels of base J (β-D-glucosyl-hydroxymethyl uracil). Base J acts as an epigenetic marker, preventing DNA cleavage by restriction enzymes [37,38, 39]. Fig 2A illustrates a progressive telomere shortening of about 1.0 kb in *Lm*TER$^{-/-}$ cells after 50 continuous in vitro passages (P5>P25>P50). The hybridization signals in *Rsa*I telomere-containing fragments decreased in size, ranging from ~3.6 - 8.5 kb in P5 to ~3.0 - 8.3 kb in P25 and ~2.5 - 8.1 kb in P50. Conversely, in *Lm*007, even after 50 consecutive in vitro passages, the *Rsa*I telomere-containing fragments remained unaltered, with a size range of approximately 3.6 to 8.5 kb (Fig 2A).

To perform a more accurate and quantitative analysis of the *Lm*TER$^{-/-}$ telomere length profile, we standardized a modification of the telomeric Flow-FISH assay [40,41]. As the negative control, we used the natural fluorescence of the parasite (depicted in Fig 2B in dark red) and the fluorescence of the PNA FITC-labeled telomeric DNA oligo probe (depicted in Fig 2B in black for *Lm*007 and gray for *Lm*TER$^{-/-}$) was used to generate the histograms. Fig 2B shows that the mean fluorescence is directly proportional to the telomere length in both *Lm*007 and *Lm*TER$^{-/-}$ cells. The distance between the observed peaks represents the difference between telomere length in the two populations analyzed (parasites collected in P5, Fig 2B - left panel, and P50, Fig 2B – right panel). The shift towards the left in the histograms of *Lm*TER$^{-/-}$ indicates a reduction in the emitted fluorescence, which is more pronounced in *Lm*TER$^{-/-}$ at P50 (Fig 2B – right panel). The progressive decrease in the emitted fluorescence observed in *Lm*TER$^{-/-}$ strongly suggests a gradual reduction in telomere length. To validate this, we calculated the molecules of equivalent soluble fluorochrome fluorescence (MESF) value and the proportional change between *Lm*007 and *Lm*TER$^{-/-}$ (S2 Table) and plotted the results in a bar graph (Fig 2B - lower right graph). The graph highlights the gradual decrease in *Lm*TER$^{-/-}$ telomere from P5 to P50, compared to *Lm*007.

For a more comprehensive visualization of telomere shortening, we also conducted an *in-situ* telomeric hybridization (telomeric FISH) using a PNA FITC-labeled telomeric probe (Dako). Fig 2C shows a representative analysis of about 100 cells/field. We observed that *Lm*TER$^{-/-}$ (P5) 's telomeric signal appears more dispersed than the well-defined telomere clusters in *Lm*007. At P50 (Fig 2D), the telomeric signal in *Lm*TER$^{-/-}$ becomes exceedingly faint, whereas in *Lm*007, the telomeric signal remains unaltered (Figs 2C-D).

Collectively, these findings undeniably indicate that the absence of *Leish*TER leads to a gradual loss of parasite telomeres with increased cell duplications (P50<P5).

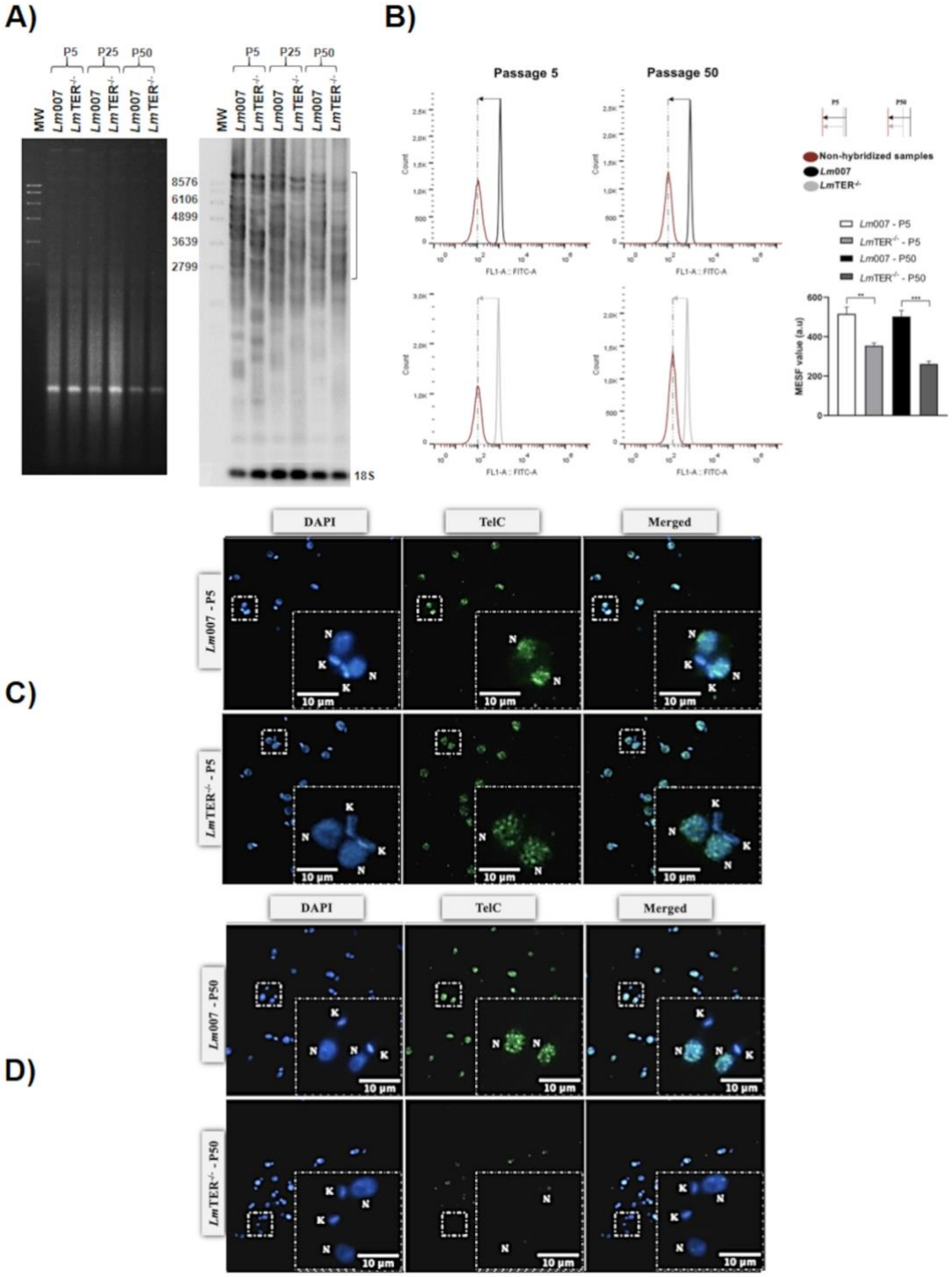

Fig 2. Ablation of *Leish*TER causes telomere shortening in *Lm*TER$^{-/-}$ during continuous in vitro passages. A) Southern blot of *Rsa*I-digested genomic DNAs from *Lm*TER$^{-/-}$ and *Lm*007 promastigotes at P5, P25, and P50, hybridized with a DIG-labeled telomeric probe (5′-TTAGGG3-3′) and a DIG-labeled 18S rRNA probe (334 bp) as the loading control. MW = DNA Molecular Weight Marker VII DIG-labeled (Roche). B) Telomeric Flow-FISH analysis of *Lm*TER$^{-/-}$ and *Lm*007 promastigotes at P5 and P50 was done using a PNA FITC-labeled telomeric DNA oligo probe $(CCCTAA)_3$ (Panagene). The histograms represent the mean fluorescence of non-hybridized parasites (in dark red), and parasites hybridized with the telomeric probe (*Lm*007 in black and *Lm*TER$^{-/-}$ in gray). Vertical lines mark the difference between peaks, and horizontal lines with arrows represent telomere length differences in the populations analyzed. The amount of fluorescence among samples was calculated using MESF, and the mean ± S.D. of technical triplicate was plotted in a graph (inferior panel - left), $*p \leq 0.05$, $***p \leq 0.001$. C) and D) Telomeric FISH of *Lm*007 and *Lm*TER$^{-/-}$ promastigotes at P5 and P50, respectively, hybridized with a PNA FITC-

labeled telomeric DNA oligo probe $(CCCTAA)_3$ (PANAGENE). The DNA in the nucleus (N) and kinetoplast (K) was counterstained, and the slides were mounted using VECTASHIELD® Antifade Mounting Medium with DAPI (Vector). Merged images were captured using the Nikon 80i fluorescence microscope and NIS elements software (v. Ar 3.10)—bars: 10 µm.

Lower expression of TERRA29 was observed in *Lm*TER$^{-/-}$ at P50

TERRA expression is known to be directly influenced by the length of the telomeres [42,43]. Hence, we investigate the potential impact of telomere shortening in the expression of TERRA from Chr29 (right arm) since it is consistently expressed in all developmental forms of the parasite [38]. RPN8 was used as the reference gene for normalizing the expression levels of TERRA29 [38].

Surprisingly, a reduction in TERRA29-R expression was observed in *Lm*TER$^{-/-}$ cells at P50 compared to *Lm*007 (Fig 3), in disagreement with what is commonly observed in model organisms where telomere shortening induces the upregulation of TERRA expression [42,43]. In the face of this result, we intend to analyze the expression of other TERRAs to verify if the downregulation is restricted to Chr29 (right arm) or is a parasite-specific feature.

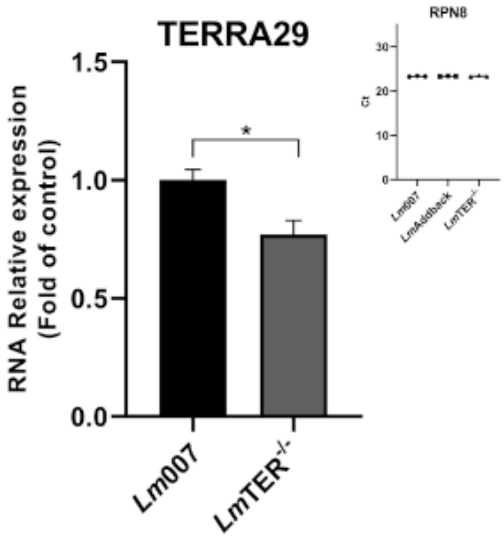

Fig 3. Lower expression of TERRA29 was observed in *Lm*TER$^{-/-}$ at P50. RT-qPCR was used to estimate TERRA29 expression in *Lm*007 and *Lm*TER$^{-/-}$ promastigotes. The expression of TERRA29 was normalized to the reference gene RPN8. $p \leq 0.05$.

The addback of *Leish*TER has a dominant negative effect and did not restore the telomere length to the *Lm*007 level

We conducted a complementation assay by the episomal expression of *Leish*TER in the knockout lineage, generating *Lm*Addback. PCR was performed to confirm the transfection

success (Fig 4A). The restoration of *Leish*TER expression was assessed by RT-qPCR, showing high levels of *Leish*TER in *Lm*Addback, which was about 10X higher than *Lm*007 (Fig 4B).

Subsequently, parasites were grown until they reached P50 and a telomeric Southern blot was performed (Fig 4C). Curiously, the telomere length was not restored in *Lm*AddBack since the telomeric restriction profile was very similar to the *Lm*TER$^{-/-}$ cells. Given that, we suspected that the overexpression of *Leish*TER would have a dominant negative effect on the parasite's telomere length.

To test this hypothesis, we constructed *Lm*pXTER cells that overexpress *Leish*TER. A lineage carrying the empty pX63Neo plasmid (*Lm*pXØ) was also used as a control for the experiments. The success of the transfection was confirmed via PCR for both *Lm*pXØ and *Lm*pXTER (see S3A and B Figs). The expression of *Leish*TER was assessed through RT-qPCR, as depicted in Fig S3C, revealing that *Lm*pXTER clones expressed approximately four times more *Leish*TER than *Lm*pXØ. Upon characterization, *Lm*pXTER displayed a phenotype similar to that observed in *Lm*TER$^{-/-}$ cells. This included alterations in the growth profiles, exhibiting lower cell density and an extended stationary phase compared to *Lm*pXØ at P5 (S3D Fig – left panel). These growth profiles were restored at P25 (S3D Fig – right panel). Regarding the cell cycle, *Lm*pXTER clones also exhibited a partial arrest at the G0/G1 phase, primarily observed at P5 (S3E Fig). Telomere shortening was observed in *Lm*pXTER, being more pronounced in clone *Lm*pXTER3 (S3F Fig; see S2 Table), in agreement with the above results.

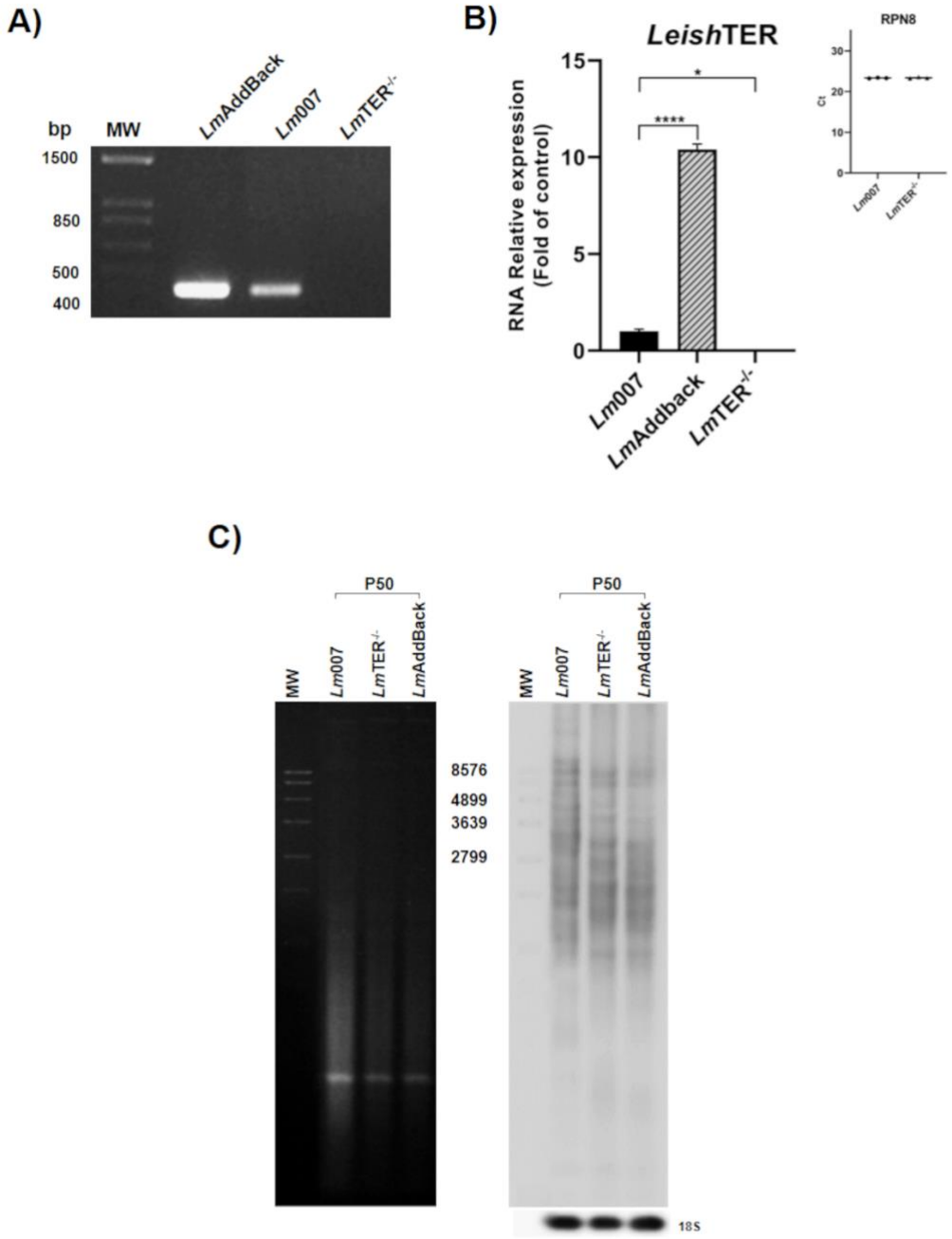

Fig 4. The addback of *Leish*TER has a dominant negative effect and did not restore the telomere length to the *Lm*007 level. A) PCR using genomic DNA from *Lm*TER$^{-/-}$, *Lm*AddBack, and *Lm*007 and a specific primer set (S1 Table) to check the presence of *Leish*TER. The PCR products were separated using a 1% agarose gel stained with ethidium bromide. MW – Molecular weight 1Kb Plus DNA ladder (Invitrogen). B) To assess the expression of *Leish*TER in *Lm*007 and *Lm*AddBack, RT-qPCR was performed, with *Lm*TER$^{-/-}$ RNA serving as the negative control. The inset displays the Ct values of RPN8, which was used as the reference gene. ***$p \leq 0.001$, ****$p \leq 0.0001$. C) Southern blot analysis of *Rsa*I-digested genomic DNAs extracted from *Lm*007, *Lm*TER$^{-/-}$, and *Lm*AddBack at P50 was hybridized with a DIG-labeled telomeric probe (5′-TTAGGG-3′)$_3$ and a DIG-labeled 18S rRNA probe (334 bp) as the loading control. MW = DNA Molecular Weight Marker VII DIG-labeled (Roche).

Phosphorylation of histone γH2A is higher in *Lm*TER$^{-/-}$without presenting DNA damage or apoptosis

We investigate whether telomere loss in *Lm*TER$^{-/-}$, like in model eukaryotes, would lead to the phosphorylation of H2A [44]. Immunofluorescence assays were done using *Lm*TER$^{-/-}$ and *Lm*007 procyclic promastigotes from P5 and P50, employing a specific anti-γH2A serum (Fig 5A). As the positive control, *Lm*007 was treated for 24 h with 10 µg/ml of phleomycin, a DNA-damage agent that induces DNA double-strand breaks [45,46,47]. Fig 5A demonstrates that γH2A was primarily detected in the nucleus of *Lm*TER$^{-/-}$ cells from P50 (~11%) and in the positive control (*Lm*007 treated with phleomycin) (~47%). The bar graph in Fig 5A quantitatively represents these findings, suggesting that telomere loss in *Lm*TER$^{-/-}$ cells can initiate phosphorylation of histone γH2A in *L. major* promastigotes just after a few population duplications, and increase after continuous in vitro passaging.

We used the TUNEL assay to check if *Lm*TER$^{-/-}$ cells present DNA fragmentation characteristic of cells entering apoptosis [48]. This experiment involved parasites in the exponential growth phase at P5 and P50. As shown in Fig 5B, *Lm*007 exhibits a higher TUNEL-positive signal than *Lm*TER$^{-/-}$. However, the percentage of *Lm*007 cells with DNA fragmentation was low (less than 10%), suggesting a non-representative condition within the cellular population [49] (Fig 5B) and that the absence of *Leish*TER did not induce DNA damage. Besides, we checked for possible plasma membrane modifications that would signal cells entering apoptosis [50]. We assessed the integrity of the *Lm*TER$^{-/-}$ plasma membrane using the AnnexinV/PI assay. The results in Fig 5C indicate that approximately 1.5% of cells from both *Lm*007 and *Lm*TER$^{-/-}$ are positive for Annexin V (Fig 5C – Q2 and Q3), with less than 0.5% showing positive PI staining, which is indicative of necrotic cells (Fig 5C – Q1). The results suggest that *Lm*TER$^{-/-}$ does not undergo apoptosis and maintains the integrity of the plasma membrane. Therefore, it is more likely that the increased γH2A phosphorylation shown in Fig. 5A is signaling a DNA replication stress process in *Lm*TER$^{-/-}$ [51].

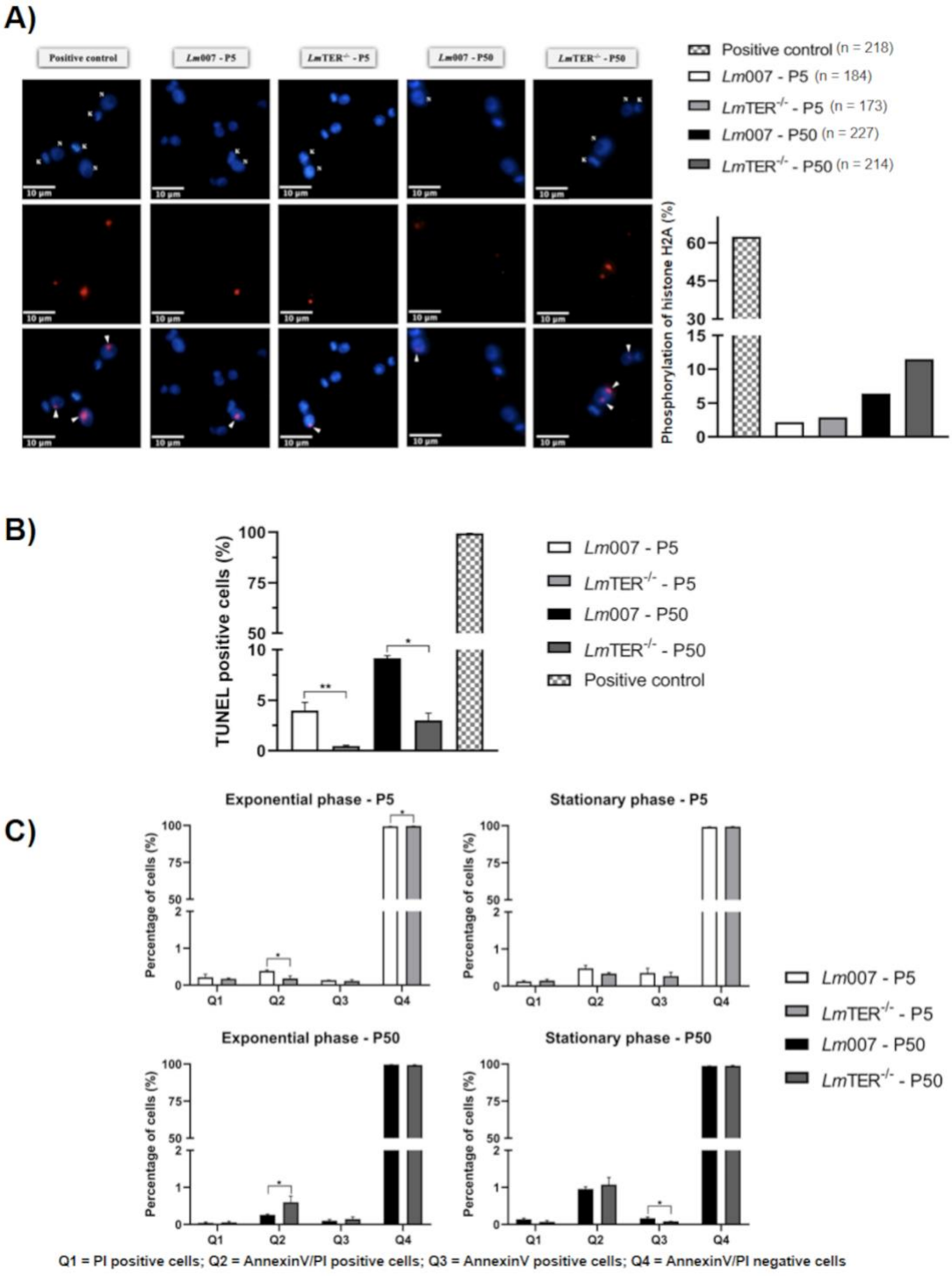

Fig 5. *Lm*TER$^{-/-}$ shows higher phosphorylation of histone γH2A, although no other DNA damage or apoptosis signal was detected. A) Immunofluorescence assay was performed using *Lm*TER$^{-/-}$ and *Lm*007 promastigotes at P5 and P50 and a specific anti-γH2A serum. As a positive control, *Lm*007 was treated with 10 μg/ml phleomycin for 24 h (hatched bar). The nucleus (N) and kinetoplast (K) were counterstained, and the slides were mounted using VECTASHIELD® Antifade Mounting Medium with DAPI. Merged images were captured using the Nikon 80i fluorescence microscope and NIS elements software (v. Ar 3.10) - scale bar: 10 μm. B) TUNEL assay was performed using *Lm*007 (white) and *Lm*TER$^{-/-}$ (light gray) promastigotes at P5 and P50 (black and dark gray, respectively) to detect DNA fragmentation. DNaseI-treated *Lm*007 (hatched bar) served as a positive control. C) AnnexinV/PI assay was conducted on *Lm*TER$^{-/-}$ and *Lm*007 promastigotes to assess plasma membrane integrity during the exponential and stationary phases at P5 (upper panel) and P50 (lower panel). All

data are presented as mean ± SD and represent triplicate experiments. Statistical analysis was performed using the student t-test, with Welch's correction applied when necessary. *$p \leq 0.05$, **$p \leq 0.01$.

*Lm*TER$^{-/-}$ exhibits intracellular alterations typical of an autophagic process

To further investigate potential cellular changes induced by *Leish*TER knockout, we conducted SEM and TEM analyses on *Lm*TER$^{-/-}$, as illustrated in Fig 6. Our observations reveal that, in comparison to *Lm*WT promastigotes (Fig 6A), no alteration in the *Lm*TER$^{-/-}$ morphology could be noticed by SEM (Figs 6C and E). All samples exhibited typical features, such as elongated bodies and free flagella. Moreover, rounded and intermediate-shaped promastigotes were observed in all groups alongside actively dividing cells (Figs 6A, C, and E).

When evaluated via TEM, the most prevalent alteration observed in *Lm*TER$^{-/-}$ cells were intense intracellular vacuolization, formation of autophagosomes, the occurrence of plasma membrane blebs and shedding at the flagella and flagellar pocket regions besides the presence of concentric membrane structures in the cytoplasm and inside the parasite mitochondrion (Figs 6D and F). These findings strongly suggest the occurrence of an autophagic process that demands further investigation. Conversely, no parasite microtubules, nuclei, or kDNA alterations were observed in *Lm*WT and *LmTER*$^{-/-}$ promastigotes (Figs 6B, D, and F).

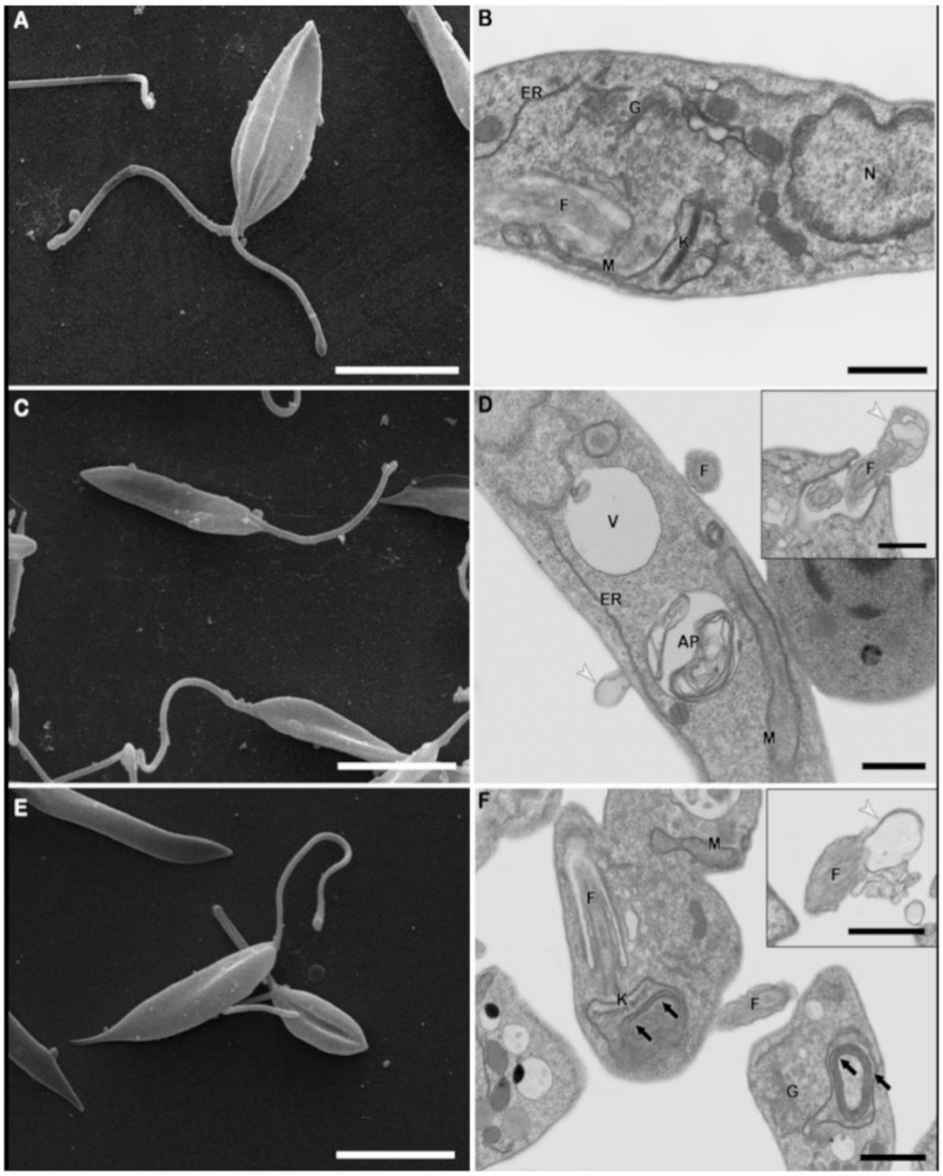

Fig 6. *Lm*TER$^{-/-}$ exhibits intracellular alterations that indicate an autophagic process. SEM and TEM analyses were conducted on wild-type (A, B) and *Lm*TER$^{-/-}$ promastigotes (C, D, E, F) at P5 (A, B, C, D) and P50 (E, F). TEM images show the nucleus (N), mitochondrion (M), kinetoplast (K), Golgi (G), endoplasmic reticulum (ER), flagellum (F), vacuole (V), autophagosomes (AP), blebs in the plasma membrane, flagella, and flagellar pocket membranes (indicated by white arrowheads) and concentric membranes within mitochondria (indicated by black arrows). Scale bars: A, C, and E: 5 μm, while B, D, and F: 1 μm.

*Lm*TER$^{-/-}$ retains the ability to transform into metacyclic form, but its in vitro infectivity index is compromised

*Lm*TER$^{-/-}$ and *Lm*007 promastigotes cultures in the stationary growth phase were subject to agglutination using peanut lectin (PNA) to select the metacyclic forms. Upon selection, a similar agglutination pattern was observed for both *Lm*007 and *Lm*TER$^{-/-}$. The non-agglutinated metacyclic forms accounted for approximately 7-8 % of the cells (data not shown), indicating that the absence of *Leish*TER does not perturb the composition of the procyclic promastigotes

plasma membrane. In contrast, parasites depleted to the TERT telomerase component present notable alterations in the procyclics plasma membrane, avoiding the parasite's transformation into metacyclics (Shiburah & Cano, personal communication).

Subsequently, we assessed the in vitro infectivity capacity of *Lm*TER$^{-/-}$ and *Lm*007 (P5 and P50), and *Lm*AddBack (P50) on Balb/c bone marrow-derived macrophages (BMDM) at 24 and 48 h. We chose BMDM because they show higher infection rates in vitro than other cell lines, such as THP-1 and J774.A and are better suited for observing and quantifying intracellular amastigotes [52]. Fig 7A is a representation of the in vitro infectivity assays that we performed. The graph in Fig 7B and S3 Table show that at 24 h, 30% of macrophages were infected with *Lm*007. About 18% were infected with *Lm*TER$^{-/-}$, both at P5, whereas with parasites at P50, there was no significant difference ($p > 0.05$) among *Lm*007 (32%), *Lm*TER$^{-/-}$ (28%) and *Lm*Addback (36%). Furthermore, at 48 h, the percentage of macrophages infected with *Lm*007 and *Lm*TER$^{-/-}$ at P5 increased to 69% and ~28%, respectively. Additionally, at P50, 59% were *Lm*007-infected macrophages, and 51% and 44% were infected with *Lm*TER$^{-/-}$ and *Lm*Addback. It is likely that the high infection rate occurred after 48 h and that independently of the parasite passage, *Lm*TER$^{-/-}$ and *Lm*Addback infected less than the control (*Lm*007).

When we estimated the number of amastigotes per infected macrophage (Fig 7C), *Lm*TER$^{-/-}$ at P5 and P50 and the *Lm*Addback showed no difference after 24 and 48 h. Still, they all showed lower numbers compared to *Lm*007. Hence, it seems that despite the ability to infect macrophages, the proliferation of the parasites inside the host cell was impacted. Finally, the estimated infectivity index for *Lm*TER$^{-/-}$ and *Lm*Addback at both infection periods (24 and 48 h) and passages (P5 and P50) was lower than the *Lm*007 (Fig 7D). Interestingly, there is also no statistically significant difference between *Lm*TER$^{-/-}$ and *Lm*Addback, showing that the complementation with *Leish*TER could not restore *Lm*TER$^{-/-}$ infectivity capacity probably because the excess of *Leish*TER exerts a dominant negative effect (see below). However, we cannot leave aside the possibility that telomere shortening (Fig 4C), which induces a decrease in parasite proliferation and cell cycle arrest (Fig 1), is implicated in a decrease in the parasite's infectious capacity.

We also tested *Lm*TER$^{-/-}$ infectivity capacity using the murine macrophage cell line RAW 264.7. The results post 24 h infection exhibited in S4 Fig confirm those obtained with BMDM (Fig 7), showing that *Lm*TER$^{-/-}$ and *Lm*Addback present low infectivity capacity compared to *Lm*007.

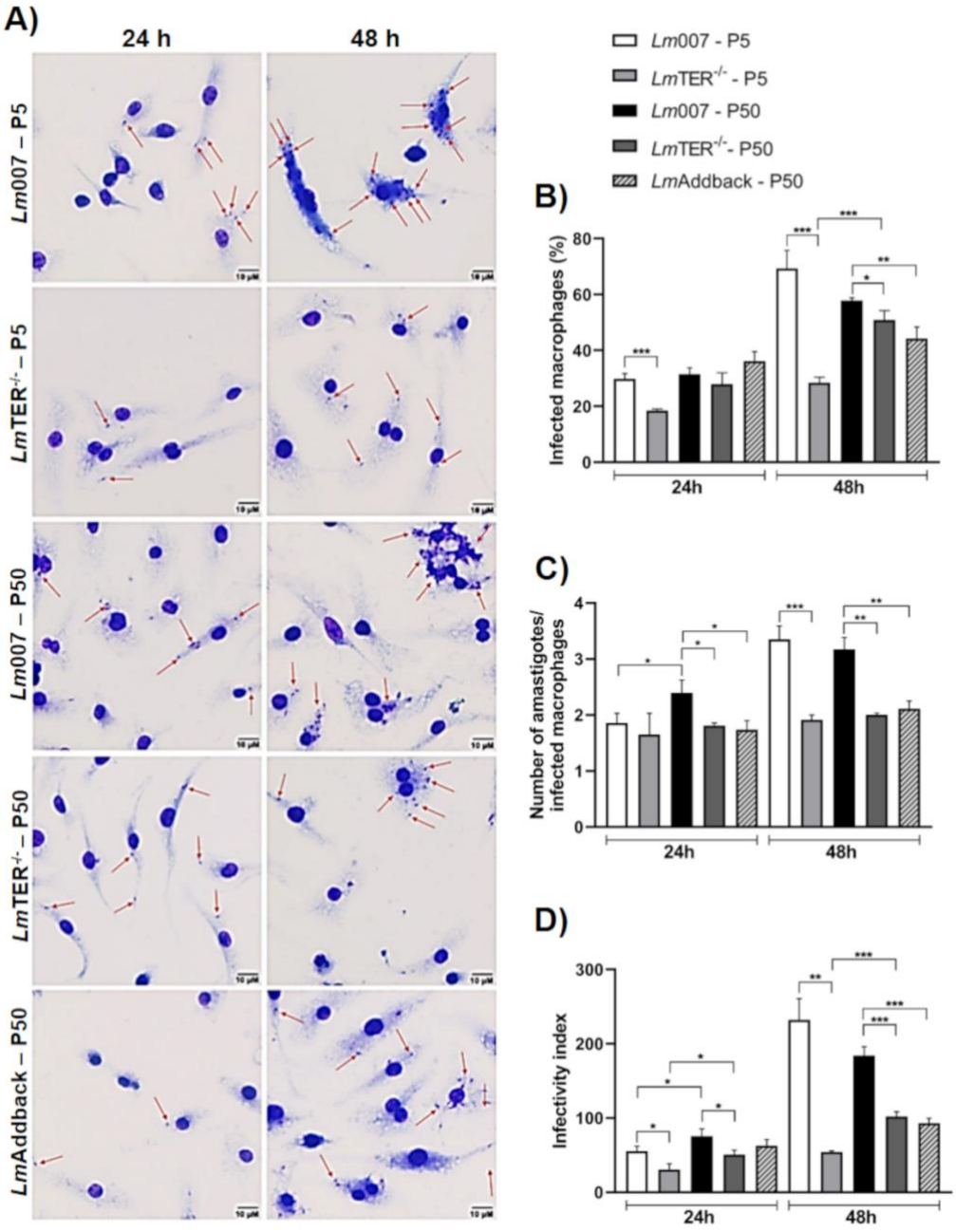

Fig 7. *Lm*TER$^{-/-}$ retains the ability to transform into metacyclic form, but its in vitro infectivity index is compromised. A) Microscopic images depict bone marrow-derived macrophages (BMDM) infected for 24 and 48 h with *Lm*007 and *Lm*TER$^{-/-}$ at P5 and P50 and *Lm*Addback at P50. Red arrows indicate *L. major* parasites internalized within the macrophages. The images were captured in representative and random fields at 40x magnification, with scale bars representing 10 μm. B) The percentage of macrophages infected for 24 and 48 h with *Lm*007 and *Lm*TER$^{-/-}$ at P5 and P50, along with *Lm*Addback at P50, is shown. C) Number of amastigotes per macrophage in infections with *Lm*007 and *Lm*TER$^{-/-}$ (both at P5 and P50) and *Lm*AddBack (P50) for 24 and 48 h is shown. D) The infectivity index of *Lm*007 and *Lm*TER$^{-/-}$ at P5 and P50 and *Lm*Addback at P50 was calculated considering the infectivity period of 24 and 48 h and are presented. All data are expressed as mean values ± S.D. and represent results from triplicate experiments. Statistical analysis was conducted using the student t-test, with Welch's correction applied when necessary. Significance levels are indicated as $*p \leq 0.05$, $**p \leq 0.01$, $***p \leq 0.001$.

Discussion

Telomeres play a pivotal role in genome stability, and telomerase is essential for maintaining telomere length. In this work, we aim to understand the impact of knocking out the *Leishmania* telomerase RNA, *Leish*TER, one of the main components of the enzyme complex. Our results show the effects of *Leish*TER on parasite survival, cellular processes, and infectivity and shed light on its potential as a therapeutic target.

Our first evidence of the harm caused by the ablation of *Leish*TER in *L. major* were the effects on parasite growth, which resemble the observed in the budding yeast *Saccharomyces cerevisiae* depleted of TER and the $Terc^{-/-}$ mouse embryonic stem cells (mESC). In yeast, TER depletion led to a decrease in growth rate and viability, whereas in mESC, the absence of Terc resulted in slow growth during extended cultures [33,53]. Our results, however, contrast with those obtained in *T. brucei*, a trypanosomatid protozoa as *Leishmania* spp. The loss of *Tb*TER and *Tb*TERT exhibited no discernible impact on cell growth even after many population doublings (~350) [25,54].

Furthermore, telomere shortening was detected in *Lm*$TER^{-/-}$ during continuous in vitro passaging, aligning with the established function of telomerase in preserving telomere length. This outcome is also consistent with findings in model eukaryotes such as mice, yeasts, and *T. brucei* [25,55,56], where the depletion of TER has a detrimental impact on telomere length maintenance. Interestingly, as shown here, part of the log phase *Lm*$TER^{-/-}$ promastigotes continued to grow in vitro until late passages (P50), suggesting that they survive even carrying short telomeres. Budding yeast depleted of TER and somatic human cells lacking telomerase activity can also survive with short telomeres [57,58]. In both cases, cells lose telomeres at every replication round until they become critically short, inducing cells to a senescence state. During senescence, cells can still avoid terminal fusions and catastrophic events of genome instability. Cells that bypass senescence, however, will face cell death or continue dividing, presenting further telomere shortening [58]. If telomeres get too short in mammals, they fuse, and cells enter crisis and eventually immortalize or transform into tumor cells. To proliferate, these cells can maintain short telomeres by reactivating telomerase or by alternative lengthening of telomeres (ALT), which usually relies on homologous recombination-mediated DNA replication [59]. In budding yeast, telomerase-depleted cells enter senescence or die after 50-100 divisions, and survivors that activate different ALT mechanisms spontaneously emerge in the cultures. Type I (~90%) and type II (~10%) survivors count on mechanisms of

recombination/amplification to maintain the telomeric DNA tracts [57,60]. Whether *Lm*TER$^{-/-}$ survivors use a still unknown ALT mechanism to maintain telomeres remains to be determined.

Another phenotype presented by *Lm*TER$^{-/-}$ cells is the phosphorylation of histone γH2A, which, in trypanosomatids, differently from mammals, occurs at the Thr^{130} [61]. γ-H2A is one of the earliest markers of DNA damage, although it can also signal replication stress, including at telomeres, and cell senescence [51,62,63,64]. Since no DNA damage was detected in *Lm*TER$^{-/-}$, we speculate that the phosphorylation of γH2A may be signaling replication stress at short telomeres, which we propose to trigger a senescence-like state in the *Lm*TER$^{-/-}$ cells as documented by their growth impairment and G0/G1 cell cycle arrest.

Trying to revert the above phenotypes, we reintroduced *Leish*TER into *Lm*TER$^{-/-}$ parasites (referred to as *Lm*Addback), but we did not succeed since *Lm*Addback did not restore telomere length to the control (*Lm*007) levels. Likely, the episomal expression of *Leish*TER, similar to budding yeast overexpressing TER (TLC1) [33], has a dominant negative effect inducing telomere shortening. This was further sustained by analyzing the overexpression of *Leish*TER, suggesting that an excess of *Leish*TER would disrupt either telomerase assembly and the complex stoichiometry or the episomally expressed *Leish*TER cannot acquire the proper secondary structure and, in both cases, inhibit enzyme activity.

In our study, we have also demonstrated a decreased expression of the long non-coding RNA TERRA29 in *Lm*TER$^{-/-}$, a phenomenon that could be attributed to the shortened telomeres or the absence of *Leish*TER. While it established that short telomeres can enhance TERRA expression in mouse tumor cells and budding yeast [42,43], it's important to mention that numerous other factors can exert influence on TERRA expression, including developmental stage, cellular stress, and telomere epigenetic modifications [43]. Therefore, further investigation is needed to determine whether the decrease in TERRA29 expression in *Leishmania* can be solely attributed to short telomeres or other factors.

Morphological transformations have also been documented in organisms lacking TER or with TER impairments. For instance, late-generation male mice deficient in TER (Terc$^{-/-}$) exhibited testicular atrophy and depletion of male germ cells [31]. Moreover, in budding yeast, *Kluyveromyces lactis* harboring mutations in the TER, aberrant "monster cells" with varying DNA content and apparent deficiencies in cell division arose [65]. Through TEM analysis, significant intracellular changes in *Lm*TER$^{-/-}$ parasites were observed, including initiating an autophagic process, which may indicate a mechanism for preserving cellular homeostasis [66].

However, no alterations in the DNA content and parasite plasma membrane that would indicate apoptotic events were detected.

The ability of procyclic promastigotes to transform into metacyclic promastigotes (infective forms) is key to establishing infection in the mammalian host [3,67]. Here, we show that *Lm*TER$^{-/-}$ preserved the ability to transform into the metacyclic form, suggesting *Leish*TER is not involved in parasite differentiation. However, *Lm*TER$^{-/-}$ exhibited a lower infectivity index than *Lm*007 across all passages and periods under scrutiny. Therefore, there appears to exist some association between reduced infectivity and telomere length. Notably, in *T. brucei*, telomerase deficient telomeres shortening increases the frequency of switch of the telomeric Variant Surface Glycoprotein-encoding genes (VSGs). VSGs are the main parasite virulent factor involved with immune evasion and are monoallelic expressed at the cell surface by a gene conversion mechanism [68]. There is no antigenic variation in *Leishmania*, but the *SCG* gene family responsible for LPG modification is mainly found near telomeres across multiple chromosomes (2, 7, 21, 25, 31, 35, and 36) [69,70]. Whether the observed telomere shortening in *Lm*TER$^{-/-}$ affected the expression of the SCG genes should be examined.

Our results corroborate the hypothesis that the absence of *Leish*TER, besides leading to telomere shortening, may induce a senescence-like phenotype in *Leishmania* promastigotes. These findings shed light on the importance of telomerase and telomere maintenance in the survival and infectivity of *Leishmania* parasites.

Further research may explore the molecular mechanisms underlying these observations and their potential implications for leishmaniasis treatment and control.

Materials and Methods

Cultivation and growth curves

Leishmania major Friedlin strain (MHOM/IL/1980/FRIEDLIN) was used in this study. All lineages of *L. major* were cultured in M199 medium, pH 7.3 (Cultilab) supplemented with 10 % (v/v) heat-inactivated fetal bovine serum (FBS) (Cultilab) [71], and 1X penicillin/streptomycin (Life Technologies, Gibco-BRL) at 26°C. Procyclic promastigotes from passage 1 (P1) were differentiated in vitro from amastigotes extracted from mice footpad lesions [72] after inoculation into the culture medium (see above) and incubation at 26°C for 24 h. Promastigotes continuous passages represent promastigotes P1 and so on being replicated in exponential growth every three days. Metacyclic promastigotes were purified from stationary

phase promastigote culture using agglutination with peanut lectin from *Arachis hypogaea* (Sigma-Aldrich), as previously described [4].

For the growth curves, the technical triplicate for each lineage was prepared with 1 x 10^6 cells/mL. The cells were fixed in PBS containing 1 % formalin and counted in a Neubauer chamber at intervals of 24 h. The data obtained were analyzed and plotted on a graph according to the mean of the technical triplicate ± S.D., using GraphPad Prism Version 8.0.2.

Establishment of experimental lineages

Obtention of *L. major* promastigotes expressing the Cas9 endonuclease and T7/RNA polymerase (*Lm*007)

L. major WT (*Lm*WT) procyclic promastigotes were transfected with pTB007. This episomal plasmid contains genes encoding the T7/RNA polymerase, the hygromycin phosphotransferase (hph), and the humanized *Streptococcus pyogenes* Cas9 nuclease (*hpCas9*) [34].

The transfection was performed as described by Kapler et al. (1990) [71] using the Gene Pulser Xcell Eukaryotic System (BioRad). Once cells were transfected, the presence of the pTB007 in the population was confirmed by PCR using primers that specifically amplify Cas9 and T7RNA polymerase genes (For-Cas9 + Rev-Cas9; T7RNAP-F + T7RNAP-R - S1 Table). Afterward, the parasites were plated in 1X M199/1 % agar, supplemented with 10 % (v/v) FBS and 30 μg/mL hygromycin to select clones. Clones of *L. major* strain expressing Cas9 and T7/RNAp (*Lm*007) were inoculated in 1X M199 liquid medium supplemented with 10 % (v/v) FBS and 30 μg/mL hygromycin B (Invitrogen).

Generation of *Leish*TER knockout (*Lm*TER$^{-/-}$) lineage

A donor DNA cassette that confers resistance to neomycin/G418 and two sgRNAs were used to obtain *Lm*TER$^{-/-}$ cells. For the in vivo transcription of guide RNAs (one for the 5' end and the other for the 3' end of *Leish*TER), sgRNA templates were generated by PCR following the protocol described in Beneke et al. (2017) [34] using both sets of primers: TracrRNA (G00) – scaffold + TER seed-5' and TracrRNA (G00) – scaffold + TER seed-3' and (see S1 Table for the sequences of the primers). The sgRNA sequences were chosen using the online tool Eukaryotic Pathogen CRISPR guide RNA/DNA Design Tool, EuPaGDT (http://grna.ctegd.uga.edu) using the default parameters described in Beneke et al. (2017) [34]. The donor DNA was also obtained by PCR using the pTNeo plasmid as a template [34].

Transfections were performed as described earlier [71]. *Lm*TER$^{-/-}$ clones were selected using solid M199 medium, as described in the previous item. *Lm*TER$^{-/-}$ cells were maintained with 40 µg/mL G418 (Sigma-Aldrich).

Selection of *Lm*TER$^{-/-}$ clones using PCR, RT-PCR, and automated sequence

A set of primers that hybridizes at the 5' upstream and 3' downstream sequences of the *Leish*TER gene (5'TER F + 3'TER R - S1 Table; S1D and E Figs) were used to confirm the generation of the knockout line. The above primers set would generate an amplicon of 2,432 bp *Lm*007 used as control and an amplicon of 2,059 bp if the donor DNA cassette replaced the *Leish*TER gene in the correct locus.

Total RNA obtained from the *Lm*TER$^{-/-}$ and from the control (*Lm*007) and a set of primers that hybridizes in the internal portion of *Leish*TER gene (TERmF and TER RT R - S1 Table; S1D Fig) were used to obtain double-stranded cDNA using SuperScript™ III One-Step RT-PCR System with Platinum™ Taq DNA Polymerase (Invitrogen), according to manufacturer's instructions.

Sequencing reactions were performed using primers that target the regions upstream and downstream of the *Leish*TER locus and internal regions of the donor DNA (S1E Fig and S1 Table). Fragments of interest were generated by PCR with further purification using the PureLink™ PCR Purification Kit (Invitrogen), and then automated Sanger sequencing was performed at IBTEC (UNESP – Botucatu). Blastn, Clustal Omega online tool (https://www.ebi.ac.uk/Tools/msa/clustalo/) and SnapGene 6.0.2. were used for in silico sequence analysis.

Complementation assay: addback of *Leish*TER in *Lm*TER$^{-/-}$ cells

*Lm*TER$^{-/-}$ cells were transfected with the plasmid pSP72-a-bla-a-LmjTER synthesized by GenOne using the pSP72-a-bla-a plasmid as the backbone. First, the transfection was performed, and 20 µg/mL of blasticidin (Invivogen) was added to the culture to select the transfectants. Then, PCR (Primers: TERmF + TER RT R – S1 Table) and RT-qPCR (Primers: TER RT F + TER RT R – S1 Table) were performed to confirm the presence of the plasmid and expression of *Leish*TER, respectively. *Lm*AddBack was maintained in 40 µg/mL G418 and 20 µg/mL Blasticidin (Invivogen).

Generation of an *L. major* lineage overexpressing *Leish*TER

L. major at the exponential growth phase were transfected with 50 µg of *Leish*TER-pX63Neo plasmid DNA (Vassilievitch & Morea, *unpublished*), which contains the *Leish*TER gene and the gene that confers resistance to neomycin. In addition, *Lm*WT was also transfected with 50 µg of empty pX63Neo plasmid [73] as a control. The pX63Neo plasmid is maintained as an episome in *Leishmania* with 40 µg/mL of G418. It is specifically used for expressing *Leishmania* genes since it signals trans-splicing and polyadenylation [73]. The selection of transfectants containing *Leish*TER-pX63Neo and pX63Neo plasmids (named *Lm*pXTER and *Lm*pXØ, respectively) was performed using 40 µg/ml G418 as the selection antibiotic. The genotype of the clones was determined by PCR, using specific primers (Px63 Neo Fw and Px63 Neo Rv - S1 Table), and the overexpression of *Leish*TER was confirmed by RT-qPCR (Primers: TER RT F and TER RT R - S1 Table).

DNA extraction and Southern blot

Genomic DNA was obtained from 2 x 10^8 cells of *L. major* using DNeasy Blood and Tissue kit (Qiagen) according to the manufacturer's instructions and phenol:chloroform extraction, according to Medina-Acosta and Cross (1993) [74] with some modifications as follow: 2 x 10^8 parasites were washed twice with 1X PBS and resuspended in TELT buffer (50 mM Tris-HC1, pH 8.0; 62.5 mM EDTA, pH 9.0; 2.5 M LiCl and 4% (v/v) Triton X-100) containing 10 µg/µl proteinase K and incubated at 56 °C for 10 min. Subsequently, 1 volume of phenol:chloroform:isoamyl alcohol (25:24:1) was added, and the tube was inverted for 5 min, followed by centrifugation at 16,000 g for 10 min. The supernatant was transferred to a new tube, and 1 ml of 100% cold ethanol was added. The tube was inverted a few times until the DNA was precipitated and centrifuged at 16,000 g for 5 min. The pellet of DNA was washed once with 70% cold ethanol, centrifuged, and air-dried. After that, the samples were resuspended in 100 µl of TE (10 mM Tris-HCl, pH 8.0/11 mM EDTA, pH 8.0) containing 50 µg/µl RNase A (Invitrogen) and incubated at 37 °C. DNA concentration and purity were evaluated by calculating the A260/280nm ratio using a spectrophotometer (Epoch, BioTek). DNA integrity was verified on 1% agarose gel.

For Southern blot, 1 µg of genomic DNA was digested with 5U *Rsa*I (Roche) at 37 ºC overnight to release the telomeric fragments [75]. The subsequent steps of the Southern blot were done using standard procedures [75, 76] with minor modifications as described in Morea et al. (2021) [38]. For the confirmation of *Leish*TER ablation in *Lm*TER$^{-/-}$, DIG-labeled TER

and alpha-tubulin probes were generated using the PCR DIG Probe Synthesis Kit (Roche) and used in the hybridization step (S1 Table, S1D Fig).

Southern blot membranes were hybridized using a DIG-labeled TELC probe (S1 Table) or a DIG-labeled 18S rRNA probe (S1 Table) as the loading control. The Telomere Restriction Fragments (TRF) location on the blots was compared to the DNA molecular weight marker VII DIG-labeled (Roche) to obtain the average of TRF.

Total protein extraction and Western blotting

Protein extracts were obtained according to de Oliveira et al. (2021) [77] using $5x10^8$ cells harvested at 2,300 g for 5 min and washed twice with 1X PBS. The pellet was resuspended in supplemented buffer A (20 mM Tris-HCl pH 7.5; 1 mM EGTA pH 8.0; 1 mM EDTA pH 8.0; 15 mM NaCl; 1mM spermidine; 0.3 mM spermine; 1mM DTT) and incubated in liquid nitrogen for 1 minute followed by incubation on ice until defrost. A solution containing 0.5 % of Nonidet P-40 (Calbiochem) and 1X protease cocktail inhibitor (Sigma-Aldrich) was added to the samples, followed by 30 min incubation on ice. The samples were then centrifuged at 16,000 g for 20 min at 4 °C; subsequently, the supernatant was transferred to a new tube, and the total protein in each extract was estimated by reading the $OD280_{nm}$ using the spectrophotometer (Epoch, BioTek). For the Western blot, 200 µg of total protein extracts were fractionated in a 10 % SDS-PAGE followed by a wet transfer to a PVDF membrane (GE Healthcare) [78]. The membranes were probed with primary antibodies, Anti-Flag (dilution 1:5,000 – Sigma-Aldrich) and Anti-*Lm*GAPDH (dilution 1:2,000 - GenScript), followed by incubation with Anti-rabbit IgG (dilution 1:50,000 - BioRad) as the secondary antibody. According to the manufacturer's instructions, immunoreactive bands were revealed by using ECL Prime Western Blotting Detection Reagent (GE Healthcare).

Total RNA isolation and RT-qPCR

Total RNA from 3 x 10^8 cells at the exponential growth phase was isolated using TRIzol reagent (Invitrogen). RNase-free DNase I treatment (Thermo Scientific™) was conducted, followed by inactivation through incubation with 1 µl of 25 mM EDTA at 65 °C for 10 min, according to the manufacturer's instructions. RNA concentration and purity were evaluated by an A_{260nm} (spectrophotometer Epoch, BioTek). The absence of genomic DNA in the RNA samples was confirmed by PCR using primers for alpha-tubulin (Primers: Alfa Fw1 + Alfa Rv1 - S1 Table) and positive control (*Lm*WT genomic DNA).

First-strand cDNA synthesis was performed using the iSCRIPT cDNA synthesis kit (BioRad) according to the manufacturer's instructions. The RT-qPCR assays were performed in technical triplicate using cDNA, iTaq Universal SYBR® Green Supermix (BioRad), and 0.5 μM of each primer specific for *Leish*TER and the subtelomeric region of chromosome 29 - right arm (S1 Table). The gene encoding the 19S proteasome non-ATPase subunit 8 (RPN8) (*Lmj*F.32.0390) was used as a control [38, 79] to normalize gene expression levels of the targets (*Leish*TER and TERRA29). RT-qPCRs were performed in 10 μL reactions, and cycle threshold (Ct) values were obtained in StepOne™ Real-Time PCR System (Applied Biosystems) using default settings. The relative gene expression data were analyzed using the $2^{-\Delta\Delta CT}$ method as described [80]. The data were expressed as means of fold change over control (relative expression), where the control data was normalized to an arbitrary value of 1. Statistical analyses were performed using GraphPad Prism version 8.0.2.

Flow cytometry protocols

DNA content analysis

1.5 x 10^7 cells at the exponential and stationary growth phase were harvested at 900 g for 5 min, washed twice with 1X PBS, fixed and permeabilized with 90% ice-cold methanol, followed by incubation at -20 °C for 20 min as described in Barak et al. (2005) [81] with some modifications [82]. Then, cells were washed once with 1X PBS, resuspended in staining solution (1X PBS containing 100 μg/mL of RNase-A (Invitrogen) and 10 μg/mL of propidium iodide (Thermo Scientific™), and incubated for 40 min at 37 ºC. Subsequently, the parasites were analyzed using flow cytometry (Acuri C6 Plus – BD Bioscience), and the DNA content analysis was performed according to de Oliveira et al. (2022) [82]. Technical triplicates were used, and 20,000 events were analyzed for each sample.

Cell proliferation tracking using carboxyfluorescein succinimidyl ester (CFSE)

1 x 10^7 cells at the exponential growth phase were labeled with 8 μM CFSE (Invitrogen) following the manufacturer's instruction. The first 20 min after labeling was considered time zero, with parasites emitting 100 % CFSE fluorescence. Then, parasites were left in culture and collected every 7 h up to 28 h, and CFSE fluorescence emission was monitored using flow cytometry [83]. About 7,000 events of each sample were analyzed. The mean fluorescent intensity (MFI) was estimated and normalized, and the mean of technical triplicate ± standard deviation was plotted in GraphPad Prism Version 8.0.2.

Telomeric Flow-FISH

Telomeric flow-FISH was performed using a modification of the Baerlocher et al. (2006) [40] method as described by da Silva et al. (2017) [41] without the human leukocytes: 1.5 x 10^7 cells were centrifuged at 900 g for 5 min at 4 °C and washed twice with 1X PBS, fixed and permeabilized with 90% ice-cold methanol, followed by incubation at -20 °C for 20 min. Then, cells were washed twice with 1X PBS (5,000 g for 5 min at 4 °C), and the pellet was gently resuspended in hybridization buffer (70 % formamide, 20 mM Tris-HCl pH 7, and 1 % BSA) containing a PNA FITC-labeled telomeric DNA oligo probe $(CCCTAA)_3$ (Panagene). The pellet was gently resuspended only in the hybridization buffer for the non-hybridized controls. Samples were protected from light and incubated at 85 ºC for 15 min, followed by overnight (~16h) incubation at room temperature. Parasites were washed in 1X Wash Solution (Dako) and incubated for 10 min at 40 ºC, then centrifuged at 5,000 g for 5 min. The supernatant was discarded, and this step was repeated, followed by an additional wash with 1X PBS and centrifugation at 5,000 g for 5 min. The pellet was resuspended in Staining solution (1X PBS containing 100 μg/mL of RNase-A and 10 μg/mL of propidium iodide) and incubated for 30 min at 37 ºC and then for 30 min at 4 ºC. Samples were subjected to flow cytometry analysis using Accuri C6 Plus (BD Bioscience). Quantum™ FITC-5 MESF beads (BioRad) were used according to the manufacturer's protocol to estimate the length of telomeres quantitatively. Technical triplicates of hybridized and non-hybridized telomeres were used. For each sample, approximately 20,000 events were analyzed.

Verification of DNA fragmentation and plasma membrane modifications by TUNEL and Annexin-V, respectively

For the TUNEL assay, 1 x 10^7 cells at P5 and P50 at the exponential growth phase were used following the manufacturer's instruction for cells in suspension. As a positive control, cells were treated with 10 units/mL Deoxyribonuclease I from bovine pancreas (Sigma-Aldrich) for 10 min. As the negative control, cells were prepared without incubation with rTdTenzyme, following the manufacturer's instructions (DeadEnd™ Fluorometric TUNEL System – Promega).

The Annexin-V assay followed the manufacturer's protocol (BioRad) using 1 x 10^6 cells. In addition, three technical replicates of *Lm*007 and *Lm*TER$^{-/-}$ promastigotes in the exponential and stationary growth phase at P5 and P50 were used. A sample not labeled with AnnexinV-FITC and PI was used as the negative control. As a positive control, cells were

treated with 3 % formaldehyde for 30 min on ice before incubation with AnnexinV:FITC. Approximately 10,000 events were collected to be analyzed in a flow cytometer.

Assessment of DNA replication by EdU labeling

Following the standard procedures as described by da Silva et al. (2017) [84], cells at exponential growth phase were incubated with 200 μM of the thymidine analog EdU (5-ethynyl-2′-deoxyuridine - Invitrogen) at 26 °C for 10.2 h (estimated doubling time of *L. major*) [85] followed by centrifugation at 900 g at 4°C for 5 min. The supernatant was discarded, and the pellet was washed twice with 1X PBS. The supernatant was discarded carefully and resuspended in cold 1X PBS, followed by the addition of ice-cold methanol (final concentration of 90%). After mixing by pipetting, the samples were incubated at -20°C for 20 min for fixation. Afterward, samples were vortexed and washed once with 1X PBS. 100 μL of cycloaddition reaction (3 mM CuSO4, 100 mM Ascorbic Acid, and 5 mM Alexa Fluor azide 488) was added in each sample and incubated for 1 h protected from light. Samples were washed once with 1X PBS, and the pellet was resuspended in 500 μL of 1X PBS. Approximately 20,000 events were collected from each sample by flow cytometry.

Sample collection and analysis using Flow cytometry

The sample collections were done using the Accuri C6 Plus flow cytometer (BD Bioscience), and the data analysis was done using both FlowJo v.10.6.5 software and GraphPad Prism Version 8.0.2. Two standard graphs were generated at FlowJo for all experiments: FSC-A x SSC-A and FSC-A and FSC-H to select the population of interest and exclude doublets and debris. In addition, due to the particularity of each experiment, additional graphs were generated to analyze the fluorescence emission related to each experiment as follow: for DNA content analysis: FL2-A x FL2-H and FL2-A x histogram; for TUNEL: SSC-A x SSC-H, FL2-A x FL2-H and FL1-A x histogram; Flow-FISH: FL2-A x FL2-H and FL1-A x histogram; for CFSE and EdU: FL1 x histogram; and Annexin V: FL2-A x FL1-A.

Telomeric FISH

For these assays, we used a protocol described before [77]. 1 x 10^7 cells from P5 and P50 were fixed with 4% paraformaldehyde for 5 min on ice, followed by several washes in 1X PBS. Then, the fixed cells were attached to glass slides coated with 0.1% poly-L-lysine (Sigma-Aldrich). Subsequently, cells were dehydrated through an ice-cold ethanol series (70 %, 85 %,

and 100 %) for 2 min each and air dried. Cells were incubated for 5 min at 85 °C and then 30 min at room temperature, protected from light, with 10 μM of PNA FITC-labeled telomeric DNA oligo probe $(CCCTAA)_3$ (Panagene). After the hybridization step, cells were washed once with Rinse solution (Dako) at room temperature for 10 seconds, followed by another washing using 1X Wash solution (Dako) at 65°C for 5 min. Afterward, a second dehydration step was followed, as described earlier. The DNA in the nucleus and kinetoplast was counterstained, and the slides were mounted using VECTASHIELD® Antifade Mounting Medium with DAPI (Vector). Approximately 100 cells/field were observed in each experiment. The slides were analyzed under a Nikon 80i fluorescence microscope, and the images were captured using the NIS elements program (Version Ar 3.10).

Detection of histone γH2A phosphorylation

The immunofluorescence assay was performed as described before [41]: 1 x 10^7 cells were harvested at 900 g for 5 min at 4°C, washed with 1X PBS, fixed in 4% paraformaldehyde, washed with 1X PBS, and then placed on a glass slide previously coated with 0.1 mg/ml of poly-L-lysine (Sigma-Aldrich). Cells were subsequently permeabilized with 0.1% Triton X-100 for 5 min, washed several times, and then incubated overnight at 4°C with the primary antibody anti-γH2A (a gift from Dr. Richard McCulloch - University of Glasgow) (dilution 1:500). Slides were washed with 1X PBS and incubated with anti-rabbit IgG AlexaFluor 594 (Invitrogen) for 2 h protected from light followed by three washes using 1X PBS. The DNA in the nucleus and kinetoplast was counterstained, and the slides were mounted using VECTASHIELD® Antifade Mounting Medium with DAPI (Vector). *Lm*007 treated with 10 μg/ml of phleomycin (Invivogen) for 24 h was used as a positive control [45]. The slides were analyzed under a Nikon 80i fluorescence microscope, and the images were captured using the NIS elements program (Version Ar 3.10).

Transmission (TEM) and Scanning Electron Microscopy (SEM) analysis

L. major procyclic promastigotes (*Lm*WT and *Lm*TER$^{-/-}$) at P5 and P50 were washed twice with 1X phosphate-buffered saline (PBS) and fixed at 4 °C for 40 min with 2.5 % glutaraldehyde (GA - Sigma-Aldrich) diluted in 0.1 M 2.5 % glutaraldehyde in 0.1 M Na-cacodylate buffer (pH 7.2). The parasites were prepared for TEM analysis as described previously [86]. Ultrathin sections were stained with uranyl acetate and lead citrate and

examined under a Jeol 1200 EX transmission electron microscope (JEOL USA Inc.) at Centro Nacional de Biologia Estrutural e Bioimagem (CENABIO, Rio de Janeiro).

For SEM analysis, the GA-fixed parasites were submitted to the procedures described by Rebello et al. (2013) [87] and examined with a Jeol JSM6390LV scanning electron microscope (JEOL USA Inc.) at Instituto Oswaldo Cruz Platform [87].

In vitro macrophage infection

In vitro infection using bone marrow-derived macrophages

Bone marrow-derived macrophages (BMDMs) were obtained from the femurs and tibias of BALB/c mice, which were differentiated in vitro as previously described [88].

A total of $3x10^5$ cells were seeded onto sterile coverslips (Olen) in 24-well plates (Nest) and incubated overnight at 37 ºC and 5 % CO_2 in RPMI medium as previously described [89]. Non-adherent cells were removed, and the infection was performed with *Lm*007, *Lm*TER$^{-/-}$ (P5 and P50), and *Lm*AddBack (P50) parasites in the stationary growth phase (MOI 10:1) for 3 h at 34ºC and 5% CO2. After this period, non-internalized parasites were removed by washing with warmed 1X PBS, and then infections were maintained for 24 or 48 h. Following the infection, the infected macrophages were fixed with methanol and stained using a Panoptic kit (Laborclin). The experiments were carried out in triplicate, and the observations were made at a magnification 40X of the optical light microscope (Leica DME). In addition, photomicrographs were taken using the EVOS XL Core Imaging System (ThermoFisher) at 40X magnification.

In vitro infection using RAW 264.7 murine macrophages

A suspension of 2 x 10^5 macrophages/mL of RAW 264.7 murine macrophages ATCC TIB-71™ (Rio de Janeiro Cell Bank – BCRJ) was cultured on 24-well plates containing 13 mm diameter glass coverslips in complete media (RPMI-1640 supplemented with 10 % FBS, 2 mM L-glutamine and 10 mM HEPES) and incubated overnight at 37 ºC, 5 % CO_2, 21 % of balanced O_2 and N_2 for macrophage step adhesion. Afterward, the macrophage culture was infected with *Lm*007 and *Lm*TER$^{-/-}$ (P5 and P50) and *Lm*Addback (P50) transgenic lines in the stationary growth phase, as described previously [90]. We used a ratio of MOI 10:1 for infections. After the incubation period (24 h), the coverslips were fixed with methanol and stained with Giemsa to visualize the macrophages and the internalized parasites. The experiments were carried out in triplicate. The observations were made at a magnification of 1,000x of the optical light

microscope (Zeiss Primo Star, Oberkochen, GER). In addition, photomicrographs were taken on a camera (Axiocam ERc5s, Axiovision software 4.8, Zeiss) attached to the microscope.

Infection analysis

The percentage of infection was calculated by dividing the number of infected macrophages by the total number of macrophages. The average number of amastigotes per infected macrophage was determined by dividing the total number of amastigotes by the total number of infected macrophages. The infectivity index was calculated by multiplying the percentage of infected macrophages by the mean number of intracellular amastigotes per infected macrophage [91].

Statistical analysis

The mean and standard deviation (S.D.) were calculated from a technical triplicate of each sample to be analyzed. A two-tailed parametric unpaired Student's *t*-test was performed when it was established that the variances among the groups were homogenous following an examination for equal variance. In cases where a significant variance difference was detected, Welch's t-test was employed. A probability level of 0.05 was chosen for statistical significance, where $*p \leq 0.05$, $**p \leq 0.01$, $***p \leq 0.001$, and $****p \leq 0.0001$. GraphPad Prism Version 8.0.2 was used to perform all the statistical analyses and to generate the graph.

Data availability

This paper does not report any original code.

All data reported in this paper can be found at **doi:10.5281/zenodo.10035539,** along with the respective statistical treatments and results obtained.

Any additional information required to reanalyze the data reported in this paper is available from the lead contact upon request.

Ethics statement

Animal procedures were approved by the Ethics Committee for Animal Experimentation of the Instituto de Biologia, Universidade Estadual de Campinas (UNICAMP) (protocol: 5719–1/2021) for experiments using mice.

Acknowledgments

The authors want to acknowledge Dr. Elton José R. Vasconcelos for the critical reading of the manuscript. Dr. Marcelo Santos da Silva, Dr. Débora Andrade da Silva, and Miss Stephany Cacete de Paiva for the comments and directions of some experiments and methodology.

Financial support

This work was supported by the São Paulo State Research Foundation (FAPESP, Fundação de Amparo à Pesquisa do Estado de São Paulo) under grant 2018/04375-2 and Conselho Nacional de Desenvolvimento Científico e Tecnológico, Brazil, CNPq under grant 302433/2019-8 to MINC. BCDO and MES are doctoral fellows from FAPESP (grants 2019/25985-6 and 2020/00316-1). LCA is a post-doctoral fellow from FAPESP (grant 2021/04253-7). VSF is an undergrad student fellow from CNPq (9/2023-PIBIC project 9434), PHGF was a master fellow from FAPESP (grant 2019/11061-7), and ACC is a young researcher fellow from FAPESP (grant 2016/21171-6).

Author contributions

Conceptualization: M.I.N.C., **Data curation:** B.C.D.O., M.I.N.C., **Formal analysis:** B.C.D.O., P.H.G.F., **Funding acquisition:** M.I.N.C., **Investigation:** B.C.D.O., M.E.S., L.H.C.A., V.S.F., P.H.G.F., M.M.B., J.I.A., **Methodology:** B.C.D.O., M.E.S., L.H.C.A., P.H.G.F., M.M.B. J.I.A., **Project administration:** M.I.N.C., **Resources:** M.I.N.C., S.G., M.N.C.S., R.F.S.M.B., A.C.C., **Supervision:** M.I.N.C., **Validation:** B.C.D.O., **Visualization:** B.C.D.O., S.G., M.N.C.S., **Writing – Original draft:** B.C.D.O., P.H.G.F., **Writing – Review & Editing:** B.C.D.O., M.E.S., L.H.C.A., P.H.G.F., S.G., M.N.C.S., J.I.A., A.C.C., M.I.N.C.

References

1. Pace, D. (2014). Leishmaniasis. *The Journal of infection*, *69 Suppl 1*, S10–S18. https://doi.org/10.1016/j.jinf.2014.07.016
2. Steck E. A. (1974). The leishmaniases. *Progress in drug research. Fortschritte der Arzneimittelforschung. Progres des recherches pharmaceutiques*, *18*, 289–351. https://doi.org/10.1007/978-3-0348-7087-0_22

3. Bates, P. A., & Rogers, M. E. (2004). New insights into the developmental biology and transmission mechanisms of *Leishmania*. *Current molecular medicine*, *4*(6), 601–609. https://doi.org/10.2174/1566524043360285
4. da Silva, R., & Sacks, D. L. (1987). Metacyclogenesis is a major determinant of *Leishmania* promastigote virulence and attenuation. *Infection and immunity*, *55*(11), 2802–2806. https://doi.org/10.1128/iai.55.11.2802-2806.1987
5. Karamysheva, Z. N., Gutierrez Guarnizo, S. A., & Karamyshev, A. L. (2020). Regulation of Translation in the Protozoan Parasite *Leishmania*. *International journal of molecular sciences*, *21*(8), 2981. https://doi.org/10.3390/ijms21082981
6. Chappuis, F., Sundar, S., Hailu, A., Ghalib, H., Rijal, S., Peeling, R. W., Alvar, J., & Boelaert, M. (2007). Visceral leishmaniasis: what are the needs for diagnosis, treatment and control?. *Nature reviews. Microbiology*, *5*(11), 873–882. https://doi.org/10.1038/nrmicro1748
7. OPAs (ORGANIZACIÓN PANAMERICANA DE LA SALUD) (2020). Atlas interactivo de leishmaniasis en las Américas: aspectos clínicos y diagnósticos diferenciales, Organizacion Panamericana de la Salud.
8. WHO (WORLD HEALTH ORGANIZATION). Leishmaniasis, Available at: https://apps.who.int/neglected_diseases/ntddata/leishmaniasis/leishmaniasis.html.
9. Sekaran, V., Soares, J., & Jarstfer, M. B. (2014). Telomere maintenance as a target for drug discovery. *Journal of medicinal chemistry*, *57*(3), 521–538. https://doi.org/10.1021/jm400528t
10. Rhodes, D., & Giraldo, R. (1995). Telomere structure and function. *Current opinion in structural biology*, *5*(3), 311–322. https://doi.org/10.1016/0959-440x(95)80092-1
11. Blackburn E. H. (1991). Structure and function of telomeres. *Nature*, *350*(6319), 569–573. https://doi.org/10.1038/350569a0
12. Blackburn, E. H., Epel, E. S., & Lin, J. (2015). Human telomere biology: A contributory and interactive factor in aging, disease risks, and protection. *Science (New York, N.Y.)*, *350*(6265), 1193–1198. https://doi.org/10.1126/science.aab3389
13. Barbé-Tuana, F.; Grun, L.K.; Pierdoná, V.; de Oliveira, B.C.D.; Paiva, S.C.; Shiburah, M.E.; da Silva, V.L.; Morea, E.G.O.; Fontes, V.S.; Cano, M.I.N. (2021). Human Chromosome Telomeres. In *Human Genome Structure, Function and Clinical Considerations* (pp. 207-243). Cham: Springer International Publishing.

14. Cano M. I. (2001). Telomere biology of trypanosomatids: more questions than answers. *Trends in parasitology*, *17*(9), 425–429. https://doi.org/10.1016/s1471-4922(01)02014-1
15. Moyzis, R. K., Buckingham, J. M., Cram, L. S., Dani, M., Deaven, L. L., Jones, M. D., Meyne, J., Ratliff, R. L., & Wu, J. R. (1988). A highly conserved repetitive DNA sequence, (TTAGGG)n, present at the telomeres of human chromosomes. *Proceedings of the National Academy of Sciences of the United States of America*, *85*(18), 6622–6626. https://doi.org/10.1073/pnas.85.18.6622
16. Autexier, C., & Lue, N. F. (2006). The structure and function of telomerase reverse transcriptase. *Annual review of biochemistry*, *75*, 493–517. https://doi.org/10.1146/annurev.biochem.75.103004.142412
17. Greider, C. W., & Blackburn, E. H. (1985). Identification of a specific telomere terminal transferase activity in Tetrahymena extracts. *Cell*, *43*(2 Pt 1), 405–413. https://doi.org/10.1016/0092-8674(85)90170-9
18. Berman, A. J., Akiyama, B. M., Stone, M. D., & Cech, T. R. (2011). The RNA accordion model for template positioning by telomerase RNA during telomeric DNA synthesis. *Nature structural & molecular biology*, *18*(12), 1371–1375. https://doi.org/10.1038/nsmb.2174
19. Zappulla, D. C., & Cech, T. R. (2006). RNA as a flexible scaffold for proteins: yeast telomerase and beyond. *Cold Spring Harbor symposia on quantitative biology*, *71*, 217–224. https://doi.org/10.1101/sqb.2006.71.011
20. Zhang, Q., Kim, N. K., & Feigon, J. (2011). Architecture of human telomerase RNA. *Proceedings of the National Academy of Sciences of the United States of America*, *108*(51), 20325–20332. https://doi.org/10.1073/pnas.1100279108
21. Blackburn, E. H., & Collins, K. (2011). Telomerase: an RNP enzyme synthesizes DNA. *Cold Spring Harbor perspectives in biology*, *3*(5), a003558. https://doi.org/10.1101/cshperspect.a003558
22. Collins K. (1999). Ciliate telomerase biochemistry. *Annual review of biochemistry*, *68*, 187–218. https://doi.org/10.1146/annurev.biochem.68.1.187
23. Lue N. F. (2004). Adding to the ends: what makes telomerase processive and how important is it?. *BioEssays : news and reviews in molecular, cellular and developmental biology*, *26*(9), 955–962. https://doi.org/10.1002/bies.20093

24. Podlevsky, J. D., & Chen, J. J. (2016). Evolutionary perspectives of telomerase RNA structure and function. *RNA biology*, *13*(8), 720–732. https://doi.org/10.1080/15476286.2016.1205768
25. Sandhu, R., Sanford, S., Basu, S., Park, M., Pandya, U. M., Li, B., & Chakrabarti, K. (2013). A trans-spliced telomerase RNA dictates telomere synthesis in Trypanosoma brucei. Cell research, 23(4), 537–551. https://doi.org/10.1038/cr.2013.35
26. Webb, C. J., & Zakian, V. A. (2016). Telomerase RNA is more than a DNA template. *RNA biology*, *13*(8), 683–689. https://doi.org/10.1080/15476286.2016.1191725
27. Chen, J. L., Blasco, M. A., & Greider, C. W. (2000). Secondary structure of vertebrate telomerase RNA. *Cell*, *100*(5), 503–514. https://doi.org/10.1016/s0092-8674(00)80687-x
28. Dey, A., & Chakrabarti, K. (2018). Current Perspectives of Telomerase Structure and Function in Eukaryotes with Emerging Views on Telomerase in Human Parasites. *International journal of molecular sciences*, *19*(2), 333. https://doi.org/10.3390/ijms19020333
29. Gupta, S. K., Kolet, L., Doniger, T., Biswas, V. K., Unger, R., Tzfati, Y., & Michaeli, S. (2013). The Trypanosoma brucei telomerase RNA (TER) homologue binds core proteins of the C/D snoRNA family. *FEBS letters*, *587*(9), 1399–1404. https://doi.org/10.1016/j.febslet.2013.03.017
30. Vasconcelos, E. J., Nunes, V. S., da Silva, M. S., Segatto, M., Myler, P. J., & Cano, M. I. (2014). The putative *Leishmania* telomerase RNA (LeishTER) undergoes trans-splicing and contains a conserved template sequence. *PloS one*, *9*(11), e112061. https://doi.org/10.1371/journal.pone.0112061
31. Blasco, M. A. (2001). The telomerase knockout mouse. Advances in Cell Aging and Gerontology, 8, 151-165. https://doi:10.1016/s1566-3124(01)08008-7
32. Feng, J., Funk, W. D., Wang, S. S., Weinrich, S. L., Avilion, A. A., Chiu, C. P., Adams, R. R., Chang, E., Allsopp, R. C., & Yu, J. (1995). The RNA component of human telomerase. *Science (New York, N.Y.)*, *269*(5228), 1236–1241. https://doi.org/10.1126/science.7544491
33. Singer, M. S., & Gottschling, D. E. (1994). TLC1: template RNA component of Saccharomyces cerevisiae telomerase. *Science (New York, N.Y.)*, *266*(5184), 404–409. https://doi.org/10.1126/science.7545955

34. Beneke, T., Madden, R., Makin, L., Valli, J., Sunter, J., & Gluenz, E. (2017). A CRISPR Cas9 high-throughput genome editing toolkit for kinetoplastids. *Royal Society open science*, *4*(5), 170095. https://doi.org/10.1098/rsos.170095

35. Quah, B. J., & Parish, C. R. (2010). The use of carboxyfluorescein diacetate succinimidyl ester (CFSE) to monitor lymphocyte proliferation. *Journal of visualized experiments : JoVE*, (44), 2259. https://doi.org/10.3791/2259

36. Lyons, A. B., & Parish, C. R. (1994). Determination of lymphocyte division by flow cytometry. *Journal of immunological methods*, *171*(1), 131–137. https://doi.org/10.1016/0022-1759(94)90236-4

37. Salic, A., & Mitchison, T. J. (2008). A chemical method for fast and sensitive detection of DNA synthesis in vivo. *Proceedings of the National Academy of Sciences of the United States of America*, *105*(7), 2415–2420. https://doi.org/10.1073/pnas.0712168105

38. Morea, E. G. O., Vasconcelos, E. J. R., Alves, C. S., Giorgio, S., Myler, P. J., Langoni, H., Azzalin, C. M., & Cano, M. I. N. (2021). Exploring TERRA during *Leishmania major* developmental cycle and continuous in vitro passages. *International journal of biological macromolecules*, *174*, 573–586. https://doi.org/10.1016/j.ijbiomac.2021.01.192

39. Borst, P., & Sabatini, R. (2008). Base J: discovery, biosynthesis, and possible functions. *Annual review of microbiology*, *62*, 235–251. https://doi.org/10.1146/annurev.micro.62.081307.162750

40. Baerlocher, G. M., Vulto, I., de Jong, G., & Lansdorp, P. M. (2006). Flow cytometry and FISH to measure the average length of telomeres (flow FISH). *Nature protocols*, *1*(5), 2365–2376. https://doi.org/10.1038/nprot.2006.263

41. da Silva, M. S., Segatto, M., Pavani, R. S., Gutierrez-Rodrigues, F., Bispo, V. D., de Medeiros, M. H., Calado, R. T., Elias, M. C., & Cano, M. I. (2017). Consequences of acute oxidative stress in *Leishmania amazonensis*: From telomere shortening to the selection of the fittest parasites. *Biochimica et biophysica acta. Molecular cell research*, *1864*(1), 138–150. https://doi.org/10.1016/j.bbamcr.2016.11.001

42. Cusanelli, E., Romero, C. A., & Chartrand, P. (2013). Telomeric noncoding RNA TERRA is induced by telomere shortening to nucleate telomerase molecules at short telomeres. *Molecular cell*, *51*(6), 780–791. https://doi.org/10.1016/j.molcel.2013.08.029

43. Deng, Z., Wang, Z., Xiang, C., Molczan, A., Baubet, V., Conejo-Garcia, J., Xu, X., Lieberman, P. M., & Dahmane, N. (2012). Formation of telomeric repeat-containing RNA (TERRA) foci in highly proliferating mouse cerebellar neuronal progenitors and

medulloblastoma. *Journal of cell science*, *125*(Pt 18), 4383–4394. https://doi.org/10.1242/jcs.108118

44. Olive, P. L. (2009). Endogenous DNA breaks: gamma-H2AX and the role of telomeres. Aging, 1(2), 154–156. https://doi.org/10.18632/aging.100025
45. McKean, P. G., Keen, J. K., Smith, D. F., & Benson, F. E. (2001). Identification and characterisation of a RAD51 gene from *Leishmania major*. *Molecular and biochemical parasitology*, *115*(2), 209–216. https://doi.org/10.1016/s0166-6851(01)00288-2
46. Sleigh M. J. (1976). The mechanism of DNA breakage by phleomycin in vitro. *Nucleic acids research*, *3*(4), 891–901. https://doi.org/10.1093/nar/3.4.891
47. Da Silveira, R.deC., Da Silva, M. S., Nunes, V. S., Perez, A. M., & Cano, M. I. (2013). The natural absence of RPA1N domain did not impair Leishmania amazonensis RPA-1 participation in DNA damage response and telomere protection. Parasitology, 140(4), 547–559. https://doi.org/10.1017/S0031182012002028
48. Nagata, S. (2000). Apoptotic DNA fragmentation. *Experimental cell research*, *256*(1), 12–18. https://doi.org/10.1006/excr.2000.4834
49. de Souza, E. M., Menna-Barreto, R., Araújo-Jorge, T. C., Kumar, A., Hu, Q., Boykin, D. W., & Soeiro, M. N. (2006). Antiparasitic activity of aromatic diamidines is related to apoptosis-like death in Trypanosoma cruzi. *Parasitology*, *133*(Pt 1), 75–79. https://doi.org/10.1017/S0031182006000084
50. Basmaciyan, L., & Casanova, M. (2019). Cell death in *Leishmania*. La mort cellulaire chez *Leishmania*. Parasite (Paris, France), 26, 71. https://doi.org/10.1051/parasite/2019071
51. Sirbu, B. M., Couch, F. B., Feigerle, J. T., Bhaskara, S., Hiebert, S. W., & Cortez, D. (2011). Analysis of protein dynamics at active, stalled, and collapsed replication forks. Genes & development, 25(12), 1320–1327. https://doi.org/10.1101/gad.2053211
52. Zauli-Nascimento, R. C., Miguel, D. C., Yokoyama-Yasunaka, J. K., Pereira, L. I., Pelli de Oliveira, M. A., Ribeiro-Dias, F., Dorta, M. L., & Uliana, S. R. (2010). In vitro sensitivity of *Leishmania* (Viannia) *braziliensis* and *Leishmania* (Leishmania) *amazonensis* Brazilian isolates to meglumine antimoniate and amphotericin B. *Tropical medicine & international health : TM & IH*, *15*(1), 68–76. https://doi.org/10.1111/j.1365-3156.2009.02414.x

53. Niida, H., Matsumoto, T., Satoh, H., Shiwa, M., Tokutake, Y., Furuichi, Y., & Shinkai, Y. (1998). Severe growth defect in mouse cells lacking the telomerase RNA component. *Nature genetics*, *19*(2), 203–206. https://doi.org/10.1038/580

54. Dreesen, O., & Cross, G. A. (2006). Consequences of telomere shortening at an active VSG expression site in telomerase-deficient Trypanosoma brucei. Eukaryotic cell, 5(12), 2114–2119. https://doi.org/10.1128/EC.00059-06

55. Blasco, M. A., Lee, H. W., Hande, M. P., Samper, E., Lansdorp, P. M., DePinho, R. A., & Greider, C. W. (1997). Telomere shortening and tumor formation by mouse cells lacking telomerase RNA. *Cell*, *91*(1), 25–34. https://doi.org/10.1016/s0092-8674(01)80006-4

56. Leonardi, J., Box, J. A., Bunch, J. T., & Baumann, P. (2008). TER1, the RNA subunit of fission yeast telomerase. *Nature structural & molecular biology*, *15*(1), 26–33. https://doi.org/10.1038/nsmb1343

57. Wellinger, R. J., & Zakian, V. A. (2012). Everything you ever wanted to know about Saccharomyces cerevisiae telomeres: beginning to end. *Genetics*, *191*(4), 1073–1105. https://doi.org/10.1534/genetics.111.137851

58. Arnoult, N., & Karlseder, J. (2015). Complex interactions between the DNA-damage response and mammalian telomeres. *Nature structural & molecular biology*, *22*(11), 859–866. https://doi.org/10.1038/nsmb.3092

59. Fasching, C. L., Bower, K., & Reddel, R. R. (2005). Telomerase-independent telomere length maintenance in the absence of alternative lengthening of telomeres-associated promyelocytic leukemia bodies. *Cancer research*, *65*(7), 2722–2729. https://doi.org/10.1158/0008-5472.CAN-04-2881

60. Grandin, N., & Charbonneau, M. (2008). Protection against chromosome degradation at the telomeres. Biochimie, 90(1), 41–59. https://doi.org/10.1016/j.biochi.2007.07.008

61. Glover, L., & Horn, D. (2012). Trypanosomal histone γH2A and the DNA damage response. Molecular and biochemical parasitology, 183(1), 78–83. https://doi.org/10.1016/j.molbiopara.2012.01.008

62. Ward, I. M., & Chen, J. (2001). Histone H2AX is phosphorylated in an ATR-dependent manner in response to replicational stress. The Journal of biological chemistry, 276(51), 47759–47762. https://doi.org/10.1074/jbc.C100569200

63. Silva, B., Arora, R., & Azzalin, C. M. (2022). The alternative lengthening of telomeres mechanism jeopardizes telomere integrity if not properly restricted. Proceedings of the

National Academy of Sciences of the United States of America, 119(39), e2208669119. https://doi.org/10.1073/pnas.2208669119

64. Mah, L. J., El-Osta, A., & Karagiannis, T. C. (2010). Gamma-H2AX: a sensitive molecular marker of DNA damage and repair. *Leukemia*, *24*(4), 679–686. https://doi.org/10.1038/leu.2010.6
65. Smith, C. D., & Blackburn, E. H. (1999). Uncapping and deregulation of telomeres lead to detrimental cellular consequences in yeast. *The Journal of cell biology*, *145*(2), 203–214. https://doi.org/10.1083/jcb.145.2.203
66. Gómez-Virgilio, L., Silva-Lucero, M. D., Flores-Morelos, D. S., Gallardo-Nieto, J., Lopez-Toledo, G., Abarca-Fernandez, A. M., Zacapala-Gómez, A. E., Luna-Muñoz, J., Montiel-Sosa, F., Soto-Rojas, L. O., Pacheco-Herrero, M., & Cardenas-Aguayo, M. D. (2022). Autophagy: A Key Regulator of Homeostasis and Disease: An Overview of Molecular Mechanisms and Modulators. *Cells*, *11*(15), 2262. https://doi.org/10.3390/cells11152262
67. Pearson, R. D., Romito, R., Symes, P. H., & Harcus, J. L. (1981). Interaction of *Leishmania donovani* promastigotes with human monocyte-derived macrophages: parasite entry, intracellular survival, and multiplication. *Infection and immunity*, *32*(3), 1249–1253. https://doi.org/10.1128/iai.32.3.1249-1253.1981
68. Hovel-Miner, G. A., Boothroyd, C. E., Mugnier, M., Dreesen, O., Cross, G. A., & Papavasiliou, F. N. (2012). Telomere length affects the frequency and mechanism of antigenic variation in Trypanosoma brucei. *PLoS pathogens*, *8*(8), e1002900. https://doi.org/10.1371/journal.ppat.1002900
69. Dobson, D. E., Scholtes, L. D., Myler, P. J., Turco, S. J., & Beverley, S. M. (2006). Genomic organization and expression of the expanded SCG/L/R gene family of *Leishmania major*: internal clusters and telomeric localization of SCGs mediating species-specific LPG modifications. *Molecular and biochemical parasitology*, *146*(2), 231–241. https://doi.org/10.1016/j.molbiopara.2005.12.012
70. Ivens, A. C., Peacock, C. S., Worthey, E. A., Murphy, L., Aggarwal, G., Berriman, M., Sisk, E., Rajandream, M. A., Adlem, E., Aert, R. et *al*. (2005). The genome of the kinetoplastid parasite, *Leishmania major*. *Science (New York, N.Y.)*, *309*(5733), 436–442. https://doi.org/10.1126/science.1112680
71. Damasceno, J. D., Obonaga, R., Santos, E. V., Scott, A., McCulloch, R., & Tosi, L. R. (2016). Functional compartmentalization of Rad9 and Hus1 reveals diverse assembly of

the 9-1-1 complex components during the DNA damage response in *Leishmania*. Molecular microbiology, 101(6), 1054–1068. https://doi.org/10.1111/mmi.13441

72. LeBowitz, J. H., Coburn, C. M., & Beverley, S. M. (1991). Simultaneous transient expression assays of the trypanosomatid parasite *Leishmania* using beta-galactosidase and beta-glucuronidase as reporter enzymes. *Gene*, *103*(1), 119–123. https://doi.org/10.1016/0378-1119(91)90402-w
73. Camacho, C., Coulouris, G., Avagyan, V., Ma, N., Papadopoulos, J., Bealer, K., & Madden, T. L. (2009). BLAST+: architecture and applications. *BMC bioinformatics*, *10*, 421. https://doi.org/10.1186/1471-2105-10-421
74. Madeira, F., Pearce, M., Tivey, A. R. N., Basutkar, P., Lee, J., Edbali, O., Madhusoodanan, N., Kolesnikov, A., & Lopez, R. (2022). Search and sequence analysis tools services from EMBL-EBI in 2022. *Nucleic acids research*, *50*(W1), W276–W279. https://doi.org/10.1093/nar/gkac240
75. Peng, D., & Tarleton, R. (2015). EuPaGDT: a web tool tailored to design CRISPR guide RNAs for eukaryotic pathogens. *Microbial genomics*, *1*(4), e000033. https://doi.org/10.1099/mgen.0.000033
76. Kapler, G. M., Coburn, C. M., & Beverley, S. M. (1990). Stable transfection of the human parasite *Leishmania* major delineates a 30-kilobase region sufficient for extrachromosomal replication and expression. *Molecular and cellular biology*, *10*(3), 1084–1094. https://doi.org/10.1128/mcb.10.3.1084-1094.1990
77. Barbiéri, C. L., Doine, A. I., & Freymuller, E. (1990). Lysosomal depletion in macrophages from spleen and foot lesions of *Leishmania*-infected hamster. *Experimental parasitology*, *71*(2), 218–228. https://doi.org/10.1016/0014-4894(90)90024-7
78. Medina-Acosta, E., & Cross, G. A. (1993). Rapid isolation of DNA from trypanosomatid protozoa using a simple 'mini-prep' procedure. *Molecular and biochemical parasitology*, *59*(2), 327–329. https://doi.org/10.1016/0166-6851(93)90231-l
79. Conte, F. F., & Cano, M. I. (2005). Genomic organization of telomeric and subtelomeric sequences of *Leishmania* (Leishmania) *amazonensis*. *International journal for parasitology*, *35*(13), 1435–1443. https://doi.org/10.1016/j.ijpara.2005.05.011
80. Chiurillo, M. A., Cano, I., Da Silveira, J. F., & Ramirez, J. L. (1999). Organization of telomeric and sub-telomeric regions of chromosomes from the protozoan parasite Trypanosoma cruzi. *Molecular and biochemical parasitology*, *100*(2), 173–183. https://doi.org/10.1016/s0166-6851(99)00047-x

81. de Oliveira, B. C. D., Shiburah, M. E., Paiva, S. C., Vieira, M. R., Morea, E. G. O., da Silva, M. S., Alves, C. S., Segatto, M., Gutierrez-Rodrigues, F., Borges, J. C. et *al*. (2021). Possible Involvement of Hp90 in the Regulation of Telomere Length and Telomerase Activity During the *Leishmania amazonensis* Developmental Cycle and Population Proliferation. *Frontiers in cell and developmental biology*, *9*, 713415. https://doi.org/10.3389/fcell.2021.713415

82. Sambrook, J., & Russell, D. W. (2001). Molecular Cloning: A Laboratory Manual, *Cold Spring Harbor Laboratory Press.*

83. Inbar, E., Hughitt, V. K., Dillon, L. A., Ghosh, K., El-Sayed, N. M., & Sacks, D. L. (2017). The Transcriptome of *Leishmania major* Developmental Stages in Their Natural Sand Fly Vector. *mBio*, *8*(2), e00029-17. https://doi.org/10.1128/mBio.00029-17

84. Livak, K. J., & Schmittgen, T. D. (2001). Analysis of relative gene expression data using real-time quantitative PCR and the 2(-Delta Delta C(T)) Method. *Methods (San Diego, Calif.)*, *25*(4), 402–408. https://doi.org/10.1006/meth.2001.1262

85. Barak, E., Amin-Spector, S., Gerliak, E., Goyard, S., Holland, N., & Zilberstein, D. (2005). Differentiation of *Leishmania donovani* in host-free system: analysis of signal perception and response. Molecular and biochemical parasitology, 141(1), 99–108. https://doi.org/10.1016/j.molbiopara.2005.02.004

86. de Oliveira, B. C. D., Assis, L. H. C., Shiburah, M. E., Paiva, S. C., Fontes, V. S., de Oliveira, L. S., da Silva, V. L., da Silva, M. S., & Cano, M. I. N. (2022). Synchronization of *Leishmania amazonensis* Cell Cycle Using Hydroxyurea. *Methods in molecular biology (Clifton, N.J.)*, *2579*, 127–135. https://doi.org/10.1007/978-1-0716-2736-5_10

87. da Silva, M. S., Monteiro, J. P., Nunes, V. S., Vasconcelos, E. J., Perez, A. M., Freitas-Júnior, L. de H., Elias, M. C., & Cano, M. I. (2013). *Leishmania amazonensis* promastigotes present two distinct modes of nucleus and kinetoplast segregation during cell cycle. *PloS one*, *8*(11), e81397. https://doi.org/10.1371/journal.pone.0081397

88. da Silva, M. S., Muñoz, P. A. M., Armelin, H. A., & Elias, M. C. (2017). Differences in the Detection of BrdU/EdU Incorporation Assays Alter the Calculation for G1, S, and G2 Phases of the Cell Cycle in Trypanosomatids. *The Journal of eukaryotic microbiology*, *64*(6), 756–770. https://doi.org/10.1111/jeu.12408

89. Ambit, A., Woods, K. L., Cull, B., Coombs, G. H., & Mottram, J. C. (2011). Morphological events during the cell cycle of *Leishmania major*. *Eukaryotic cell*, *10*(11), 1429–1438. https://doi.org/10.1128/EC.05118-11

90. Sangenito, L. S., Rodrigues, H. D., Santiago, S. O., Bombaça, A. C. S., Menna-Barreto, R. F., Reddy, A., ... & Santos, A. L. (2021). In vitro effects of bis (N-[4-(hydroxyphenyl) methyl]-2-pyridinemethamine) zinc perchlorate monohydrate 4 on the physiology and interaction process of *Leishmania amazonensis*. *Parasitology International, 84*, 102376.

91. Rebello, K. M., Menna-Barreto, R. F., Chagas-Moutinho, V. A., Mota, E. M., Perales, J., Neves-Ferreira, A. G., Oliveira-Menezes, A., & Lenzi, H. (2013). Morphological aspects of Angiostrongylus costaricensis by light and scanning electron microscopy. *Acta tropica*, *127*(3), 191–198. https://doi.org/10.1016/j.actatropica.2013.05.002

92. Zamboni, D. S., & Rabinovitch, M. (2003). Nitric oxide partially controls Coxiella burnetii phase II infection in mouse primary macrophages. *Infection and immunity*, *71*(3), 1225–1233. https://doi.org/10.1128/IAI.71.3.1225-1233.2003

93. Ferreira, B. A., Coser, E. M., Saborito, C., Yamashiro-Kanashiro, E. H., Lindoso, J. A. L., & Coelho, A. C. (2023). In vitro miltefosine and amphotericin B susceptibility of strains and clinical isolates of *Leishmania* species endemic in Brazil that cause tegumentary leishmaniasis. *Experimental parasitology*, *246*, 108462. https://doi.org/10.1016/j.exppara.2023.108462

94. Colhone, M. C., Arrais-Silva, W. W., Picoli, C., & Giorgio, S. (2004). Effect of hypoxia on macrophage infection by *Leishmania amazonensis*. *The Journal of parasitology*, *90*(3), 510–515. https://doi.org/10.1645/GE-3286

95. de Mesquita Barbosa, A., Dos Santos Costa, S., da Rocha, J. R., Montanari, C. A., & Giorgio, S. (2015). Evaluation of the leishmanicidal and cytotoxic effects of inhibitors for microorganism metabolic pathway enzymes. Biomedicine & pharmacotherapy = Biomedecine & pharmacotherapie, 74, 95–100. https://doi.org/10.1016/j.biopha.2015.07.040

Supplementary Material

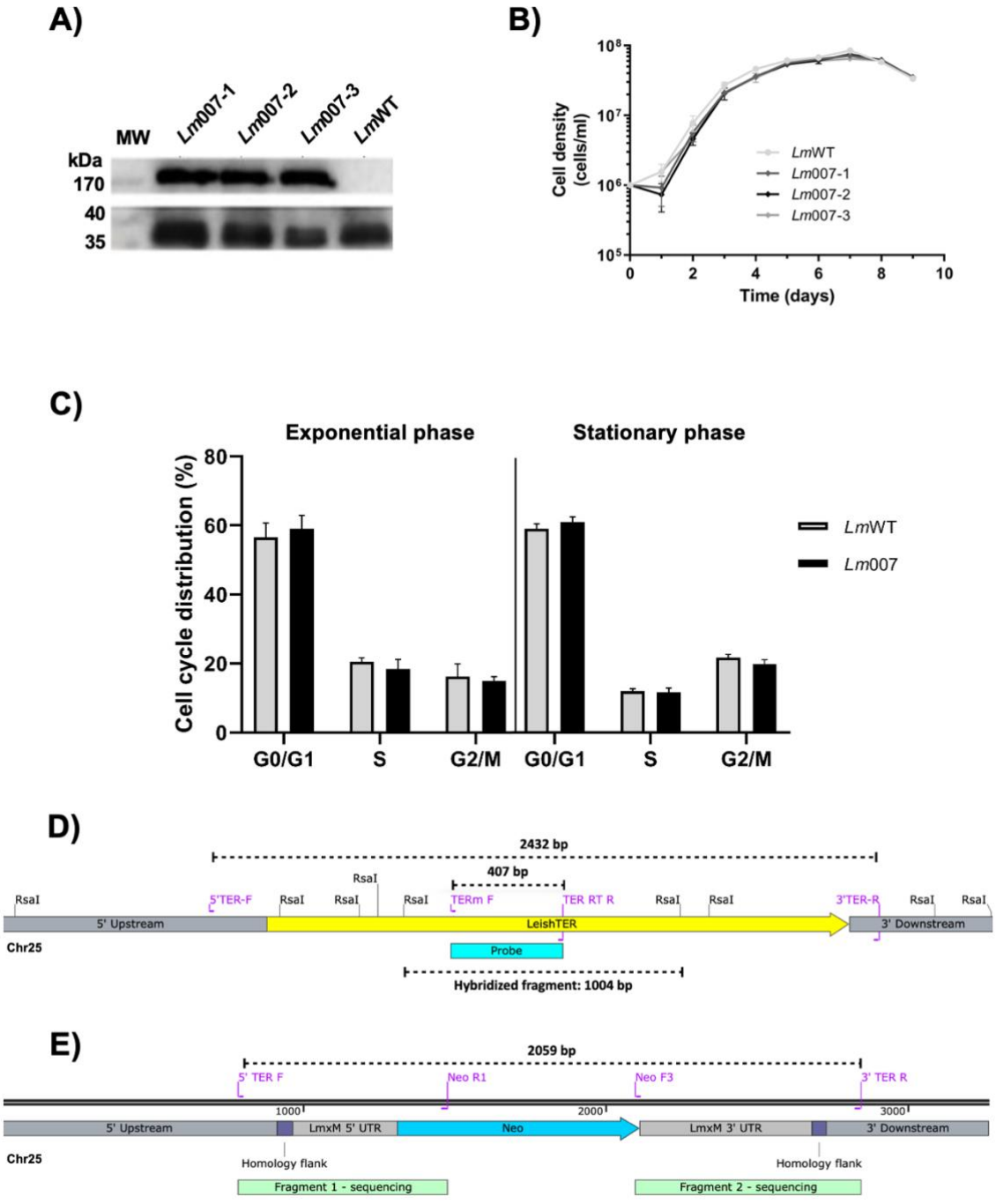

S1 Fig. Episomal expression of Cas9 does not interfere with proliferation and cell cycle progression in *L. major*. A) Western blot analysis using an anti-Flag antibody was done to verify the expression of Cas9 in *Lm*007 clones. Anti-*Lm*GAPDH antibody served as the loading control, and a molecular weight marker (Page Ruler, Invitrogen) was used for reference. B) Growth curves of *Lm*007 and wild-type parasites were generated by daily cell counting (every 24 h) using a Neubauer chamber. The graph represents the mean values of technical triplicates. C) Cell cycle profiles of *Lm*007-1 clone and *Lm*WT at P5 are depicted. Cell cycle analyses were conducted on days 3 (exponential growth phase - left graph) and 5 (stationary phase - right graph). D) The schematic map illustrates the *Leish*TER locus in *Lm*WT. The position of each primer set used for PCR amplification (5' TER F + 3' TER R – S1 Table) and RT-PCR (TERm F + TER RT R – S1 Table) are signaled (purple), along with the expected amplicon sizes (2432 bp and 407 bp, respectively). The position of the *Rsa*I restriction sites, the primers used to generate the DIG-labeled TER probe (in royal blue), and the size of the fragment hybridized with the probe

(1004 bp) are also shown. E) A schematic map of the *Leish*TER gene locus at chromosome 25 after gene edition using CRISPR/Cas9 is shown. The primer set (5' TER F + 3' TER R – S1 Table) was used to confirm the insertion of the donor DNA cassette that replaced *Leish*TER. The expected amplicon size (2059 bp) and the primers used for DNA sequencing analysis (5' TER F + Neo R1; Neo F3 + 3' TER R – S1 Table) are indicated.

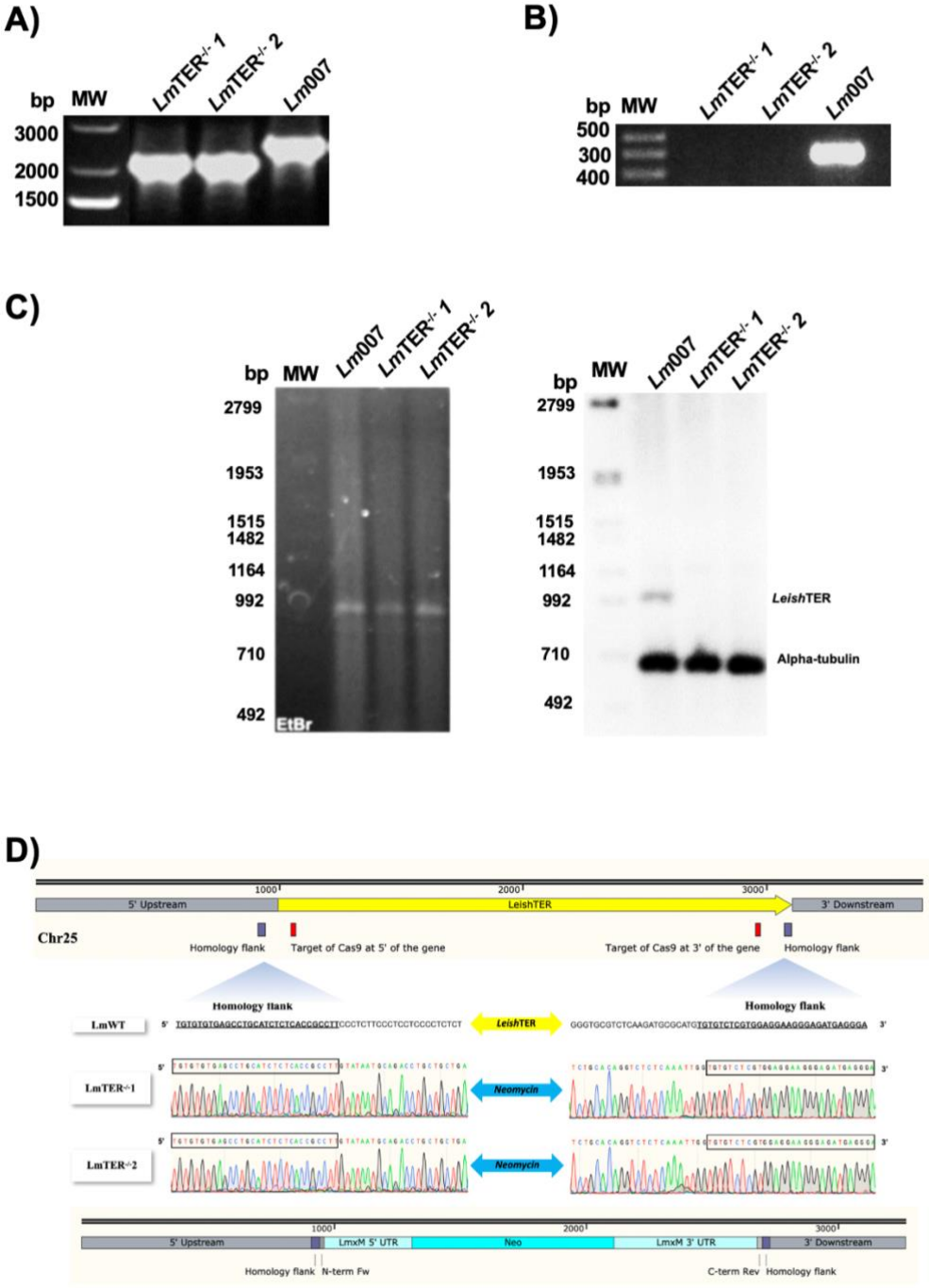

S2 Fig. Generation of *Leish*TER double knockout (*Lm*TER$^{-/-}$) was successfully achieved. A) PCR amplification was performed using specific primer sets to validate the edition of the *Leish*TER locus. The PCR products were separated in a 1% agarose gel stained with ethidium bromide. A molecular weight marker (1 Kb Plus DNA ladder, Invitrogen) was included for reference. B) RT-PCR was conducted using the TERm F and TER RT R primer set (S1 Table), which amplifies an internal *Leish*TER fragment of 407 bp, and total RNA obtained from *Lm*TER$^{-/-}$ clones and *Lm*007. The cDNA samples were fractionated in a 1% agarose gel stained with ethidium bromide. A molecular weight marker (1 Kb Plus DNA ladder, Invitrogen) was used for reference. C) Southern blot analysis was performed using *Rsa*I digested-DNA obtained from *Lm*007 and *Lm*TER$^{-/-}$ clones, hybridized with a DIG-labeled TER probe (S1 Table). Additionally, a DIG-labeled Alpha-tubulin probe (~700 bp) served as the loading control (S1 Table). DNA molecular weight marker VII, DIG-labeled (Roche), was employed for reference. D) The diagram illustrates the outcomes of the edited and unedited *Leish*TER locus. The top image portrays the wild-type *Leish*TER locus, highlighting the homology regions (purple) and the sgRNAs target regions (red). Electropherograms (middle image) indicate the positions of the 5' and 3' homology regions containing shared

sequences between *Lm*WT and *Lm*TER$^{-/-}$ clones. The integration of the donor DNA cassette containing the neomycin resistance gene within the *Leish*TER locus (both alleles) is depicted (bottom image).

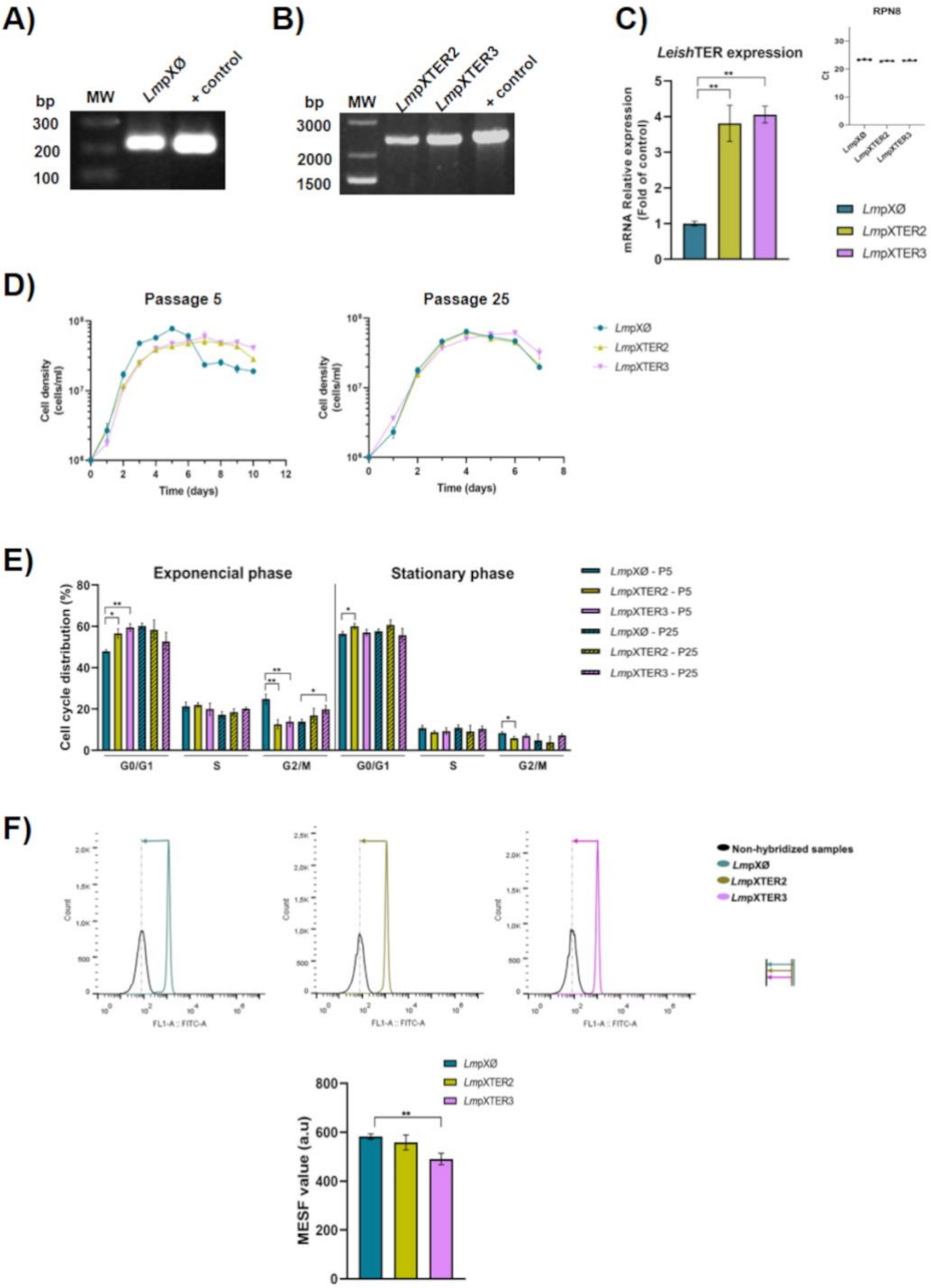

S3 Fig. The creation of a *Leish*TER overexpressor lineage, known as *Lmp*XTER, has a dominant negative effect on the parasite similar to the depletion of *Leish*TER. A) PCR using a specific primer set, was carried out to verify the acquisition of the control lineage carrying the pX63Neo plasmid, denoted as *Lmp*XØ. B) Clones overexpressing *Leish*TER, designated as *Lmp*XTER2 and *Lmp*XTER3, were also confirmed by PCR using the same primer set as in A). C) *Leish*TER expression was assessed by RT-qPCR using total RNA extracted from *Lmp*XTER2, *Lmp*XTER3 and *Lmp*XØ. The upper right panel displays the Ct values of the reference gene RPN8. D) Growth curves of *Lmp*XØ, *Lmp*XTER2, and *Lmp*XTER3 at P5 (left panel) and P25 (right panel) were obtained by daily counting using a Neubauer chamber. E) Cell cycle analyses of *Lmp*XØ, *Lmp*XTER2 and *Lmp*XTER3 at P5 and P25 were conducted using parasites in the exponential (left panel) and stationary growth phases (right panel). F) A PNA FITC-labeled telomeric DNA oligo probe $(CCCTAA)_3$ (Panagene) was used to perform the

Flow-FISH analysis. The histograms represent the mean fluorescence of non-hybridized parasites (in black) and parasites hybridized with the telomeric probe (*Lm*pXØ in green, *Lm*pXTER2 in yellow, and *Lm*pXTER3 in pink). Vertical lines mark the difference between peaks, and horizontal lines with arrows represent telomere length differences in the populations analyzed. The amount of fluorescence among samples was calculated using MESF, and the means ± S.D. of technical triplicate was plotted in the graph (bottom). All data are presented as mean ± SD and represent triplicate experiments. Statistical analysis was conducted using the student t-test, with Welch's correction applied when necessary (*$p \leq 0.05$, **$p \leq 0.01$).

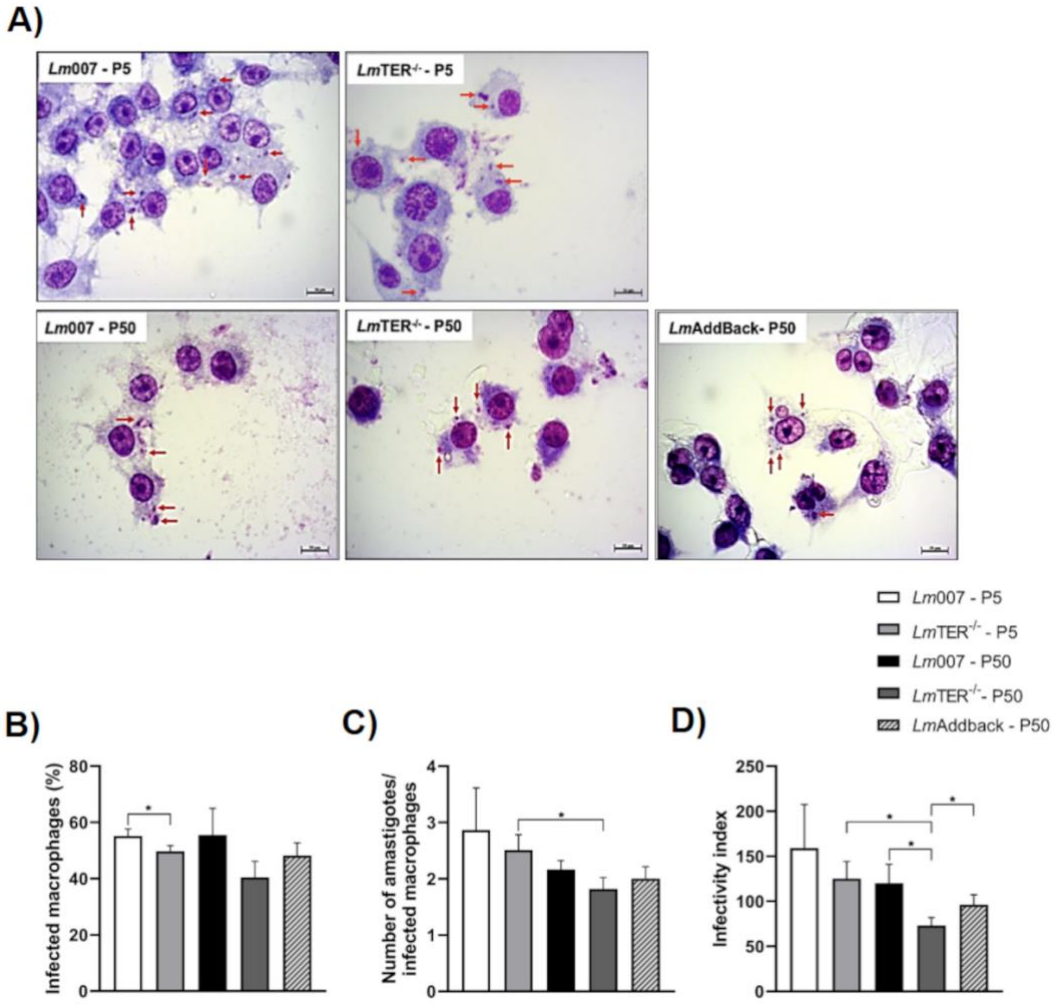

S4 Fig. The reduced infectivity of BMDM by *Lm*TER$^{-/-}$ was validated through a subsequent in vitro experiment using RAW 264.7 cells. A) Photomicrographs depict RAW 264.7 macrophages infected for 24 h with *Lm*007 and *Lm*TER$^{-/-}$ at P5 and P50, as well as with *Lm*Addback at P50. Red arrows indicate internalized *L. major* parasites. Images were captured randomly at 1000X magnification. Scale bars = 10 μm. B) Percentage of RAW 264.7 macrophages infected with *Lm*007 and *Lm*TER$^{-/-}$ (P5 and P50), and *Lm*AddBack (P50). C) Number of amastigotes per macrophage in infections with *Lm*007 and *Lm*TER$^{-/-}$ (P5 and P50), and *Lm*AddBack (P50). D) The estimated infectivity index of *Lm*007, *Lm*TER$^{-/-}$ at P5 and P50 and *Lm*AddBack at P50 in RAW 264.7 macrophages. All data are presented as mean ± SD and represent triplicate experiments. Statistical analysis was conducted using the Student t-test with Welch's correction as needed. *$p \leq 0.05$.

S1 Table. Oligonucleotide sequences

Name	Sequence 5’ - 3’	Reference
For-Cas9	CCGAAGAGGTCGTGAAGAAG	Current work
Rev-Cas9	GCCTTATCCAGTTCGCTCAG	Current work
T7RNAP-F	TAAGCGCGGCAAGCGCCCGA	Current work
T7RNAP-R	GACCTACTACGCCAGCATTT	Current work
5’ TER F	GGTTCTTTCCCCTTGCACTG	Current work
5’ TER R	CAATCTCCCGTGTGGTGCTT	Current work
3’ TER R	TTCTGCGGTTCAGCACTACA	Current work
Neo R1	AGGTCGGTCTTGACAAAAAGAACC	Current work
Neo F3	TGACGAGTTCTTCAGCTCCG	Current work
TracrRNA (G00) – scaffold	AAAAGCACCGACTCGGTGCCACTTTTT CAAGTTGATAACGGACTAGCCTTATTT TAACTTGCTATTTCTAGCTCTAAAAC	[34]
TER-seed 5’	GAAATTAATACGACTCACTATAGGAGG TGTCGGACGATGTCCTAGTTTTAGAGC TAGAAATAGC	Current work, generated at http://grna.ctegd.uga.edu

TER-seed 3’	GAAATTAATACGACTCACTATAGGAGC GTGGCGTCGATAAAAACGTTTTAGAGC TAGAAATAGC	Current work, generated at http://grna.ctegd.uga.edu
N-term For (TER)	TGTGTGTGAGCCTGCATCTCTCACCGC CTTGTATAATGCAGACCTGCTGC	Current work, generate at http://www.leishgedit.net/Home.html
C-term Rev (TER)	TCCCTCATCTCCCTTCCTCCACGAGACA CACCAATTTGAGAGACCTGTGC	Current work, generate at http://www.leishgedit.net/Home.html
DIG-labeled TelC probe	CCCTAACCCTAACCCTAACCCTAACCC TAA	[41, 81]
Lmj 18s RNA Fw	AGTGTGGAGATCGAAGATGATTAG	Current work
Lmj 18s RNA Rv	CCCTGAGACTGTAACCTCAAAG	Current work
DIG-labeled 18S rRNA probe	AGTGTGGAGATCGAAGATGATTAGAG ACCATTGTAGTCCACACTGCAAACGAT GACACCCATGAATTGGGGATCTTATGG GCCGGCCTGCGGCAGGGTTTACCCTGT GTCAGCACCGCGCCCGCTTTTACCAAC TTACGTATCTTTTCTATTCGGCCTTTAC CGGCCACCCACGGGAATATCCTCAGCA	Current work

	CGTTTTCTGTTTTTTCACGCGAAAGCTT TGAGGTTACAGTCTCAGGG	
AlfaTub-1 Fw	CGAACAACTACGCTCGTGGC	Current work
AlfaTub-1 Rv	GCCACCCACAGCGTGGAACA	Current work
DIG-labeled Alpha-Tubuline probe	CGAACAACTACGCTCGTGGCCACTACA CGATCGGCAAGGAGATCGTCGACCTTG CGCTGGACCGCATTCGCAAGCTGGCGG ACAACTGCACTGGTCTCCAGGGCTTTA TGGTGTTCCACGCTGTGGGTGGC	Current work
TERm F	TGCTTGCATGTCTGTCCTTC	Current work
TER RT F	GAGAACTAGCACGGCCACTC	Current work
TER RT R	GAGGATCGCGCTACAAAGTC	Current work
DIG-labeled TER probe	TGCTTGCATGTCTGTCCTTCGTCTCAGC ACGCGCGTGCGCGCACACTATGCCGGC CCTTCATCGCTCAACGGCTCTTTTTCCG TTTCGCACCTGTGCCCTCAGGAGCGCG TAAGCACGCCTAAGCACACACCGTCAC GCAGAATCAGACCCCACGCGTGATTGC AAGCGATGCGGCCTCTCACTGCAGTCG AGGTGGGGCAACGGGCGCAGTCCGCCT TCTCCCTTTCTCATTTGCTTTTCAGTAT GCTGGCCTTCTCGCCGTCGGTGAGGGT	Current work

	GTTATGTGTGTGCGTGCGGGCGTGTGG	
	TGCACCACCATGGACTGTGAGAACTAG	
	CACGGCCACTCAGGCATGCACACATAC	
	ACGTGCACGTGCACGTGCACACGCGCG	
	TGCACCGACTTTGTAGCGCGATCCTC	
SUBCHRO. 29R-F	ATGGGGATTAAGGGAAGCAC	[38]
LMCHR29_RV_2	CCCGTACCCGTACCTTATCC	Current work
RPN8 F	ATGAACCGCCGCAAGCT	[38]
RPN8 R	GGCGCGACGACGATCTTTGATT	[38]
pX63 Neo Fw	CACCACCCTCAACCACCC	Current work
pX63 Neo Rv	CAATACGCAAACCGCCTC	Current work

S2 Table. Flow-FISH (MESF ± SD analysis) of *Lm*007, *Lm*TER$^{-/-}$, *Lm*pXØ and *Lm*pXTER cells

Samples	MESF value (a.u.) ± SD	Proportional change (MESF analysis)
*Lm*007 - P5	516.3 ± 34.65	1
*Lm*TER$^{-/-}$ - P5	354.3 ± 13.43	0,69
*Lm*007 - P50	502.7 ± 30.83	1
*Lm*TER$^{-/-}$ - P50	261.7 ± 14.29	0,52
*Lm*pX0 - P25	582.3 ± 11.02	1

*Lm*pXT2 - P25	558.7 ± 30.57	0,96
*Lm*pXT3 - P25	491 ± 23.07	0,84

S3 Table. In Vitro Infectivity Assessment of *Lm*TER$^{-/-}$, *Lm*007 (P5 and P50), and *Lm*AddBack (P50) on Balb/c Bone Marrow-Derived Macrophages (BMDM)

Samples	Infected macrophages (%) ± S.D.	Number of amastigotes/infected macrophages ± S.D.	Infectivity index (%) ± S.D.
*Lm*007 – P5 – 24 h	29.8 ± 1.96	1.86 ± 0.17	55.4 ± 6.67
*Lm*TER$^{-/-}$ - P5 – 24 h	18.5 ± 0.61	1.65 ± 0.37	30.7 ± 7.65
*Lm*007 – P50 – 24 h	31.5 ± 2.27	2.4 ± 0.22	75.7 ± 9.62
*Lm*TER$^{-/-}$ - P50 – 24 h	27.9 ± 4.05	1.81 ± 0.04	50.5 ± 6.21
*Lm*Addback – P50 – 24 h	36.1 ± 3.49	1.74 ± 0.16	63 ± 8.09
*Lm*007 – P5 – 48 h	69.2 ± 6.52	3.35 ± 0.24	232 ± 28.7

*Lm*TER$^{-/-}$ - P5 – 48 h	28.5 ± 1.95	1.91 ± 0.08	54.3 ± 1.48
*Lm*007 – P50 – 48 h	57.8 ± 1.02	3.18 ± 0.20	184 ± 12.1
*Lm*TER$^{-/-}$ - P50 – 48 h	50.8 ± 3.42	2 ± 0.03	102 ± 6.42
*Lm*Addback – P50 – 48 h	44.2 ± 4.19	2.11 ± 0.14	92.9 ± 6.71

3.2 Capítulo 2

Relatório da Bolsa Estágio de Pesquisa no Exterior (BEPE) financiada pela FAPESP (Processo: 2022/05039-1)

Structural assessment of the core domains of *Leishmania major* telomerase RNA (*Leish*TER)

Beatriz C D de Oliveira[1], Arthur de Oliveira Passos[1], Kaitlin Klotz[2], Kausik Chakrabarti[2], Maria I N Cano[1]

[1]Department of Chemical and Biological Sciences, Biosciences Institute, São Paulo State University (UNESP), Botucatu, SP, Brazil
[2]Department of Biological Sciences, University of North Carolina, Charlotte, NC, USA

Abstract

Leishmaniases are neglected tropical diseases caused by different species of *Leishmania*, a protozoa parasite belonging to the Trypanosomatidae family. Every year, about 1 million people worldwide are threatened by the disease. Besides its high incidence rate, there is still no efficient prevention and treatment. Therefore, a deeper understanding of parasite biology will help develop new therapies to treat the disease. Telomeres are key to maintaining genome stability and integrity and, thus, are considered potential targets for drug design. *Leishmania* spp. telomeres, similarly to other eukaryotes, are nucleoprotein structures formed by repetitive DNA in double and single-stranded forms, with the single strand protruding towards the end of the chromosome (known as the 3' G-overhang). Telomeres are maintained by telomerase, a ribonucleoprotein complex minimally composed of a protein subunit, the Telomerase Reverse Transcriptase (TERT), and a noncoding RNA, the telomerase RNA (TER). The *Leishmania* TER (*Leish*TER), like *Trypanosoma brucei* TER (*Tb*TER), is one of the largest TER described so far, making it difficult to characterize its structure due to its large size and sequence diversity. Current information about *Leish*TER's putative architecture and secondary structure is mainly based on bioinformatics analysis. At the University of North Carolina, Charlotte, USA, Dr. Chakrabarti's group and colleagues used an approach to characterize unusual long RNA structures at single-nucleotide resolution, such as *Tb*TER. The methodology combines in-cell chemical probing (in vivo and ex vivo) using DMS (dimethyl sulfate) and NAI (2-methyl nicotinic acid imidazolide) with targeted high-throughput RNA sequencing and mutational mapping. We proposed collaborating with Dr. Chakrabarti's group to apply this methodology to elucidate the *Leish*TER structural domains. Due to the known structural similarities between *Tb*TER and *Leish*TER, we intended to learn the methodology at Dr. Chakrabarti's lab and apply it in our lab in Brazil (Telomeres Lab) to gather information about *Leish*TER structure and further from other lncRNAs like TERRA. The results from the pilot experiment showed to be successful, where the different NAI concentrations tested revealed similar structures for the first 242 nt, with 100 mM and 150 mM concentrations showing the best mutation rates. The obtained results confirmed predicted structures obtained by our group (Vasconcelos et al., 2014), including Helix II (TBE), the template, and the template proximal helix (TPH). The structure of the first ~100 nt of *Leish*TER closely resembled *Tb*TR, and the presence of 5’ CCGUCA 3’ motif at the proximal 3' end of TBE is similar to TBE of *Tetrahymena thermophila*. Nucleotides in the TPH base showed low reactivity, indicating rigidity, while the

apex exhibited reactivity. The *Leish*TER template mostly comprised single-stranded elements, except for a few nucleotides suggesting involvement in long-range or transient interactions. Thus, further experiments are required for confirmation and a comprehensive understanding of the *Leish*TER structure.
Furthermore, RNA chemical probing combined with bioinformatic analysis will be a great addition to the project's second part, which involves uncovering novel species-specific RNA-protein interactions in *Leishmania*. Discovering the *Leish*TER binding partners is crucial to understanding its role inside the cell since important protein partners associated with TER are involved in the biogenesis and assembly of the telomerase complex. Thus, we intend to obtain information about proteins interacting with *Leish*TER domains (e.g., template region, Helix II (TBE), pseudoknot) using RNA-centric approaches (i.e., MS2-RNA and S1m affinity tag) followed by mass spectrometry analysis.

1. Introduction

1.1 Leishmania spp and leishmaniases

Parasites of the *Leishmania* genus belong to the Trypanosomatidae family, order Kinetoplastida (PACE, 2014; STECK, 1974), and cause diseases known as leishmaniases. They are unicellular and digenetic parasites with three main morphological forms. Procyclic promastigotes are highly proliferative forms found in the invertebrate host's digestive tract (phlebotomine sand flies), characterized by presenting an elongated shape and a flagellum. The metacyclic promastigotes, which are the infective forms with a short body and a longer flagellum, are located at the anterior of the insect's gut and cannot proliferate, and the amastigotes are highly proliferative forms found inside of the vertebrate host, presenting an oval shape and an inapparent flagellum (BATES and ROGERS, 2004; PEARSON and SOUSA, 1996; da SILVA and SACKS, 1987; STECK, 1974).

Leishmaniases are endemic in more than 80 countries, and despite the high incidence rate and vast global distribution, no effective prophylactic measures and treatments are available. Therefore, improving our knowledge about these parasites' molecular machinery and physiology is essential, increasing the possibility of finding new therapeutic targets.

1.2 Telomeres and telomerase

Telomeres are nucleoprotein structures formed by repetitive DNA in double and single-stranded forms. In most vertebrates and *Leishmania* spp., the telomeric DNA comprises the conserved 5' TTAGGG 3' sequence (CANO, 2001). One telomeric strand is rich in guanine (G) and extends ahead of its complementary strand, forming a single-stranded protrusion known as a 3' G overhang (BLACKBURN et al., 2015). The 3' G overhang and the double-stranded DNA are the sites of interacting proteins involved in telomere maintenance, protection of the ends,

and telomerase recruitment and regulation (FERNANDES et al., 2020; DMITRIEV et al., 2003). Besides their importance, the telomeres shorten with each cell cycle division due to the end replication problem (OLOVNIKOV, 1973; WATSON, 1972). When they reach a critical length, the coding DNA may be affected and could bring severe consequences to the cells, such as genomic instability, cell cycle arrest, and even senescence (EISENBERG, 2011; CHAN and BLACKBURN, 2004). A way to overcome this is through telomerase, a ribonucleoprotein complex minimally composed of a protein subunit known as Telomerase Reverse Transcriptase (TERT) and the telomerase RNA (TER or TR), which can replenish telomeres (COLLINS, 1999).

The TERT component contains the catalytic core of the enzyme that works as a specialized reverse transcriptase that uses the template provided by TER to synthesize telomeric DNA at the 3' end of the G-rich strand (ZHANG et al., 2011; AUTEXIER and LUE, 2006). TERT is highly conserved, and it is composed of four structural and functional domains: the TEN domain (Telomerase Essential N-terminal), the TRBD (Telomerase RNA Binding Domain), the RT (Reverse Transcriptase) domain, and CTE (C-Terminal Extension) domain (BARBÉ-TUANA et al., 2021; ZHANG et al., 2011). Unlike TERT, TER is a unique molecule since it varies in nucleotide sequence and size among organisms (PODLEVSKY and CHEN, 2016). However, despite its extensive sequence divergence, TER has some conserved structural domains that allow interactions with TERT (ZHANG et al., 2011). Among the conserved structures of TER are the template boundary element (TBE, or Helix II), located in the 5' end of the molecule. TBE works as a barrier preventing the reverse transcription of telomeric DNA to occurs beyond the template and is also involved in the interaction with the TERT TRBD domain (WEBB and ZAKIAN, 2016; BLACKBURN and COLLINS, 2011; COLLINS, 1999). In addition, the template region is a single-stranded sequence, normally composed of a one-and-a-half reverse copy of the telomeric repeat sequence (LUE, 2004). Moreover, TER also has two other important elements involved in TERT-TER interaction and enzyme processivity: the pseudoknot and the stem terminus element (STE) (called CR4/CR5 in humans and Helix IV in trypanosomatids) (DEY and CHAKRABARTI, 2018; PODLEVSKY et al., 2016; CHEN et al., 2000). Besides that, the TER of some organisms may contain additional domains, such as the H/ACA box present in mammals (BARBÉ-TUANA et al., 2021) and the C/D box in flagellates, including trypanosomatids (GUPTA et al., 2013).

1.3 Characterization of Telomerase RNA in Leishmania major using chemical probing read by mutational profiling

Leishmania telomerase RNA (*Leish*TER) is a lncRNA of ~2,113 nt encoded by a single copy gene on chromosome 25. RNA polymerase II transcribes *Leish*TER, which undergoes *trans*-splicing, adding a polyA tail in the 3' portion and a 5' SL (spliced leader) cap. The previous analysis of its predicted structure showed that the template sequence (5' ACCCUAACCCUA 3') is 12 nt long, single-stranded as a multiloop secondary structure, and located close to the TBE element. In addition, it also contains a sequence of ~45 nt-long small nucleolar RNA domain (a C/D box snoRNA) which is part of the snoU90 (or scaRNA7) found in human Cajal bodies (VASCONCELOS et al., 2014). Most of the information we have gathered about the *Leish*TER structure is based solely on in-silico structural modeling predictions. Thus, finding other ways to elucidate the LeishTER core domain structures and compare them with the previous in-silico results would be important.

Therefore, due to the known structural similarities between *Tb*TER and *Leish*TER (VASCONCELOS et al., 2014), we propose collaborating with Dr. Chakrabarti's group to apply the same methodology they used in *Trypanosoma brucei* to elucidate the *Tb*TER core domains structures (DEY et al., 2021).

The methodology comprises chemical probing, high-throughput sequencing, and mutational profiling. The chemical probes they used were DMS (dimethyl sulfate) and NAI (2-methyl nicotinic acid imidazolide). These chemical probes can react with RNA causing modifications in the molecule that can be mapped (STROBEL et al., 2018). DMS is a base-specific probe that reacts with unpaired adenine (at position N1) and cytosine (at position N3), triggering the methylation of the bases. Paired bases have low reactivity to DMS, while unpaired bases show a high reactivity towards the probe. Therefore, DMS allows the analysis of Watson-Crick base-pairing. NAI, in contrast, is a generalist probe and works as a SHAPE reagent (Selective 2'-hydroxyl acylation analyzed by primer extension). SHAPE can modify the RNA backbone by acylating the ribose 2'-hydroxyl group of flexible nucleotides. Both NAI and DMS penetrate very easily into the cell and can modify the RNA molecule in unpaired positions (DEY et al., 2021; STROBEL et al., 2018). The resultant chemically-modified RNAs are subsequently reverse-transcribed into cDNA under error-prone reactions in the presence of Mn^{2+} at the positions containing modified nucleotides, increasing nucleotide misincorporation and deletions (nucleotide skipping). Thus, the newly synthetized cDNA strand contains more random mutations than the controls (KRISTEN et al., 2020; SMOLA et al., 2015). As controls,

RNA samples are treated with the chemical's solvents (e.g., ethanol and DMSO for DMS and NAI, respectively), which remove the false positive reactivity signal that can occur due to natural loss of the reverse transcriptase processivity (SMOLA & WEEKS, 2018; STROBEL et al., 2018). The mutated cDNA molecules are further used to generate cDNA libraries and sequenced using high-throughput Next Generation Sequencing (NGS) methods. The raw RNA sequencing data is directly deposited in the ShapeMapper2 software that can detect the mutations caused by the chemical probes and compares them to the unmodified nucleotides (DEY et al., 2021; SMOLA & WEEKS, 2018). ShapeMapper2 creates reactivity or mutational profiling (SMOLA & WEEKS, 2018) since the RNA unstructured regions normally react highly towards the chemical probe, while structured regions show low reactivity (STROBEL et al., 2018). Thus, only the unstructured regions will be chemically modified. Therefore, information about the RNA structure can be obtained based on ShapeMapper2's analysis of the reactivity results. Finally, the secondary structure model of the RNA is obtained using RNA structure and VARNA.

This methodology showed that depending on the parasite's developmental stage (insect and mammalian), *Tb*TER forms at least two different conformers with distinct folding topologies and that *Tb*TERT does not affect TER folding in vivo. Their results suggest that in *T. brucei*, the conformational changes observed in TER are key for parasite development.

Compared to available in-silico tools to obtain TER secondary structures, the methodology used by Dey and colleagues (2021) was very successful in analyzing the architecture of long noncoding RNAs (lncRNAs), such as *Tb*TER. And as shown in our pilot experiment results here, it was also a good way to assess *Leish*TER's secondary structure.

Therefore, the methodology learned at Dr. Chakrabarti's lab should be successfully applied at our laboratory in Brazil (Telomeres Lab - UNESP/Botucatu), not only for *Leish*TER structural studies but also to other *Leishmania* ncRNAs of our interest, such as TERRA.

1.4 *TER-proteins interaction*

It is worth reminding that besides having the template used by TERT, TER is required for telomerase processivity and the assembly of the RNP complex. The RNA component TER works as a structural scaffold for additional proteins to bind to telomerase (BERMAN et al., 2011; ZAPPULLA and CECH, 2006), for processivity and function. We have previously shown that among the protein subunits, the *Leishmania* telomerase RNP contains molecular chaperones probably involved in the conformation and assembly of the complex (de

OLIVEIRA et al., 2021). In addition, work from Cech lab and others have shown that the p65 protein in ciliates copurifies with TER and TERT as well as promotes proper folding of TER for telomerase holoenzyme assembly and activity (HE et al., 2021; SINGH et al., 2012; BERMAN et al., 2010). Although homologs of p65 have not been found outside ciliate ancestry, the complex of dyskerin, NHP2, NOP10, and GAR1 that bind with the H/ACA domain of human TER are thought to be the functional analog of p65 chaperone in human telomerase (ROAKE & ARTANDI, 2020; BERMAN et al., 2010). Indeed, these H/ACA binding proteins facilitate human TER folding by enabling the human CR4/5 domain to adopt a particular conformation that engages with TERT (CHEN et al., 2018; EGAN & COLLINS, 2012). Interestingly, in *T. brucei* and *Leishmania* TER, the human H/ACA type snoRNP domain is replaced by a unique C/D box snoRNP domain. However, the core group of proteins that binds this unique domain in flagellated protozoa remains unknown. Once assembled, the telomerase RNP can be recruited to telomeres. Recruitment depends on the coordinated action of telomeric proteins associated with the complex and DNA polymerase alpha, enabling telomeres elongation and C-strand synthesis (BARBÉ-TUANA et al., 2021). Therefore, the crosstalk between the shelterin and CST telomeric proteins and the telomerase RNP complex (BARBÉ-TUANA et al., 2021) is crucial for genome stability and integrity since they regulate telomerase activity and telomere maintenance, avoiding local DNA damage response (BLACKBURN et al.,2015; EISENBERG, 2011). However, just a few of the well-known shelterin and shelterin-like telomeric proteins (i.e., human TRF1 and TRF2, TTAGGG binding factor) share some level of structural and functional conservation with the trypanosomatids (ASSIS et al., 2021; LI, 2021; FERNANDES et al., 2020; VIVIESCAS & CANO, 2019). In these protozoa, including *Leishmania*, the telomeric chromatin mainly consists of species-specific proteins, with a few exceptions (ASSIS et al., 2021; LI, 2021). Moreover, the knowledge about the trypanosomatids proteins involved with telomerase biogenesis that would interact with the TERT and the TER components is poor (de OLIVEIRA et al., 2021; SANDHU et al., 2013). Thus, identifying new trypanosomatids' telomerase subunits would be of great value to understanding the importance of telomeres for parasite homeostasis. Furthermore, the telomerase interactions and function comprehension can enlighten telomere organization and genome stability. For mammals, this knowledge essentially highlights the significance of telomere/telomerase biology in health and disease (BARBÉ-TUANA et al., 2021; AUTEXIER and LUE, 2006).

Thus, besides the structural and functional insights into the *Leish*TER molecule that we foresee acquiring, we aim to examine the interactions between *Leish*TER and its unknown partners, which can help to uncover novel species-specific RNA-protein interactions in *Leishmania*. For this purpose, we will try to use either the MS2 RNA tagging approach, which can specifically bind an MS2 coat protein (HAN et al., 2020), or the S1m aptamer, a modified streptavidin (SA)-binding RNA that exhibits a greater affinity for SA compared to the original S1. It binds to SA adopting a four-repeat conformation (4S1m) and seems to surpass the MS2 in efficiency (LEPPEK & STOECKLIN, 2013). The strategy that we succeed in applying first will be used.

2. Objectives

2.1 General objective

Access the structure of *Leish*TER core domains and identify its protein partners.

2.2 Specific objectives

- Learn the RNA chemical probing coupled with high-throughput sequencing and mutational profiling (done in the U.S.A.);
- Determine the structure of the core domains of telomerase RNA from *L. major* in single-nucleotide resolution through chemical probing and mutational profiling (*in progress*);
- Define the stage-specific requirements of the telomerase RNA structural domains in the procyclic and metacyclic promastigotes, in vivo and ex vivo (*in progress*);
- Uncover novel species-specific RNA-protein interactions in *Leishmania* by combining the information obtained from the RNA chemical probing read by mutational profiling with RNA-centric approaches and mass spectrometry analysis (*in progress*).

3. Materials and methods

3.1 Culture of Leishmania major cells

Leishmania major strain *Friedlin* (MHOM/IL/1980/FRIEDLIN) was cultured at 26°C in 1X M199 media, pH 7.3, supplemented with 10% heat-inactivated fetal bovine serum (FBS) (Avantor) (KAPLER et al., 1990), and 1X penicillin/streptomycin (Life Technologies, Gibco-BRL). *L. major* strain carrying the pTB007 plasmid (*Lm*007) was cultured in media supplemented with 30 μg/ml of hygromycin (Invitrogen). Metacyclic promastigotes were

selected through agglutination of stationary culture using peanut lectin from *Arachis hypogaea* (Sigma-Aldrich) (da Silva and Sacks, 1987).

3.2 Total RNA extraction to check LeishTER expression

Total RNA from exponentially growing promastigotes (3 x 10^8 cells) was isolated using TRIzol reagent (Invitrogen) following the manufacturer's instructions. The extracted RNA was treated with DNase I recombinant, RNase-free (Roche), and cleaned using RNA Clean & Concentrator-5 kit (Zymo Research). RNA concentration and quality were evaluated by Nanodrop (ThermoFisher). An RT-PCR reaction was set up to check *Leish*TER expression, using *SuperScript* II (TermoFisher) and TER RT R primer (Table 2) to generate the cDNA, followed by PCR using GoTaq Green Master Mix (Promega) and a set of primers (TERm F + TER RT R - Table 2) that internally hybridize to *Leish*TER generating a 407 bp amplicon (Figure 2).

3.3 Obtention of L. major promastigotes carrying the pTB007 plasmid (Lm007)

Promastigote procyclic cells in the exponential growth phase were transfected with 25 μg of pTB007 plasmid following two different protocols: The old method and the Cytomix method (KAPLER et al., 1990; ROBINSON & BEVERLEY, 2003). After the transfections, the transfected cultures were incubated overnight at 26°C, and the next day 30 μg/ml of hygromycin was added to the culture to select the transfectants.

After recovery of the cultures from transfection, DNA of the transfected cultures (*Lm*007) and control (*Lm*WT) was extracted as follows: 1x10^6 cells were harvested at 2300 g at 4°C, washed with cold 1X PBS, and resuspended in 10 μl of lysis buffer W (30 mM Tris pH 8.0; 50 mM NaOH; 5 mM $CaCl_2$) and 5 μg/μl of Proteinase K, followed by 30 min incubation at 50°C and 10 min at 95°C to inactivate the enzyme. The DNA was immediately used in a PCR reaction to check the presence of pTB007 in the transfected populations. The PCR reaction used a set of primers that hybridized an internal region of the Cas9 gene (Table 2), generating an amplicon of 127 bp.

3.4 Design of primers for the SHAPE experiment

For the pilot experiment performed in the U.S.A., primers that would hybridize the beginning of *Leish*TER in the 5' region, generating a 242 bp amplicon comprising the catalytic core (TBE/Helix II + template) were designed. Besides the sequence that would hybridize to the

target, adapters to the TruSeq barcodes (see Table 2 for primers details) were added in the 5' end of the primers. Each sample was generated using a Universal Rv Primer and a specific Adapter sequence (Table 3).

For the experiments to be performed in Brazil, five primer sets were designed to cover the entire sequence of *Leish*TER (Fig. 1), where each set will generate an amplicon of ~445 bp. For the Illumina platform, each primer comprises a specific region of *Leish*TER + specific sequence (Table 2).

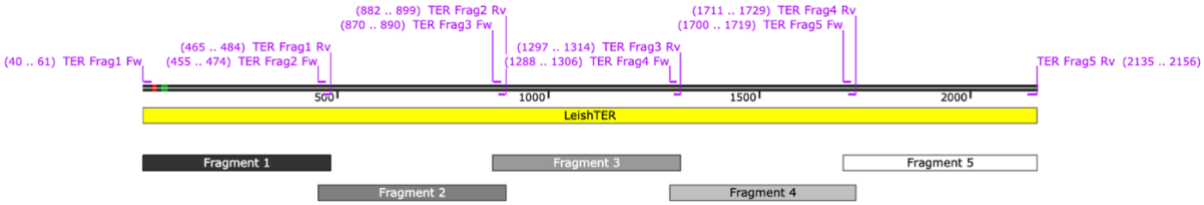

Figure 1. Strategy to map the entire *Leish*TER sequence. The diagram shows the position of the five primer sets comprising specific target sites inside of *Leish*TER + specific nucleotide sequence for the Illumina platform (in purple). Each set will generate a ~445 bp fragment.

3.5 Pilot experiment of in vivo RNA chemical probing using NAI

Three cultures of *L. major* WT procyclic promastigotes in the exponential growth phase were harvested separately at 900 g for 5 min at 4°C. The pellet was resuspended in bicine-buffered media (1 M of bicine pH 8.3 diluted in 1X M199 media to a final concentration of 200 mM of bicine). Each sample was treated with different concentrations of NAI (50 mM, 100 mM, and 150 mM) to test which would work best for *Leish*TER chemical probing. Samples were incubated for 15 min at 37°C. As controls, separated cultures were treated with NAI solvent (DMSO). After treatment, total RNA was extracted by TRIzol following the manufacturer's instructions and then treated with DNase I recombinant, RNase-free (Roche). After DNase treatment, the RNA samples were cleaned using RNA Clean & Concentrator-5 kit (Zymo Research).

3.6 cDNA synthesis and purification

cDNA for the *Leish*TER gene was synthesized using a gene-specific reverse primer (TER RT R - Table 2) and the SuperScript II enzyme (ThermoFisher Scientific). The error-prone reverse transcriptase reaction was done in the presence of manganese ion to facilitate the incorporation of non-complementary nucleotides in the cDNA, thus creating mutations complementary to the

unprotected/chemically modified RNA nucleotides (DEY et al., 2021). The resultant cDNA was purified using AxyPrep Mag PCR Clean-Up Kit (Axygen®) and submitted to a second strand synthesis performed using NEBNext® UltraTM II Non-Directional RNA Second Strand Synthesis Module (New England BioLabs).

For the experiments to be performed in Brazil, a new primer hybridizing in the extremity of the 3' end of *Leish*TER was designed to generate the cDNA (Table 2).

3.7 Library construction and sequencing

A PCR reaction was performed to amplify the catalytic core of *Leish*TER (template region and TBE) using specific primers (Table 2) and the Q5® High-Fidelity DNA Polymerase (New England BioLabs). A second PCR was done to introduce TruSeq barcodes (see Table 3 for details). The Qubit dsDNA HS Assay Kit (ThermoFisher) was used to check the quantification of the libraries, and their quality was analyzed using Agilent 5200 – Fragment Analyzer. These libraries were sent to sequencing at NovoGene using the HiSeq platform.

In Brazil, the cDNA sequencing will be performed using the MiSeq platform at the Molecular Biology – Hemocenter Laboraty at HCFMB (Hospital das Clínicas - Botucatu Medicine University, UNESP) in collaboration with Dr. Rejane Maria Tommasini Grotto, Dr. Guilherme Targino Valente, and Dr. Leonardo Nazario de Moraes.

3.8 Data processing and analysis

The sequencing data's mean quality score and per sequence quality score were analyzed using the MultiQC tool (https://multiqc.info/). Then, the ShapeMapper2 algorithm was used to detect the mutation frequency according to instructions at https://github.com/Weeks-UNC/shapemapper2. The calculation of chemical reactivity for each nucleotide of the RNA molecule was done according to the following equation: $R = mutr_m - mutr_u$, where R is the chemical reactivity, $mutr_m$ refers to the mutation rate calculated for chemically modified RNA samples, and $mutr_u$ refers to the mutation rate calculated for untreated control RNA samples. RNA secondary structures were modeled using RNA structure software.

3.9 RNA-centric approaches to uncover novel species-specific RNA-protein interactions in Leishmania

*Leish*TER will be tagged with two different aptamers in two different approaches, one of them involves the MS2 aptamer (HILGARTHB & LANIGAN, 2020), and the other one is the S1m aptamer (LEPPEK & STOECKLIN, 2013).

For the MS2 approach, *Leish*TER will be fused to 6 MS2 stem-loops in its 5' region through overlap PCR, followed by purification of the PCR product using Wizard SV Gel and PCR Clean-Up System (Promega). The generated amplicon ("6X MS2 + *Leish*TER") will have, respectively, *BamH*I and *Bgl*II restriction sites at the 5' and 3' ends to be cloned into the pX63Neo *Leishmania* expression vector. The recombinant plasmid will be transfected and expressed in a *Leish*TER knockout lineage (de OLIVEIRA and CANO, in preparation) to avoid competition with the endogenous *Leish*TER. Nuclear cell extracts will be immunoprecipitated with an anti-MS2 antibody, and the pull-down products will be fractionated in SDS-PAGE gels followed by in-gel digestion of protein bands, or the pool will be trypsin digested and directly used to identify the endogenous interaction partners by mass spectrometry analysis. Processed samples will be sent for mass spectrometry analysis.

The identified peptides will be analyzed using MaxQuant (https://www.maxquant.org/) or Proteome Discoverer Software (ThermoFisher).

Since the MS2 strategy is more laborious, we also intend to try a similar strategy that allows the fusion of *Leish*TER to the S1m aptamer (LEPPEK & STOECKLIN, 2013). Once the cells are transfected and expressing the *Leish*TER fused to S1m aptamer, nuclear cells extracts will be used in affinity purification assays using Dynabeads™ MyOneTM Streptavidin C1 (ThermoFisher), according to the manufacturer's specifications. The procedure will be improved as necessary at the steps of optimization. The pull-down of *Leish*TER interacting partners will be performed, followed by their identification by mass spectrometry (see above).

4. Results and discussion

4.1 Confirmation of LeishTER expression in LmWT

The *L. major* WT strain *Friedlin* (MHOM/IL/1980/FRIEDLIN) used in the experiments performed at Dr. Chakrabarti's lab was kindly donated by Dr. David Sacks from NIH (National Institutes of Health). Once the culture arrived, total RNA was extracted, and the expression of *Leish*TER was checked. As observed in Fig. 2, the parasites expressed the telomerase RNA as expected, and the next experiments could be carried on.

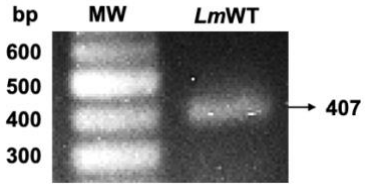

Figure 2. Confirmation of *Leish*TER expression in *Lm*WT cells. RT-PCR using the TERm F and TER RT R primers and total RNA from *Lm*WT. The expression of *Leish*TER was detected by amplifying a cDNA fragment of 407 bp. cDNA samples were fractionated in a 1% agarose gel stained with gel-red. MW – Molecular weight, GeneRuler 100 bp DNA ladder (Thermo Scientific).

4.2 Obtainment of L. major carrying the pTB007 expression vector

Since one of the project's goals was to analyze the *Leish*TER structure without TERT, generating a full knockout lineage for the TERT component was demanding. To reach this goal, we used the CRISPR/Cas9 system described by Beneke et al. (2017) and the same tools (i.e., primer sets and the DNA donor cassette) used by Mark Shiburah, a Ph.D. student from our lab in Brazil. Therefore, *Leishmania major* WT (*Lm*WT) promastigotes were transfected with pTB007. This episomal plasmid contains the genes encoding the T7 RNA polymerase, responsible for the *in vivo* transcription of sgRNAs from transfected DNA templates (BENEKE et al., 2017), the hygromycin phosphotransferase (hph) gene that confers resistance to hygromycin (BLOCHLINGER AND DIGGLMANN, 1984), and the humanized *Streptococcus pyogenes* Cas9 nuclease gene (hSpCas9), responsible for cleaving the two strands of DNA for further gene editing (RAN et al., 2013). The transfection was performed using the "Old method" protocol (KAPLER et al., 1990). The presence of pTB007 in the transfected population (*Lm*007) was confirmed by PCR (Lane 2 – Fig. 3). Since the BEPE was interrupted, the experiments using the TERT full knockout lineage will be performed in our lab in Brazil, using a well-characterized parasite clone.

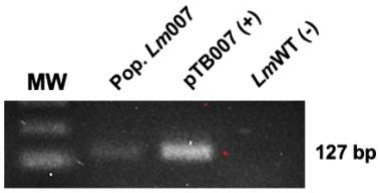

Figure 3. Confirmation of the presence of pTB007 plasmid in the *Lm*007 population. PCR using the For-Cas9 and Rev-Cas9 primers and genomic DNA from *Lm*007 non-cloned population. The presence of the plasmid pTB007 was detected by the amplification of the Cas9 region (127 bp – Lane 2). As a positive control, PCR was performed using the pTB007 plasmid DNA (lane 3) and LmWT genomic DNA as the negative control (lane 4). The PCR products were fractionated in a 2% agarose gel stained with gel red. MW – Molecular weight, GeneRuler 100 bp DNA ladder (Thermo Scientific).

4.3 Structural analysis of the in vivo-treated LeishTER using different concentrations of NAI

4.3.1 Quality and concentration analysis of the pre-made libraries

A pilot experiment was carried out by checking which concentration of NAI would work for *Leish*TER chemical probing. To start, we used the same concentration used by Dey et al. (2021), 100 mM of NAI, and two other concentrations, 50 mM NAI and 150 mM NAI were used. The concentration of the pre-made libraries was checked by Qubit (Table 1), the purity ($A_{260/280}$ and $A_{260/230}$ absorbance ratios – Table 1) by Nanodrop, and the quality of the libraries was checked by Agilent 5200 – Fragment Analyzer (Figure 4).

Table 1. Concentration and purity of pre-made libraries

Sample	Concentration (ng/µl)	Absorbance 260/280	Absorbance 260/230
Treated with 50 mM NAI	48,3	1,95	2,23
Treated with 100 mM NAI	45,6	1,94	2,25
Treated with 150 mM NAI	34,9	1,97	2,20
Untreated – control of 50 mM NAI	60,0	1,93	2,23
Untreated – control of 100 mM NAI	59,0	1,95	2,22
Untreated – control of 150 mM NAI	57,0	1,93	2,05

A)

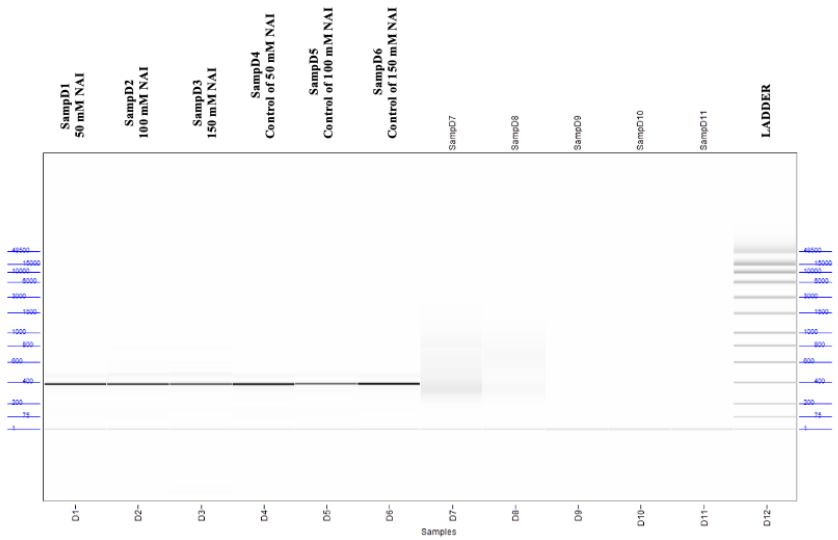

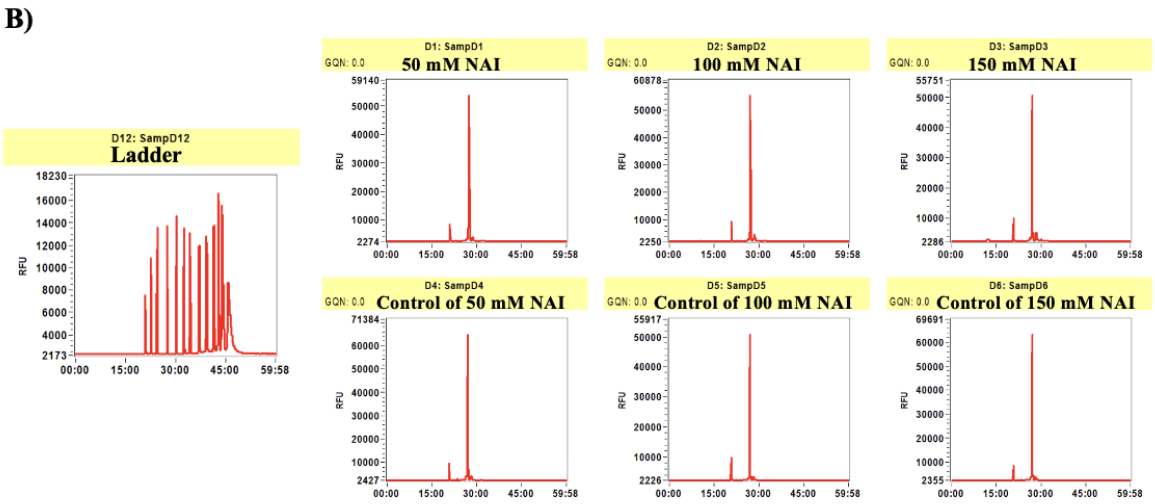

Figure 4. Quality analysis of the pre-made libraries. A) Gel image from the Agilent 5200 – Fragment Analyzer of pre-made libraries: lanes 1-3 treated samples with different concentrations of NAI (50 mM, 100 mM, and 150 mM, respectively), lanes 4-6 untreated controls incubated with DMSO, lane 12 – ladder; B) Electropherograms showing the peaks related to the bands of the samples from image (A): electropherogram on the left shows the peaks of all bands of the ladder (from 1 to 48,500 bp), the others electropherograms show the smaller ladder band (left peak of 1 bp), and the fragment band (~380 bp - higher peak).
*Lanes 7 and 8 are samples that ran together from another researcher.

As observed in Table 1 and Figure 4 results, the pre-made libraries were of good quality and concentration, where the fragment of interest was high. Then, the samples were diluted to 2 ng/µl and sent to sequence at NovoGene.

4.3.2 Analysis of the sequencing results

The sequencing was performed using the HiSeq PE 150 (Illumina). Since the sequencing was conducted from 5' to 150 bp inside of the target and from 3' to 150 bp inside of the target, the sequencing resulted in a total of 12 samples, with two replicas from each condition (50 mM NAI, 100 mM NAI, 150 mM NAI, control of 50 mM NAI, control of 100 mM NAI, and control of 150 mM NAI).

MultiQC accessed the sequencing data quality through *Sequence Quality Histograms* that show the mean quality value across each base position in the read and the *Per Sequence Quality Scores* that show the number of reads with average quality scores (Figure 5A and 5B, respectively). In Figures 5A and 5B, the samples present higher Phred scores (>30), relying on the green area of the graphs, which indicates a high-quality base call with a lower probability of being incorrect.

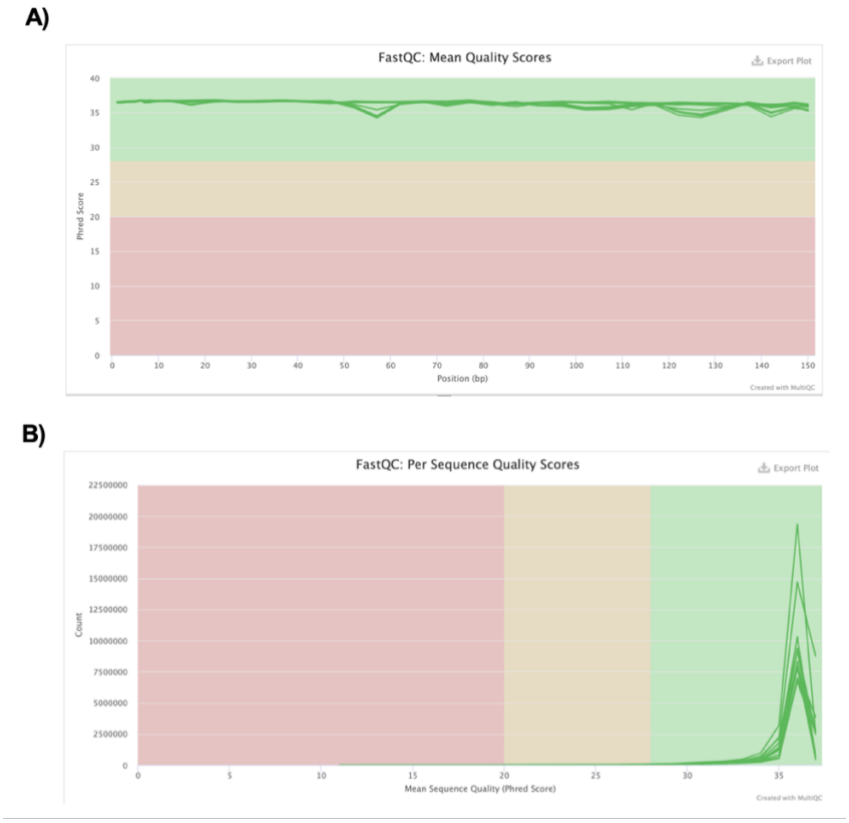

Figure 5. Quality analysis of the sequencing data. A) Sequence Quality Histograms; B) Per Sequence Quality Scores. The graphs were generated using the MultiQC tool (https://multiqc.info/).

4.3.3 SHAPE-MaP reactivity profiles analysis

SHAPE reagents prefer reacting with the 2'-hydroxyl groups found in RNA nucleotides that possess conformational flexibility. Thus, the SHAPE reactivity profile shows the reactivity of each nucleotide from the target sequence towards the SHAPE reagent used (in this case, NAI), where a flexible nucleotide presents a higher reactivity to the SHAPE reagent than a non-flexible nucleotide (SMOLA et al., 2015). SHAPE reactivity profiles offer a concise assessment of the overall success of an experiment. This way, a small number of negative gray bars (no-data points) indicate a high level of data acquisition, and small error bars reflect a high degree of precision and accuracy in the obtained results (SMOLA et al., 2015). SHAPE-MaP reactivity profiles from the *E. coli* 16S rRNA (SMOLA et al., 2015) were used as references to analyze the success or failure of the experiment results. In Fig. 6A, there is an example of a high-quality reactivity profile with no gray bars and small error bars; in Fig. 6B, a poor-quality reactivity profile with a high abundance of gray bars and error bars. Therefore, our results (Figs. 6C-E) showed a high-quality reactivity profile since they are very similar, showing few differences.

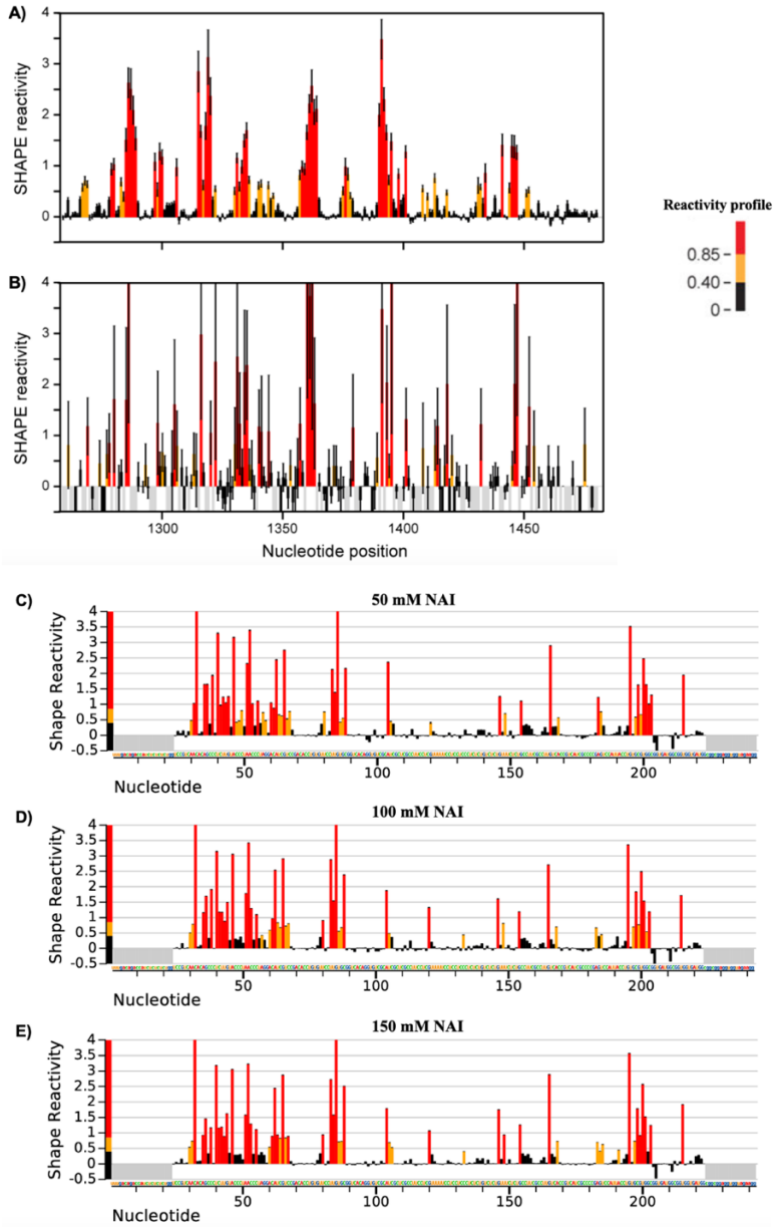

Figure 6. SHAPE-MaP reactivity profiles. Example of a High-quality (A) and Poor-quality (B) reactivity profile for the *E. coli* 16S rRNA (SMOLA et al., 2015), C) Reactivity profiles of samples treated with 50 mM NAI (C), 100 mM (D), and 150 mM NAI and their respective controls. Reactivities below 0.4 are colored black, between 0.4 and 0.85 orange, and above 0.85 red. Gray bars in (B) indicate missing data points (corresponding to a background mutation rate above 5% or read depth below 10). In C-E, the gray bars indicate the primers' hybridization regions excluded from the reactivity profile. Error bars indicate standard errors.

Besides the reactivity profile, ShapeMapper also generates a variety of histograms that serve as valuable tools for distinguishing between successful and problematic experiments. These histograms aid in identifying and differentiating experiments that yield favorable results from those that encounter difficulties or issues. These histograms will mainly show the mutation rate, read depths, and normalized reactivity. For a successful experiment is expected a mutation rate in the untreated sample is between 0 and 0.2% and a strong shift toward higher mutation

rates in the treated sample (Fig. 7A - left panel); a read depth above 2000 (Fig. 7A - middle panel); and reactivities mostly positive, with smaller standard errors than most of the reactivities (Fig. 7A - right panel) (SMOLA et al., 2015). In Figures 7B-D (middle panel), all experiments were successful, showing low standard errors, and most of the reactivities were positive (right panel from Figs. 7B-D), giving high read depths (from 8 to 14 million reads). Also, a higher mutation rate was detected in the treated samples (modified) than in the untreated (left panel from Figs. 7B-D). However, it is worth mentioning that in the sample treated with 50 mM NAI, the mutation rate was lower than in samples treated with 100 mM and 150 mM NAI, indicating that a higher concentration of NAI (100 mM or 150 mM) should be used in further experiments.

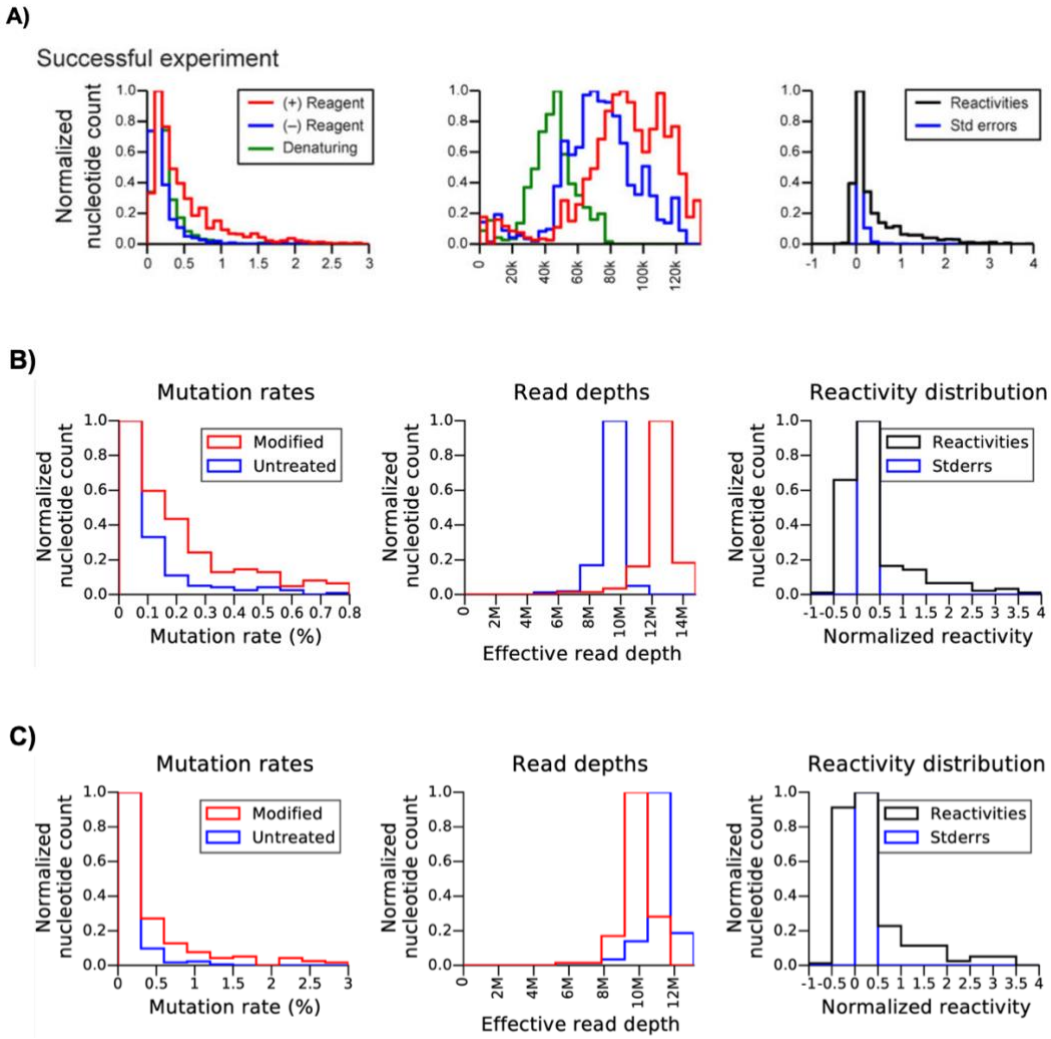

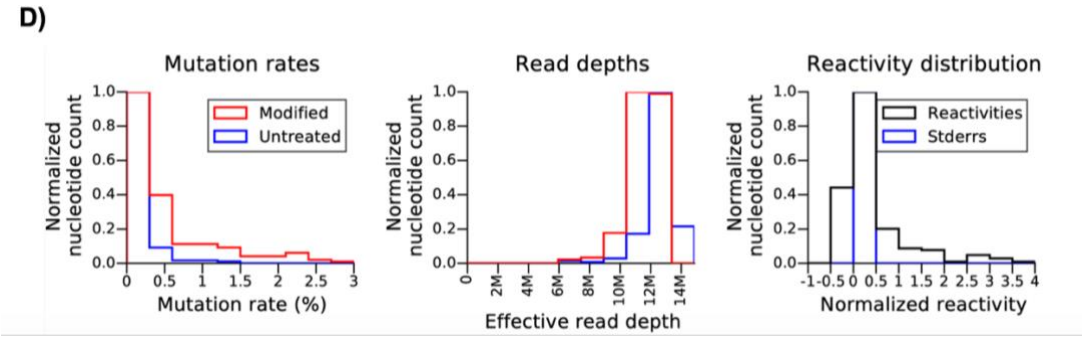

Figure 7. Histograms generated by ShapeMapper indicate the success of the NAI treatment. A) Histograms showing an example of successful experiment data from the *E. coli* 16S rRNA (SMOLA et al., 2015), Histograms generated by ShapeMapper to verify the data obtained from samples treated with 50 mM NAI (B), 100 mM NAI (C) and 150 mM (D) and their respective controls.

4.3.4 *Leish*TER structure analysis

In 2014, our group published the predicted secondary structure of *Leish*TER from the first 139 nt (39 nt from the spliced leader sequence + 100 nt from *Leish*TER) through *in silico* analysis (Fig. 8A). In the currently pilot experiment shown in Figs. 8B-D, we used the RNA chemical probing read by mutational profiling, to generate the partial structure of *Leish*TER by testing different concentrations of NAI. Independently of NAI concentrations, the results obtained were very similar among them (Figs. 8B-D) and to that obtained in 2014 (Fig. 8A), where we can see from the 5' going towards inside the molecule the following structures: Helix II (TBE), the template, and template proximal helix (TPH).

It is important to remind that the RNA structure software uses the sequence information to generate possible structures of the molecule of interest. The beginning of the *Leish*TER structure (1 to 102 nt) closely resembles the *Tb*TER structure described by DEY et al. (2021). First, it is possible to observe that, similar to the in-silico model obtained in 2014 (Fig. 8A), the template domain is positioned between two stem-loop helix arrangements (Helix II and TPH) (Figs. 8B-D).

According to our previous work (VASCONCELOS et al., 2014), the first nucleotide of *Leish*TER molecule is already part of Helix II (TBE), and since the forward primer designed for the cDNA sequencing (LmTERTBEFw-Adp - Table 2) hybridizes to the first 23 nt of *Leish*TER, the reactivity profile of the these nucleotides can't be accessed by SHAPEMapper2, because the software exclude the primer sequence for reactivity profile analysis (Fig. 6C-E – gray bars in both extremities). However, we could still check how the nucleotides are organized to form the structure. The Helix II in *Leish*TER contains in its apex an eight nucleotides loop

(5' UCUCUCUC3') (Fig. 8B-D), which is different from *Tb*TER Helix II that contains a six nucleotides loop (5′ UCUCGU3′) (DEY et al., 2021) and from *Tetrahymena* TER that has a five loop (5′ GUAAU 3′) apex (MCCORMICK-GRAHAM & ROMERO, 1995). Similarly to *Tetrahymena thermophila*, the TBE in *Leish*TER also contains, at the 3' end, the CCGUCA motif (positioned from nt 25 to 30), which is known to play a crucial role in the demarcation of the template boundaries (RICHARDS et al., 2006; VASCONCELOS et al., 2014). Nucleotides positioned in the base of TPH show low reactivity towards NAI (< 0.4), which indicates that they are not flexible (Fig. 8B-D). At the same time, the six nucleotides present in the apex (5' UUGUGC 3') are reactive to NAI (orange > 0.4 and red >08) (Fig. 8B-D). Most of the nucleotides from the *Leish*TER template (Fig. 8B-D – from nucleotide 46 to 57) are also reactive to NAI, being mainly composed of single-stranded elements and, thus, lacking any intra- or inter-molecular interactions except for nucleotides 50U, 54C, and 56U that had low reactivity to NAI, suggesting they are likely involved in long-range or transient interactions.

A new *in silico* analysis performed by our collaborator (Dr. Elton Vasconcelos – University of Leeds) showed the presence of a possible pseudoknot structure between positions 81 and 1,832 using SPOT-RNA (data not shown). The putative pseudoknot is probably located three nucleotides upstream of the template. However, to confirm that and get accurate information about the remaining part of the *Leish*TER structure, we will need more data and comparison among replicates and a full context of the entire structure to understand better how this RNA is folded *in vivo*.

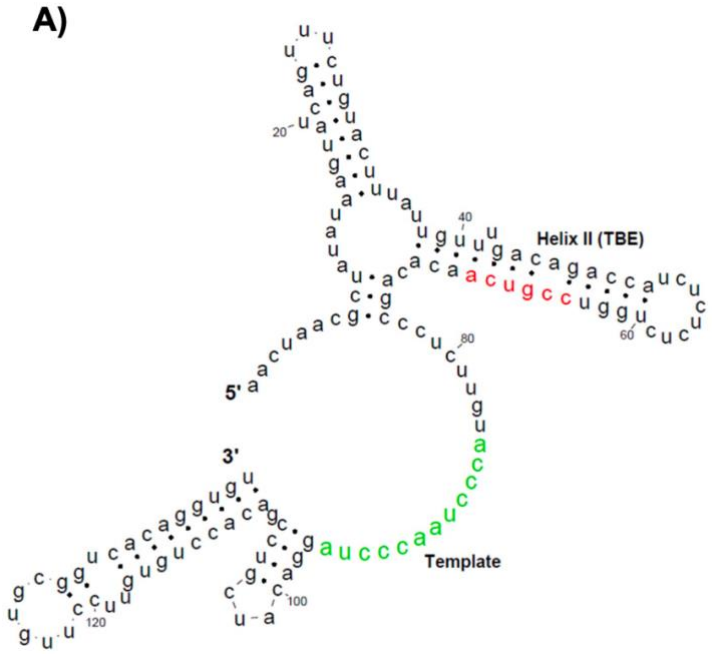

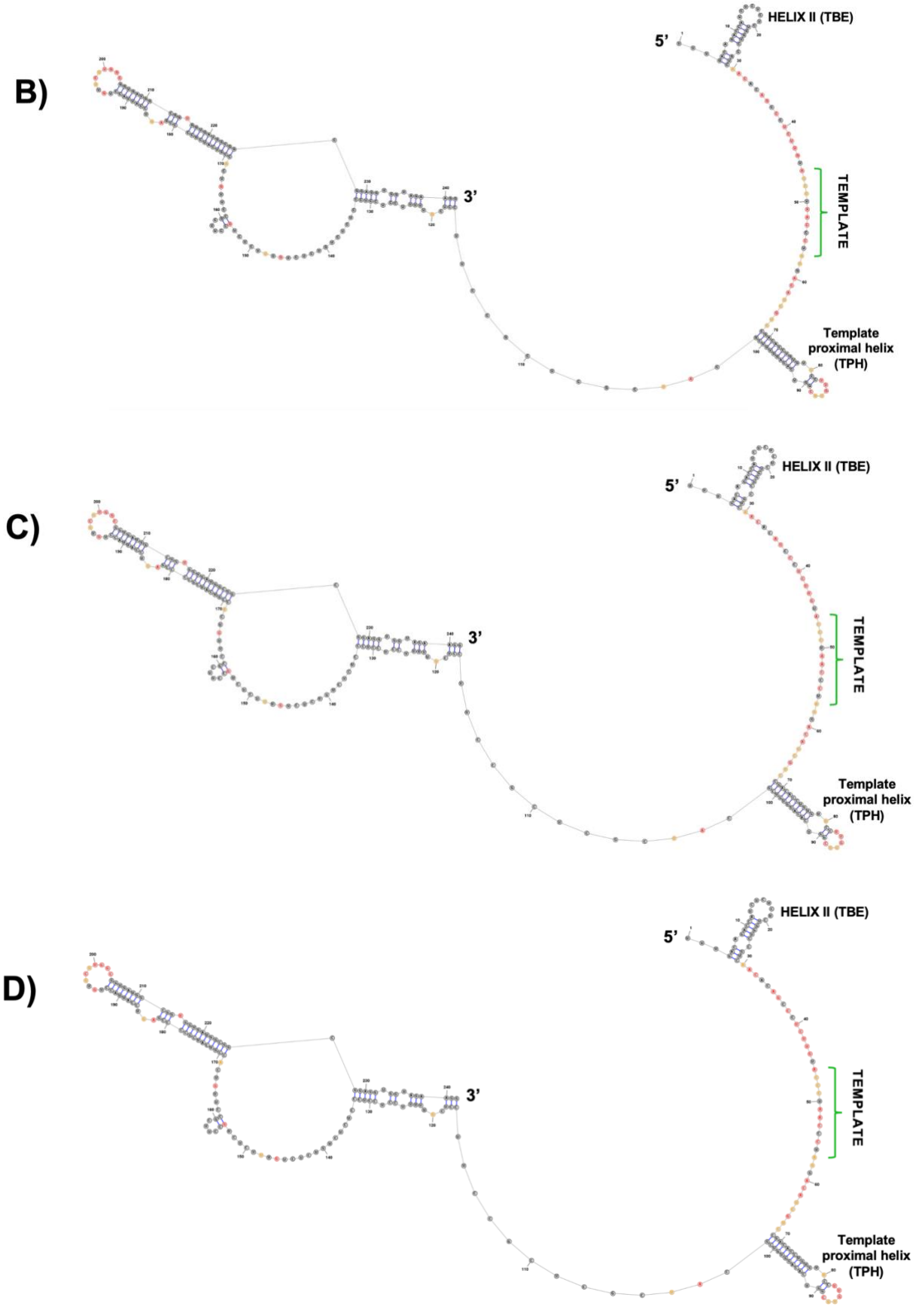

Figure 8. Predicted *Leish*TER secondary structure obtained in-silico and by chemical probing. A) Proposed secondary structure of *Leish*TER obtained through in silico analysis (Vasconcelos et al., 2014) shows the Helix II,

containing a CCGUCA motif (red) and the single-stranded template sequence (green) followed by two helices positioned towards the 3' end. B), C), and D) Structures generated in the RNA structure software using data from ShapeMapper2 highlighting Helix II (TBE) in the 5' end, the template sequence highlighted in green, followed by the template proximal helix.

5. Conclusions

The RNA chemical probing using NAI showed to be an easy and successful way to probe *Leish*TER. According to our preliminary results, all the concentrations resulted in very similar structures of the first 242 nt of the RNA, although the best concentrations of NAI according to the mutation rate results obtained through the probing were the 100 mM and 150 mM (Fig. 7). Thus, for the continuation of this project we will use 100 mM NAI.

The results obtained in this pilot experiment confirmed the presence of some structures obtained in silico in 2014: Helix II (TBE), the template, and the template proximal helix (TPH). The first 242 nt of *Leish*TER's structure closely resembled *Tb*TR. In this model, the *Leish*TER TBE started from the 1st nucleotide and contained a CCGUCA motif at its proximal 3' end, similar to *Tetrahymena thermophila*. Nucleotides in the base of TPH showed low reactivity to NAI, indicating rigidity, while the apex was reactive. Most of the *Leish*TER template consisted of single-stranded elements, except for a few nucleotides with low reactivity, suggesting their involvement in long-range or transient interactions. A possible pseudoknot structure was identified near the template region through in-silico analysis performed by Elton Vasconcelos. However, further experiments are needed to confirm the pseudoknot's presence and understand the entire structure of *Leish*TER.

Here is worth mentioning that due to the interruption of BEPE, some of the project's objectives couldn't be accomplished in the U.S.A. However, the project's main goal, which was to learn the RNA chemical probing read by mutational profiling, was accomplished thanks to Dr. Chakrabarti and his Ph.D. student Kaitlin Klotz. Efforts are being made to apply this technique in our lab in Brazil. We started a collaboration with Dr. Rejane Maria Tommasini Grotto, Dr. Guilherme Targino Valente, and Dr. Leonardo Nazario de Moraes from the Molecular Biology – Hemocenter Laboraty at HCFMB (Hospital das Clínicas - Botucatu Medicine University, UNESP) that will help us to conduct the sequencing and analysis. Alongside the *Leish*TER secondary structure study, we will also try to identify *Leish*TER protein partners using either the MS2 tagging or the S1m aptamer approach, followed by mass spectrometry analysis.

Supplementary material

Table S1. Oligonucleotide sequences

Oligonucleotide name	Sequence (5' → 3')
For-Cas9	CCGAAGAGGTCGTGAAGAAG
Rev-Cas9	GCCTTATCCAGTTCGCTCAG
TERm F	TGCTTGCATGTCTGTCCTTC
TER RT R	GAGGATCGCGCTACAAAGTC
LmTERTBEFw-Adp	ccctacacgacgctcttccgatctnnnnnTTTGACAGACCATCTCTCTCTGG
CatCoreLmTERR2Adp	gactggagttcagacgtgtgctcttccgatctnnnnnCCTTCTACCACCTCCGCCG
Universal Rv Primer	AATGATACGGCGACCACCGAGATCTACACTCTTTCCCTACACGACGCTCTTCCG
Adpt 1	CAAGCAGAAGACGGCATACGAGATCGTGATGTGACTGGAGTTCAGAC
Adpt 2	CAAGCAGAAGACGGCATACGAGATACATCGGTGACTGGAGTTCAGAC
Adpt 3	CAAGCAGAAGACGGCATACGAGATGCCTAAGTGACTGGAGTTCAGAC
Adpt 4	CAAGCAGAAGACGGCATACGAGATTGGTCAGTGACTGGAGTTCAGAC
Adpt 19	CAAGCAGAAGACGGCATACGAGATCGTTTCACGTGACTGGAGTTCAGAC
Adpt 23	CAAGCAGAAGACGGCATACGAGATATCCACTCGTGACTGGAGTTCAGAC
TER FragX Fw	TCGTCGGCAGCGTCAGATGTGTATAAGAGACAG[target sequence – Forward]
TER FragX Rv	GTCTCGTGGGCTCGGAGATGTGTATAAGAGACAG[target sequence – Reverse]
TER RT R2	CGTCTTCCCTCATCTCCCTTCC

X: Adaptor sequences

X: Gene-specific sequences

Table S2. Information about the TruSeq barcodes

Sample	**Barcodes**
Treated with 50 mM NAI	Universal Rv Primer + Adpt 1
Treated with 100 mM NAI	Universal Rv Primer + Adpt 2
Treated with 150 mM NAI	Universal Rv Primer + Adpt 3
Untreated – control of 50 mM NAI	Universal Rv Primer + Adpt 4
Untreated – control of 100 mM NAI	Universal Rv Primer + Adpt 19
Untreated – control of 150 mM NAI	Universal Rv Primer + Adpt 23

References

ASSIS, L., ANDRADE-SILVA, D., SHIBURAH, M. E., DE OLIVEIRA, B., PAIVA, S. C., ABUCHERY, B. E., FERRI, Y. G., FONTES, V. S., DE OLIVEIRA, L. S., DA SILVA, M. S., & CANO, M. (2021). Cell Cycle, Telomeres, and Telomerase in *Leishmania* spp.: What Do We Know So Far? Cells, 10(11), 3195. https://doi.org/10.3390/cells10113195

AUTEXIER, C., & LUE, N. F. (2006). The structure and function of telomerase reverse transcriptase. Annual Review of Biochemistry, 75, 493–517. https://doi.org/10.1146/annurev.biochem.75.103004.142412

BARBE-TUANA, F.; GRUN, L.K.; PIERDONÁ, V.; DE OLIVEIRA, B.C.D.; PAIVA, S.C.; SHIBURAH, M.E.; DA SILVA, V.L.; MOREA, E.G.O.; FONTES, V.S.; CANO, M.I.N. Human Chromosome Telomeres. (2021). In Human Genome Structure, Function and Clinical Considerations; Haddad, L.A., Ed.; Springer: Cham, Switzerland, 207–243. https://doi.org/10.1007/978- 3-030-73151-9_7

BATES, P. A., & ROGERS, M. E. (2004). New insights into the developmental biology and transmission mechanisms of *Leishmania*. Current Molecular Medicine, 4(6), 601–609. https://doi.org/10.2174/1566524043360285
Beneke, T., Madden, R., Makin, L., Valli, J., Sunter, J., & Gluenz, E. (2017). A CRISPR Cas9 high- throughput genome editing toolkit for kinetoplastids. Royal Society Open Science, 4(5), 170095. doi:10.1098/rsos.170095

BERMAN, A. J., AKIYAMA, B. M., STONE, M. D., & CECH, T. R. (2011). The RNA accordion model for template positioning by telomerase RNA during telomeric DNA synthesis. Nature Structural & Molecular Biology, 18, 1371–1375. https://doi.org/10.1038/nsmb.2174

BLACKBURN, E. H., & COLLINS, K. (2011). Telomerase: an RNP enzyme synthesizes DNA. Cold Spring Harbor Perspectives in Biology, 3(5), a003558. https://doi.org/10.1101/cshperspect.a003558

BLACKBURN, E. H., EPEL, E. S., & LIN, J. (2015). Human telomere biology: A contributory and interactive factor in aging, disease risks, and protection. Science, 350(6265), 1193–1198. https://doi.org/10.1126/science.aab3389

BLOCHLINGER, K., & DIGGELMANN, H. (1984). Hygromycin B phosphotransferase as a selectable marker for DNA transfer experiments with higher eukaryotic cells. *Molecular and cellular biology*, *4*(12), 2929–2931. https://doi.org/10.1128/mcb.4.12.2929-2931.1984

CANO M. I. (2001). Telomere biology of trypanosomatids: more questions than answers. Trends in Parasitology, 17(9), 425– 429. https://doi.org/10.1016/s1471-4922(01)02014-1

CHAN, S. R., & BLACKBURN, E. H. (2004). Telomeres and telomerase. Philosophical Transactions of the Royal Society of London. Series B, Biological sciences, 359(1441), 109–121. https://doi.org/10.1098/rstb.2003.1370

CHEN, J. L., BLASCO, M. A., & GREIDER, C. W. (2000). Secondary structure of vertebrate telomerase RNA. Cell, 100(5), 503–514. https://doi.org/10.1016/s0092-8674(00)80687-x

COLLINS K. (1999). Ciliate telomerase biochemistry. Annual Review of Biochemistry, 68, 187–218. https://doi.org/10.1146/annurev.biochem.68.1.187

da SILVA, R., & SACKS, D. L. (1987). Metacyclogenesis is a major determinant of *Leishmania* promastigote virulence and attenuation. *Infection and immunity*, *55*(11), 2802–2806. https://doi.org/10.1128/iai.55.11.2802-2806.1987

de OLIVEIRA, B., SHIBURAH, M. E., PAIVA, S. C., VIEIRA, M. R., MOREA, E., DA SILVA, M. S., ALVES, C. S., SEGATTO, M., GUTIERREZ-RODRIGUES, F., BORGES, J. C., CALADO, R. T., & CANO, M. (2021). Possible Involvement of Hsp90 in the Regulation of Telomere Length and Telomerase Activity During the *Leishmania amazonensis* Developmental Cycle and Population Proliferation. Frontiers in Cell and Developmental Biology, 9, 713415. https://doi.org/10.3389/fcell.2021.713415

DEY, A., & CHAKRABARTI, K. (2018). Current perspectives of telomerase structure and function in eukaryotes with emerging views on telomerase in human parasites.International Journal of Molecular Sciences,19(2), 333. https://doi.org/10.3390/ijms19020333

DEY, A.; MONROY-EKLUND, A.; KLOTZ, K.; SAHA, A; DAVIS, J.; Li, B.; LAEDERACH, A.; CHAKRABARTI, K. (2021). In vivo architecture of the telomerase RNA catalytic core in Trypanosoma brucei. Nucleic Acids Research, 49, 12445– 12466. https://doi.org/10.1093/nar/gkab1042

DMITRIEV, P. V., PETROV, A. V., & DONTSOVA, O. A. (2003). Yeast telosome complex: components and their functions. Biochemistry. Biokhimiia, 68(7), 718–734. https://doi.org/10.1023/a:1025022630840

EGAN, E.D., AND K. COLLINS., 2012. An enhanced H/ACA RNP assembly mechanism for human telomerase RNA. Mol Cell Biol. 32:2428-2439.

EISENBERG, D. T. A. (2011). An evolutionary review of human telomere biology: The thrifty telomere hypothesis and notes on potential adaptive paternal effects. American Journal of Human Biology, 23(2), 149–167. https://doi.org/10.1002/ajhb.21127

FERNANDES, C.A.H.; PEREZ, A.M.; BARROS, A.C.; DREYER, T.R.; DA SILVA, M.S.; MOREA, E.G.O.; FONTES, M.R.M.; CANO, M.I.N. (2019). Dual cellular localization of the *Leishmania amazonensis* Rbp38 (LaRbp38) explains its affinity for telomeric and mitochondrial DNA. Biochimie, 162, 15–25. http://dx.doi.org/10.1016/j.biochi.2019.03.017

GUPTA, S.K.; KOLET, L.; DONIGER, T.; BISWAS, V.K.; UNGER, R.; TZFATI, Y.; MICHAELI, S. (2013). The Trypanosoma brucei telomerase RNA (TER) homolog binds core proteins of the C/D snoRNA family. FEBS Letter., 587, 1399–1404. https://doi.org/10.1016/j.febslet.2013.03.017

HAN, S., ZHAO, B. S., MYERS, S. A., CARR, S. A., HE, C., & TING, A. Y. (2020). RNA-protein interaction mapping via MS2- or Cas13-based APEX targeting. Proceedings of the National Academy of Sciences of the United States of America, 117(36), 22068–22079. https://doi.org/10.1073/pnas.2006617117

HE, Y., Y. WANG, B. LIU, C. HELMLING, L. SUSAC, R. CHENG, Z.H. ZHOU, AND J. FEIGON. 2021. Structures of telomerase at several steps of telomere repeat synthesis. Nature. 593:454-459.

HILGARTH, R. S., & LANIGAN, T. M. (2019). Optimization of overlap extension PCR for efficient transgene construction. *MethodsX*, *7*, 100759. https://doi.org/10.1016/j.mex.2019.12.001

KAPLER, G. M., COBURN, C. M., & BEVERLEY, S. M. (1990). Stable transfection of the human parasite *Leishmania major* delineates a 30-kilobase region sufficient for extrachromosomal replication and expression. *Molecular and cellular biology*, *10*(3), 1084–1094. https://doi.org/10.1128/mcb.10.3.1084-1094.1990

KRISTEN, M., PLEHN, J., MARCHAND, V., FRIEDLAND, K., MOTORIN, Y., HELM, M., & WERNER, S. (2020). Manganese ions individually alter the reverse transcription signature of modified ribonucleosides. Genes, 11(8), 950. Https://doi.org/10.3390/genes11080950

LEPPEK, K., & STOECKLIN, G. (2014). An optimized streptavidin-binding RNA aptamer for purification of ribonucleoprotein complexes identifies novel ARE-binding proteins. *Nucleic acids research*, *42*(2), e13. https://doi.org/10.1093/nar/gkt956

LI, B. (2021). Keeping Balance Between Genetic Stability and Plasticity at the Telomere and Subtelomere of Trypanosoma brucei. Frontiers in Cell and Developmental Biology, 9, 699639. https://doi.org/10.3389/fcell.2021.699639

LUE N. F. (2004). Adding to the ends: what makes telomerase processive and how important is it?. BioEssays: news and reviews in molecular, cellular and developmental biology, 26(9), 955–962. https://doi.org/10.1002/bies.20093

MCCORMICK-GRAHAM, M., & ROMERO, D. P. (1995). Ciliate telomerase RNA structural features. *Nucleic acids research*, *23*(7), 1091–1097. https://doi.org/10.1093/nar/23.7.1091

OLOVNIKOV A. M. (1973). A theory of marginotomy. The incomplete copying of template margin in enzymic synthesis of polynucleotides and biological significance of the phenomenon. Journal of Theoretical Biology, 41(1), 181–190. https://doi.org/10.1016/0022-5193(73)90198-7

PACE D. (2014). Leishmaniasis. The Journal of Infection, 69, 10–18. https://doi.org/10.1016/j.jinf.2014.07.016
PEARSON, R. D., & SOUSA, A. Q. (1996). Clinical Spectrum of Leishmaniasis. Clinical Infectious Diseases, 22(1), 1–13. https://doi.org/10.1093/clinids/22.1.1

PODLEVSKY, J. D., LI, Y., & CHEN, J. J.-L. (2016). The functional requirement of two structural domains within telomerase
RNA emerged early in eukaryotes. Nucleic Acids Research, gkw605. doi:10.1093/nar/gkw605

PODLEVSKY, J. D., & CHEN, J. J. (2016). Evolutionary perspectives of telomerase RNA structure and function. RNA Biology, 13(8), 720–732. https://doi.org/10.1080/15476286.2016.1205768

RAN, F. A., HSU, P. D., WRIGHT, J., AGARWALA, V., SCOTT, D. A., & ZHANG, F. (2013). Genome engineering using the CRISPR-Cas9 system. *Nature protocols*, *8*(11), 2281–2308. https://doi.org/10.1038/nprot.2013.143

RICHARDS, R. J., THEIMER, C. A., FINGER, L. D., & FEIGON, J. (2006). Structure of the Tetrahymena thermophila telomerase RNA helix II template boundary element. *Nucleic acids research*, *34*(3), 816–825. https://doi.org/10.1093/nar/gkj481

ROAKE, C.M., AND S.E. ARTANDI. 2020. Regulation of human telomerase in homeostasis and disease. Nat Rev Mol Cell Biol. 21:384-397.

ROBINSON, K. A., & BEVERLEY, S. M. (2003). Improvements in transfection efficiency and tests of RNA interference (RNAi) approaches in the protozoan parasite *Leishmania*. *Molecular and biochemical parasitology*, *128*(2), 217–228. https://doi.org/10.1016/s0166-6851(03)00079-3

SANDHU, R., SANFORD, S., BASU, S., PARK, M., PANDYA, U. M., LI, B., & CHAKRABARTI, K. (2013). A trans-spliced telomerase RNA dictates telomere synthesis in Trypanosoma brucei. Cell Research, 23(4), 537–551. https://doi.org/10.1038/cr.2013.35

SINGH, M., Z. WANG, B.K. KOO, A. PATEL, D. CASCIO, K. COLLINS, AND J. FEIGON. 2012. Structural basis for telomerase RNA recognition and RNP assembly by the holoenzyme La family protein p65. Mol Cell. 47:16-26.

SMOLA, M. J., RICE, G. M., BUSAN, S., SIEGFRIED, N. A., & WEEKS, K. M. (2015). Selective 2′-hydroxyl acylation analyzed by primer extension and mutational profiling (SHAPE-MaP) for direct, versatile and accurate RNA structure analysis. Nature Protocols, 10(11), 1643–1669. doi:10.1038/nprot.2015.103

SMOLA, M. J., & WEEKS, K. M. (2018). In-cell RNA structure probing with SHAPE-MaP. Nature Protocols, 13(6), 1181– 1195. doi:10.1038/nprot.2018.010

STECK E. A. (1974). The leishmaniases. Progress in drug research. Fortschritte der Arzneimittelforschung. Progres Des Recherches Pharmaceutiques, 18, 289–351. https://doi.org/10.1007/978-3-0348-7087-0_22

STROBEL, E. J., YU, A. M., & LUCKS, J. B. (2018). High-throughput determination of RNA structures. Nature reviews. Genetics, 19(10), 615–634. https://doi.org/10.1038/s41576-018-0034-x

VASCONCELOS, E. J., NUNES, V. S., DA SILVA, M. S., SEGATTO, M., MYLER, P. J., & CANO, M. I. (2014). The putative *Leishmania* telomerase RNA (LeishTER) undergoes trans-splicing and contains a conserved template sequence. PloS One, 9(11), e112061. https://doi.org/10.1371/journal.pone.0112061

VIVIESCAS, M. A., SEGATO, M., AND CANO, M. I. N. (2019). Chaperones and their role in telomerase ribonucleoprotein biogenesis and telomere maintenance. Current. Proteomics 16, 31–43. doi: 10.2174/1570164615666180713103133

WATSON J. D. (1972). Origin of concatemeric T7 DNA.Nature: New biology,239(94), 197–201. https://doi.org/10.1038/newbio239197a0

WEBB, C. J., & ZAKIAN, V. A. (2016). Telomerase RNA is more than a DNA template. RNA Biology, 13(8), 683–689. https://doi.org/10.1080/15476286.2016.1191725

ZAPPULLA, D. C., & CECH, T. R. (2006). RNA as a flexible scaffold for proteins: yeast telomerase and beyond. Cold Spring Harbor Symposia on Quantitative Biology, 71, 217–224. https://doi.org/10.1101/sqb.2006.71.011

ZHANG, Q., KIM, N. K., & FEIGON, J. (2011). Architecture of human telomerase RNA. Proceedings of the National Academy of Sciences of the United States of America, 108(51), 20325–20332. https://doi.org/10.1073/pnas.1100279108

3.3 Capítulo 3

Geração de linhagem de *Leishmania major* duplo nocaute para o TER e para a TERT

Introdução

As leishmanioses, doenças tropicais negligenciadas, carecem de tratamentos eficazes e métodos de controle. Suas diversas manifestações clínicas incluem formas cutânea, cutânea difusa, mucocutânea e visceral, sendo esta última a mais grave (Chappuis et. al., 2007). Diante da importância dessas doenças e da falta de tratamentos, vacinas e protocolos de profilaxia eficazes, torna-se crucial a compreensão aprofundada da biologia molecular do parasito. Uma das maquinarias moleculares relacionadas à estabilidade do genoma e proliferação celular é a maquinaria telomérica.

Os telômeros são estruturas nucleoproteicas encontradas nas extremidades de cromossomos lineares de seres eucariontes e são compostos por repetições em tandem de uma sequência não codificante de DNA organizadas em dupla fita e simples fita protrusa ou 3'G-overhang (Blackburn, 1991; Blackburn et al., 2015). Essas estruturas são mantidas pela telomerase, um complexo ribonucleoproteico que possui como núcleo catalítico a transcriptase reversa da telomerase (TERT) e o RNA da telomerase (TER).

O componente TERT é uma transcriptase reversa que sintetiza novas sequências teloméricas (Autexier e Lue, 2006). A TERT possui quatro domínios estruturais e funcionais, incluindo os exclusivos das TERTs, como o TEN (Telomerase Essential N-terminal) e o TRBD (Telomerase RNA Binding Domain) na região N-terminal, essenciais na interação com ácidos nucleicos e proteínas do complexo telomerase (Autexier e Lue, 2006). Na região carboxi-terminal estão presentes o domínio transcriptase reversa (RT), sendo conservado entre as RTs e crucial para a catálise enzimática, e o domínio CTE (C-Terminal Extention), o qual é menos conservado entre as espécies e está também associado com a atividade enzimática da enzima (Hukezalie e Wong, 2013). Por outro lado, o componente TER, um RNA não codificante, atua como molde para a TERT na síntese do DNA telomérico, desempenhando papel crucial na montagem do complexo telomerase (Gilson e Géli, 2007; Zappulla e Cech, 2006). A estrutura secundária do TER é conservada, mas seu tamanho e composição variam entre espécies (Theimer e Feigon, 2006). O motivo TBE (Template Boundary Element) e o molde encontram-se na porção 5' da molécula. Enquanto o TBE está envolvido com a interação com o domínio TRBD da TERT, o molde é usado como substrato pela TERT para a adição de novos nucleotídeos nos telômeros (Blackburn e Collins; Lai et al., 2012). Já outras regiões como o

pseudoknot, o STE e o stem IV, são essenciais para a interação TERT-TER e para a montagem do complexo telomerase (Webb e Zakian, 2016; Jiang et al., 2013). Além disso pode haver regiões adicionais como o domínio H/ACA box, na porção 3' no TER de humanos, e o domínio BOX C/D snoRNA presente em organismos como *T. brucei* e *L. major* (Barbé-Tuana et al., 2021; Gupta et al., 2013; Vasconcelos et al., 2014). Em *Leishmania major*, tanto a TERT como o TER são codificados por genes de cópia única, localizados nos cromossomos 36 e 25, respectivamente (Giardini et al., 2006; Vasconcelos et al., 2014).

Pesquisas realizadas com organismos modelo, como *S. cerevisiae* e *T. brucei*, demonstraram que o nocaute de um dos componentes da telomerase, seja TERT ou TER, provoca o encurtamento dos telômeros (Lundblad & Szostak, 1989; Dreesen et al., 2005; Singer & Gottschling, 1994; Sandhu et al., 2013). Este fenômeno, conforme corroborado nesta tese, assim como na pesquisa de doutorado de nosso colega, Mark Ewusi Shiburah (pré-print doi.org/10.1101/2023.11.10.566596), mostra que em *Leishmania major*, a ausência tanto do TER quanto da TERT também resulta no encurtamento dos telômeros, associado a danos significativos nos parasitos, incluindo prejuízos na proliferação celular e impacto na capacidade de infecção. Diante desse contexto, propus a geração de mutantes duplos nocaute para o TER e a TERT, com o objetivo de avaliar os efeitos combinados da ausência desses dois componentes nos parasitos e compará-los com os mutantes previamente obtidos em nosso laboratório. Após a obtenção dessa nova linhagem de mutantes, a confirmação do nocaute foi realizada e o comprimento dos telômeros foi analisado. Investigações futuras serão conduzidas em nosso laboratório para caracterizar outros fenótipos que esses mutantes podem apresentar.

Objetivos

Objetivo geral

- Gerar uma linhagem duplo nocaute para TERT e TER

Objetivos específicos

- Confirmar o nocaute dos genes que codificam a TERT e o TER.

Materiais e métodos

Cultura celular de *Leishmania major*

Formas promastigotas de *Leishmania major*, cepa *Friedlin* (MHOM/IL/1980/FRIEDLIN) foram cultivadas a 26ºC em meio de cultura comercial M199 1X, pH 7,3 (Cultilab)

suplementado com 10% de soro fetal bovino inativado (SFB) (Cultilab) inativado pelo calor (Kapler et al., 1990), com a adição de solução de 1X de antibióticos penicilina/estreptomicina (Life Technologies, Gibco- BRL). A linhagem *L. major* expressando a T7 RNA polimerase e a Cas9 (Lm007) foi cultivada em meio 199 suplementado com 30 μg/ml de higromicina. A linhagem LmTER$^{-/-}$ foi cultivada em meio 199 suplementado com 30 μg/ml de higromicina e 40 μg/ml de G418. A linhagem duplo nocaute LmTER$^{-/-}$/TERT$^{-/-}$ foi cultivada em meio 199 suplementado com 30 μg/ml de puromicina e 40 μg/ml de G418.

Transfecção e obtenção de linhagens clonais de *Leishmania major* nocaute para o TER e TERT

Para a obtenção de linhagem nocaute para o TER e TERT, uma linhagem nocaute para o TER obtida anteriormente (LmTER$^{-/-}$) e que expressa a Cas9 e a T7/RNAp foi utilizada. Para a transfecção foram utilizados dois moldes de sgRNAs, um para a extremidade 5' e outro para a extremidade 3' do gene da TERT (Tabela 1), além do cassete de DNA doador que contém o gene que confere resistência à Puromicina. As reações de PCR para gerar os sgRNAs e o DNA doador foram realizadas seguindo as orientações oferecidas por Beneke et al. (2017). A ferramenta online LeishGEdit (http://www.leishgedit.net/Home.html) foi utilizada para a escolha das sequências dos sgRNA e dos iniciadores específicos para amplificar os fragmentos de DNA doador. A transfecção dos sgRNAs e do DNA doador foi realizada conforme descrito anteriormente em Kapler et al. (1990). A seleção de transfectantes foi realizada em placa sólida de M199 2x/ágar 2% suplementado com 20% (v/v) de soro fetal bovino contendo 30 μg/ml de higromicina, 30 μg/ml de puromicina e 40 μg/ml de G418. As colônias escolhidas foram inoculadas em meio líquido M199 1x suplementado com 10% (v/v) soro fetal bovino e com 30 μg/ml de puromicina e 40 μg/ml de G418.

Tabela 1. Sequência dos moldes sgRNAs utilizados.

Molde de sgRNA	Sequência (5' – 3')	Descrição
1	5'GAAATTAATACGACTCACTATAGGGTACCATG AACGAGGCAAGGGTTTTAGAGCTAGAAATAGCA AGTTAAAATAAGGCTAGTCCGTTATCAACTTGAA AAAGTGGCACCGAGTCGGTGCTTTT 3'	Utilização dos iniciadores TracrRNA + 5-sgRNATERT Ben (124 pb).
2	5'GAAATTAATACGACTCACTATAGGTAACCCCAA CACTCACAGAGGTTTTAGAGCTAGAAATAGCAA GTTAAAATAAGGCTAGTCCGTTATCAACTTGAAA AAGTGGCACCGAGTCGGTGCTTTT 3'	Utilização dos iniciadores TracrRNA + 3-sgRNATERT Ben(124 pb).

x: região promotora da T7/RNAp;
x: sequência complementar a região alvo;
x sequência do *sgRNA scaffold*.

Extração de DNA genômico de *L. major* e confirmação da ausência do gene que codifica a TERT

Formas promastigotas em fase exponencial de crescimento de *L. major* foram submetidas a extração de DNA utilizando o kit *DNeasy Blood & Tissue* (*Qiagen*) seguindo as recomendações do fabricante. As amostras foram então tratadas com 10 µg/µl RNase A (Invitrogen) e a concentração e pureza do DNA foram avaliadas por espectrofotometria de absorção (OD_{260nm}), utilizando o equipamento *Epoch* (*BioTek*). A integridade do DNA foi verificada em gel de agarose 1%. Para verificar a ausência do gene que codifica a TERT, uma PCR utilizando iniciadores específicos foram utilizados (PWTF1 e PWTR7 - Tabela 2). A linhagem foi nomeada de $LmTER^{-/-}/TERT^{-/-}$.

RT-PCR para verificar a ausência da expressão da TERT em parasitos $LmTER^{-/-}$ /$LmTERT^{-/-}$

Extrato total de RNA de formas promastigotas de clones de $LmTER^{-/-}$, $LmTER^{-/-}/LmTERT^{-/-}$ e do controle Lm007 foi isolado seguindo as recomendações do fabricante do reagente TRIzol (Invitrogen). Para estes ensaios, foi utilizado $3x10^8$ células em fase exponencial de crescimento. Após a extração, o RNA foi tratado com DNase I, RNase free (ThermoFisher) seguindo as recomendações do fabricante. A reação foi inativada usando 1 µl de 25 mM de EDTA e incubada a 65ºC por 10 minutos. A concentração e pureza do RNA foram avaliadas por espectrofotometria de absorção (OD260nm), utilizando o equipamento Epoch (BioTek). Para a RT-PCR foi utilizado o kit SuperScriptTM III One-Step RT-PCR System with PlatinumTM

Taq DNA Polymerase da Invitrogen, seguindo as recomendações do fabricante, utilizando iniciadores específicos para o gene da TERT (5'TERT F + 5'TERT R - Tabela 2).

Sequenciamento dos clones LmTER$^{-/-}$/LmTERT$^{-/-}$

Para o sequenciamento foram utilizados iniciadores específicos que hibridizam nas regiões 5' (PWTF1 – Tabela 2) e 3' (PWTR7 – Tabela 2) do lócus gênico da TERT e iniciadores que hibridizam na porção 5' (Puro1 UTR 5' Rv – Tabela 2) e 3' (Puro2 UTR 3' Fw – Tabela 2) do DNA doador. Essas regiões foram escolhidas pois, elas abrangem uma porção do lócus da TERT selvagem, mantida após o nocaute e que contém a região de homologia, e uma porção do DNA doador, o que permite analisar se o nocaute ocorreu no local esperado. Os fragmentos de interesse foram gerados por PCR com posterior purificação dos produtos de PCR utilizando o PureLink™ PCR Purification Kit (Invitrogen), e então foram sequenciados no IBTEC (UNESP – Botucatu) utilizando a técnica de Sanger. As análises foram realizadas através da ferramenta online Clustal Omega (https://www.ebi.ac.uk/Tools/msa/clustalo/) e SnapGene 6.0.2.

Tabela 2. Sequência dos iniciadores utilizados

Nome do inciador	Sequência (5' – 3')
5'TERT F	GCCTCGTTTCCATCAATTCC
5'TERT R	GAAAACGATCTCTCGAATGCTGT
Puro1 UTR 5' Rv	TTCGTGAGAGAAACCTGTAG
Puro2 UTR 3' Fw	AATACAGGCACGGTCCT
PWTF1	GGTACGTCATAGGCACTTGAAAG
PWTR7	TGTGTGTCTGCAATCAGCC

Resultados

Linhagem de *L. major* duplo nocaute para a TERT e TER (LmTER$^{-/-}$/LmTERT$^{-/-}$) foram obtidas com sucesso

O sucesso do nocaute duplo da TERT em linhagem LmTER$^{-/-}$ foi confirmado através de PCR, RT-PCR e também por sequenciamento Sanger com foco nas regiões de homologia (local que o DNA doador foi inserido no locus específico através de reparo dirigido).

Na figura 1A observa-se o mapa do lócus gênico da TERT no cromossomo 36 de *Leishmania major* WT e na figura 1B o mapa do mesmo lócus após a substituição do gene da

TERT pelo cassete de DNA doador que confere resistência à puromicina. Ainda nesses mapas podem ser observados os sítios de hibridização dos iniciadores utilizados na confirmação do nocaute da TERT (PWTF1 + PWTR7 – Tabela 2), no ensaio de RT-PCR (5’ TERT F + 5’ TERT R – Tabela 2) e no sequenciamento (PWTF1 + Puro1 UTR 5’ Rv; Puro2 UTR 3’ Fw + PWTR7 – Tabela 2) (Fig. 1A e 5B).

O conjunto de iniciadores PWTF1 + PWTR7 permitem a geração de um amplicon de 4831 pb para aqueles que possuem o gene da TERT e um amplicon de 2.228 pb é gerado naqueles que tiveram o gene da TERT substituído pelo DNA doador (Fig 1A e 1B). Dessa forma, foi confirmado o duplo nocaute do gene da TERT, pois nos clones isolados e selecionados houve amplificação de apenas um fragmento com amplicon de 2.228 pb referente a amplificação do gene que confere resistência à puromicina no lócus onde se encontrava a TERT (Fig. 1C). Nos controles (LmTER$^{-/-}$ e Lm007), por sua vez, ocorreu a amplificação de um fragmento de 4.831 pb indicando a presença do gene que codifica a TERT no locus específico no cromossomo 36 (Fig. 1C).

Para a RT-PCR, caso o gene que codifica a TERT fosse expresso, os iniciadores utilizados (5’ TERT F + 5’ TERT R) gerariam um cDNA de 692 pb (Fig. 1A). Como pode ser observado na figura 1D, nos dois clones analisados não houve amplificação, enquanto nos controles que expressam a TERT, há a amplificação de um cDNA de 692 pb.

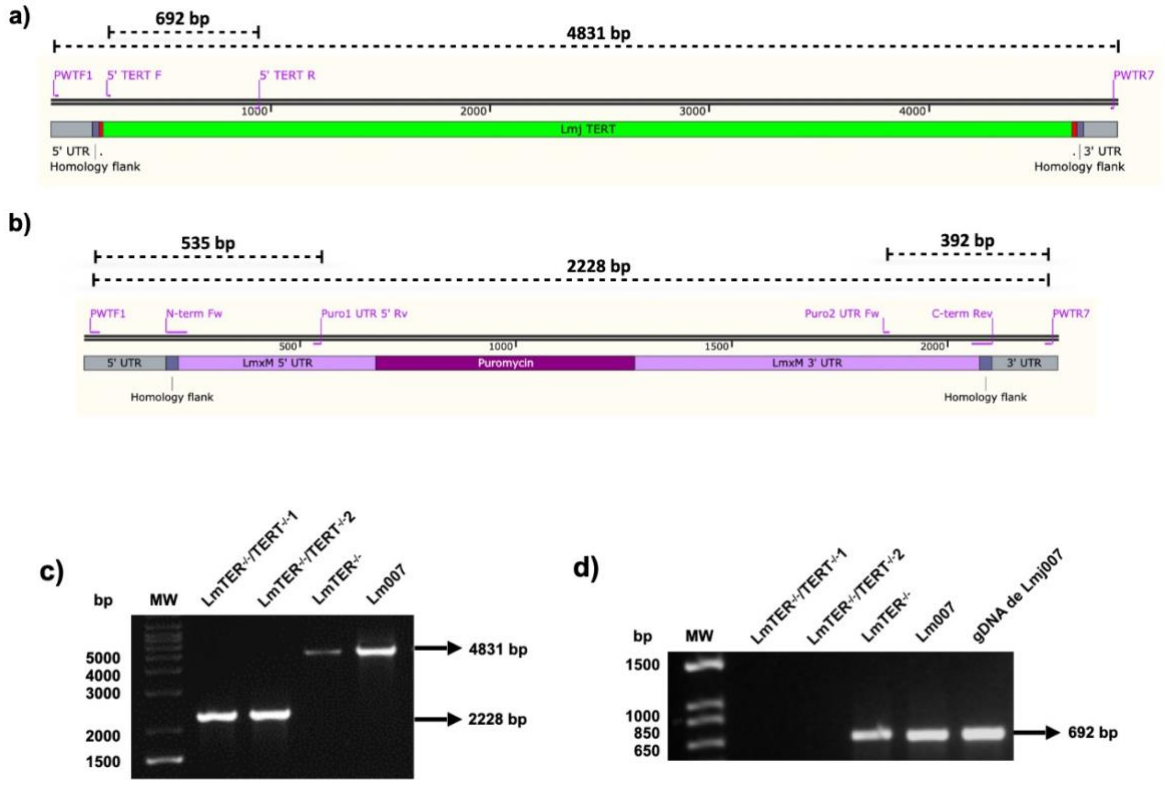

Figura 1. Mapas esquemáticos do lócus da TERT antes e depois do nocaute e confirmação via PCR e RT-PCR do nocaute da TERT. a) Mapa esquemático do lócus gênico da TERT WT evidenciando os conjuntos de iniciadores utilizados para a PCR e RT-PCR indicando o tamanho dos amplicons esperados; b) Mapa esquemático do lócus gênico da TERT após o nocaute mostrando os conjuntos de iniciadores utilizados para confirmar o nocaute da TERT e para a realização do sequenciamento, indicando o tamanho dos amplicons esperados; c) PCR utilizando os iniciadores PWTF1 e PWTR7, os quais geram um amplicon de 4831 pb referente a TERT selvagem (presente em LmTER$^{-/-}$ e Lm007) e um amplicon de 2228 pb nas linhagens LmTER$^{-/-}$/LmTERT$^{-/-}$ devido a substituição do gene da TERT pelo cassete de DNA doador. Gel de agarose 1% corado com brometo de etídeo. MW - Molecular weight 1 KB plus DNA ladder (Invitrogen); d) RT-PCR utilizando os iniciadores 5' TERT F e 5' TERT R, os quais geram um fragmento de cDNA de 692 pb nas linhagens que contém a TERT selvagem (LmTER$^{-/-}$ e Lm007), englobando uma parte da região 5'UTR da TERT e uma parte da região interna da TERT, como pode ser observado na figura **a**. Gel de agarose 1% corado com brometo de etídeo. MW - Molecular weight 1 KB plus DNA ladder da Invitrogen.

Após a confirmação por PCR e RT-PCR da ausência do gene da TERT, as amostras foram enviadas ao IBTEC (UNESP/Botucatu) para a realização do sequenciamento Sanger usando iniciadores específicos (Tabela 2). Na imagem 2A pode ser observado em vermelho os sítios alvos dos sgRNAs, os quais são adjacentes as regiões de homologia (em roxo) utilizadas para o reparo direcionado por recombinação homóloga. Na porção 5' da molécula encontra-se a primeira região de homologia, a qual é a mesma entre os controles com TERT WT e os clones LmTER$^{-/-}$/TERT$^{-/-}$. A partir dessa região seguindo para o interior do gene percebe-se que a sequência de nucleotídeos entre os clones LmTER$^{-/-}$/LmTERT$^{-/-}$ são iguais entre si, porém diferentes em comparação com a TERT WT (Fig. 2B), o mesmo pode ser observado na porção 3' da molécula (Fig. 2B). Esse é o resultado esperado para linhagens nocaute para a TERT. Sendo assim, esse resultado confirmou os resultados obtidos por PCR e RT-PCR e o sucesso na obtenção de linhagens duplo nocaute para o TER e para a TERT (LmTER$^{-/-}$/LmTERT$^{-/-}$).

Figura 2. Confirmação do nocaute do gene da TERT por sequenciamento Sanger. a) Mapa esquemático do lócus da TERT selvagem, destacando as regiões de homologia na porção 5' e 3' UTR (roxo) e as regiões alvo dos sgRNAs (vermelho); b) Eletroferogramas provenientes do sequenciamento Sanger para confirmar o nocaute da TERT. Os fragmentos de interesse foram amplificados por PCR e então sequenciados pelo método Sanger. Através da análise dos eletroferogramas é possível observar a similaridade entre as regiões de homologia (porção 5 'e 3 ' UTR sublinhados em LmWT e enquadrados em LmTER$^{-/-}$/TERT$^{-/-}$). As diferenças após essas regiões (sentido interno do gene) mostram que ocorreu a integração do DNA doador que contém o gene que confere resistência a puromicina no lócus da TERT, mostrando que o nocaute do gene funcionou; c) Mapa esquemático do lócus da TERT após o nocaute e integração do cassete de DNA doador. Os mapas apresentados foram idealizados utilizando-se o programa SnapGene® versão 6.0.2.

Conclusões e perspectivas

Como já evidenciado neste trabalho e no trabalho de doutorado de Mark Shiburah, observou-se que nem o gene do TER nem o da TERT são indispensáveis para a sobrevivência do parasito. Esses resultados preliminares indicam que também é viável obter linhagens nocautes para ambos os alelos de cada gene sem causar a morte imediata do parasito. No entanto, é essencial explorar as possíveis consequências decorrentes da ausência simultânea de ambos os genes nos parasitos, fazendo uma comparação desses resultados com os obtidos em linhagens que possuem apenas um dos genes ausentes. Esta análise será conduzida pelo nosso grupo de pesquisa, oferecendo perspectivas valiosas para o entendimento mais aprofundado desses mecanismos genéticos em *Leishmania*.

Referências

AUTEXIER, C., & LUE, N. F. (2006). The structure and function of telomerase reverse transcriptase. Annual review of biochemistry, 75, 493–517. https://doi.org/10.1146/annurev.biochem.75.103004.142412

BARBÉ-TUANA, F., GRUN, L. K., PIERDONÁ, V., DE OLIVEIRA, B. C. D., PAIVA, S. C., SHIBURAH, M. E., ... & CANO, M. I. N. (2021). Human Chromosome Telomeres. In Human Genome Structure, Function and Clinical Considerations (pp. 207-243).
Cham: Springer International Publishing.

BLACKBURN E. H. (1991). Structure and function of telomeres. Nature, 350(6319), 569–573. https://doi.org/10.1038/350569a0

BLACKBURN, E. H., & COLLINS, K. (2011). Telomerase: an RNP enzyme synthesizes DNA. Cold Spring Harbor perspectives in biology, 3(5), a003558. https://doi.org/10.1101/cshperspect.a003558

BLACKBURN, E. H., EPEL, E. S., & LIN, J. (2015). Human telomere biology: A contributory and interactive factor in aging, disease risks, and protection. Science (New York, N.Y.), 350(6265), 1193–1198. https://doi.org/10.1126/science.aab3389

CHAPPUIS, F., SUNDAR, S., HAILU, A., GHALIB, H., RIJAL, S., PEELING, R. W., ALVAR, J., & BOELAERT, M. (2007). Visceral leishmaniasis: what are the needs for diagnosis, treatment and control?. Nature reviews. Microbiology, 5(11), 873–882. https://doi.org/10.1038/nrmicro1748

DREESEN, O., LI, B., & CROSS, G. A. (2005). Telomere structure and shortening in telomerase-deficient Trypanosoma brucei. *Nucleic acids research*, *33*(14), 4536–4543. https://doi.org/10.1093/nar/gki769

GIARDINI, M. A., LIRA, C. B., CONTE, F. F., CAMILLO, L. R., DE SIQUEIRA NETO, J. L., RAMOS, C. H., & CANO, M. I. (2006). The putative telomerase reverse transcriptase

component of *Leishmania amazonensis*: gene cloning and characterization. *Parasitology research*, *98*(5), 447–454. https://doi.org/10.1007/s00436-005-0036-4

GILSON, E., & GÉLI, V. (2007). How telomeres are replicated. Nature reviews. Molecular cell biology, 8(10), 825–838. https://doi.org/10.1038/nrm2259

GUPTA, S. K., KOLET, L., DONIGER, T., BISWAS, V. K., UNGER, R., TZFATI, Y., & MICHAELI, S. (2013). The Trypanosoma brucei telomerase RNA (TER) homologue binds core proteins of the C/D snoRNA family. FEBS letters, 587(9), 1399–1404. https://doi.org/10.1016/j.febslet.2013.03.017

HUKEZALIE, K. R., & WONG, J. M. (2013). Structure-function relationship and biogenesis regulation of the human telomerase holoenzyme. The FEBS journal, 280(14), 3194–3204. https://doi.org/10.1111/febs.12272

JIANG, J., MIRACCO, E. J., HONG, K., ECKERT, B., CHAN, H., CASH, D. D., MIN, B., ZHOU, Z. H., COLLINS, K., & FEIGON, J. (2013). The architecture of Tetrahymena telomerase holoenzyme. Nature, 496(7444), 187–192. https://doi.org/10.1038/nature12062

LAI, A. C., NGUYEN BA, A. N., & MOSES, A. M. (2012). Predicting kinase substrates using conservation of local motif density. Bioinformatics (Oxford, England), 28(7), 962–969. https://doi.org/10.1093/bioinformatics/bts060

LUNDBLAD, V., & SZOSTAK, J. W. (1989). A mutant with a defect in telomere elongation leads to senescence in yeast. *Cell*, *57*(4), 633–643. https://doi.org/10.1016/0092-8674(89)90132-3

SANDHU, R., SANFORD, S., BASU, S., PARK, M., PANDYA, U. M., LI, B., & CHAKRABARTI, K. (2013). A trans-spliced telomerase RNA dictates telomere synthesis in Trypanosoma brucei. *Cell research*, *23*(4), 537–551. https://doi.org/10.1038/cr.2013.35

SINGER, M. S., & GOTTSCHLING, D. E. (1994). TLC1: template RNA component of Saccharomyces cerevisiae telomerase. *Science (New York, N.Y.)*, *266*(5184), 404–409. https://doi.org/10.1126/science.7545955

THEIMER, C. A., & FEIGON, J. (2006). Structure and function of telomerase RNA. Current opinion in structural biology, 16(3), 307–318. https://doi.org/10.1016/j.sbi.2006.05.005

VASCONCELOS, E. J., NUNES, V. S., DA SILVA, M. S., SEGATTO, M., MYLER, P. J., & CANO, M. I. (2014). The putative *Leishmania* telomerase RNA (LeishTER) undergoes trans-splicing and contains a conserved template sequence. PloS one, 9(11), e112061. https://doi.org/10.1371/journal.pone.0112061

WEBB, C. J., & ZAKIAN, V. A. (2016). Telomerase RNA is more than a DNA template. RNA biology, 13(8), 683–689. https://doi.org/10.1080/15476286.2016.1191725

ZAPPULLA, D. C., & CECH, T. R. (2006). RNA as a flexible scaffold for proteins: yeast telomerase and beyond. Cold Spring Harbor symposia on quantitative biology, 71, 217–224. https://doi.org/10.1101/sqb.2006.71.011

4 Conclusões

- A ausência de *Leish*TER causou encurtamento dos telômeros e comprometeu a proliferação dos parasitos, levando os mesmos a um estado semelhante a senescência replicativa, o que sublinha a importância de *Leish*TER na sobrevida do parasito. Aqui ressaltam-se que a ausência de *Leish*TER induziu alterações morfológicas e ativação de processos autofágicos, indicando adaptações celulares para manter a homeostase, sem evidências de apoptose. Embora a capacidade de transformação na forma infectiva metacíclica tenha sido preservada, a infectividade dos parasitos mutantes foi reduzida, sugerindo uma associação entre telômeros mais curtos e menor infectividade. Essas descobertas respaldam a noção de que a ausência de *Leish*TER é de certa forma deletéria para *Leishmania.* Além disso, a superexpressão de *Leish*TER teve um efeito dominante negativo nos parasitos, gerando fenótipos semelhantes aos observados nas linhagens duplo nocaute para *Leish*TER. Esses resultados evidenciam a importância da telomerase na sobrevivência e infectividade desses parasitos, abrindo caminho para investigações adicionais sobre os mecanismos moleculares subjacentes e suas possíveis implicações como potenciais alvos no tratamento da leishmaniose.

- A técnica SHAPE-MaP usando NAI mostrou-se uma abordagem bem-sucedida para investigar a estrutura secundária de *Leish*TER. Os resultados preliminares confirmaram a presença de estruturas previamente preditas *in silico*, incluindo a Hélice II (TBE) e o molde, e mostram conservação da estrutura secundária do *Leish*TER com a de *Tb*TR. Atualmente novos experimentos estão sendo conduzidos e esperamos desvendar em breve a estrutura secundária completa de *Leish*TER.

- Estudos preliminares realizados nesse trabalho demonstraram que tanto o gene TER quanto o gene TERT não são essenciais para a sobrevivência do parasito, possibilitando a obtenção de linhagens nocautes para ambos os alelos de cada gene sem causar sua morte imediata. No entanto, é crucial investigar a longevidade desses parasitos em cultura e as sua possíveis implicações biológicas, comparando esses resultados com linhagens que têm apenas um dos genes ausentes.

- Em síntese, os resultados obtidos ressaltam a importância do RNA da telomerase na manutenção dos telômeros, no crescimento celular e na capacidade infectiva de *Leishmania major*. Esses achados ampliam a compreensão do papel da telomerase na biologia do parasito e abrem caminhos para investigações futuras sobre a longevidade desses parasitos, bem como a presença ou ausência de mecanismos alternativos de elongamento telomérico por meio de recombinação homóloga.

5 Referências

AKHOUNDI, M., KUHLS, K., CANNET, A., VOTÝPKA, J., MARTY, P., DELAUNAY, P., & SERENO, D. (2016). A Historical Overview of the Classification, Evolution, and Dispersion of *Leishmania* Parasites and Sandflies. *PLoS neglected tropical diseases*, *10*(3), e0004349. https://doi.org/10.1371/journal.pntd.0004349

ARMANIOS, M., & BLACKBURN, E. H. (2012). The telomere syndromes. *Nature reviews. Genetics*, *13*(10), 693–704. https://doi.org/10.1038/nrg3246

ASSIS, L. H. C., ANDRADE-SILVA, D., SHIBURAH, M. E., DE OLIVEIRA, B. C. D., PAIVA, S. C., ABUCHERY, B. E., FERRI, Y. G., FONTES, V. S., DE OLIVEIRA, L. S., DA SILVA, M. S., & CANO, M. I. N. (2021). Cell Cycle, Telomeres, and Telomerase in *Leishmania* spp.: What Do We Know So Far?. *Cells*, *10*(11), 3195. https://doi.org/10.3390/cells10113195

AUTEXIER, C., & LUE, N. F. (2006). The structure and function of telomerase reverse transcriptase. *Annual review of biochemistry*, *75*, 493–517. https://doi.org/10.1146/annurev.biochem.75.103004.142412

AZZALIN, C. M., REICHENBACH, P., KHORIAULI, L., GIULOTTO, E., & LINGNER, J. (2007). Telomeric repeat containing RNA and RNA surveillance factors at mammalian chromosome ends. *Science* (New York, N.Y.), 318(5851), 798–801. https://doi.org/10.1126/science.1147182

BARBÉ-TUANA, F., GRUN, L. K., PIERDONÁ, V., DE OLIVEIRA, B. C. D., PAIVA, S. C., SHIBURAH, M. E., ... & CANO, M. I. N. (2021). Human Chromosome Telomeres. In Human Genome Structure, Function and Clinical Considerations (pp. 207-243).
Cham: Springer International Publishing.

BATES P. A. (1994). Complete developmental cycle of *Leishmania mexicana* in axenic culture. *Parasitology*, *108 (Pt1)*, 1–9. https://doi.org/10.1017/s0031182000078458

BLACKBURN E. H. (1991). Structure and function of telomeres. *Nature*, *350*(6319), 569–573. https://doi.org/10.1038/350569a0

BLACKBURN, E. H., & COLLINS, K. (2011). Telomerase: an RNP enzyme synthesizes DNA. *Cold Spring Harbor perspectives in biology*, *3*(5), a003558. https://doi.org/10.1101/cshperspect.a003558

BLACKBURN, E. H., EPEL, E. S., & LIN, J. (2015). Human telomere biology: A contributory and interactive factor in aging, disease risks, and protection. *Science (New York, N.Y.)*, *350*(6265), 1193–1198. https://doi.org/10.1126/science.aab3389

BLASCO, M. A. (2001). *The telomerase knockout mouse. Advances in Cell Aging and Gerontology, 151–165.* doi:10.1016/s1566-3124(01)08008-7

CANO, M. I., DUNGAN, J. M., AGABIAN, N., & BLACKBURN, E. H. (1999). Telomerase in kinetoplastid parasitic protozoa. *Proceedings of the National Academy of Sciences of the United States of America*, *96*(7), 3616–3621. https://doi.org/10.1073/pnas.96.7.3616

CANO M. I. (2001). Telomere biology of trypanosomatids: more questions than answers. *Trends in parasitology*, *17*(9), 425–429. https://doi.org/10.1016/s1471-4922(01)02014-1

CARREGAL, V. M., LANZA, J. S., SOUZA, D. M., ISLAM, A., DEMICHELI, C., FUJIWARA, R. T., RIVAS, L., & FRÉZARD, F. (2019). Combination oral therapy against *Leishmania amazonensis* infection in BALB/c mice using nanoassemblies made from amphiphilic antimony(V) complex incorporating miltefosine. *Parasitology research*, *118*(10), 3077–3084. https://doi.org/10.1007/s00436-019-06419-2

CASH, D. D., & FEIGON, J. (2017). Structure and folding of the Tetrahymena telomerase RNA pseudoknot. *Nucleic acids research*, *45*(1), 482–495. https://doi.org/10.1093/nar/gkw1153

CHAN, S. R., & BLACKBURN, E. H. (2004). Telomeres and telomerase. *Philosophical transactions of the Royal Society of London. Series B, Biological sciences*, *359*(1441), 109–121. https://doi.org/10.1098/rstb.2003.1370

CHAPPUIS, F., SUNDAR, S., HAILU, A., GHALIB, H., RIJAL, S., PEELING, R. W., ALVAR, J., & BOELAERT, M. (2007). Visceral leishmaniasis: what are the needs for diagnosis, treatment and control?. *Nature reviews. Microbiology*, *5*(11), 873–882. https://doi.org/10.1038/nrmicro1748

CHEN, J. L., & GREIDER, C. W. (2004). An emerging consensus for telomerase RNA structure. *Proceedings of the National Academy of Sciences of the United States of America*, *101*(41), 14683–14684. https://doi.org/10.1073/pnas.0406204101

COLLINS K. (1999). Ciliate telomerase biochemistry. *Annual review of biochemistry*, *68*, 187–218. https://doi.org/10.1146/annurev.biochem.68.1.187

CUPOLILLO, E.; BOITÉ, M. C.; PORROZZI, R. (2014). Considerações sobre a Taxonomia do Gênero *Leishmania*. In: *Leishmanioses do continente americano*. Editora FIOCRUZ. p. 39–51.

da SILVA, M. S., PEREZ, A. M., DA SILVEIRA, R.DEC., DE MORAES, C. E., SIQUEIRA-NETO, J. L., FREITAS, L.DEH., JR, & CANO, M. I. (2010). The *Leishmania amazonensis* TRF (TTAGGG repeat-binding factor) homologue binds and co-localizes with telomeres. *BMC microbiology*, *10*, 136. https://doi.org/10.1186/1471-2180-10-136

DA SILVA, R., & SACKS, D. L. (1987). Metacyclogenesis is a major determinant of *Leishmania* promastigote virulence and attenuation. *Infection and immunity*, *55*(11), 2802–2806. https://doi.org/10.1128/iai.55.11.2802-2806.1987

DAMASCENO, J. D., SILVA, G., TSCHUDI, C., & TOSI, L. R. (2017). Evidence for regulated expression of Telomeric Repeat-containing RNAs (TERRA) in parasitic trypanosomatids. *Memorias do Instituto Oswaldo Cruz*, *112*(8), 572–576. https://doi.org/10.1590/0074-02760170054

DESJEUX P. (1992). Human leishmaniases: epidemiology and public health aspects. *World health statistics quarterly. Rapport trimestriel de statistiques sanitaires mondiales*, *45*(2-3), 267–275.

DMITRIEV, P. V., PETROV, A. V., & DONTSOVA, O. A. (2003). Yeast telosome complex: components and their functions. *Biochemistry. Biokhimiia*, *68*(7), 718–734. https://doi.org/10.1023/a:1025022630840

EISENBERG D. T. (2011). An evolutionary review of human telomere biology: the thrifty telomere hypothesis and notes on potential adaptive paternal effects. *American journal of human biology : the official journal of the Human Biology Council*, *23*(2), 149–167. https://doi.org/10.1002/ajhb.21127

FENG, J., FUNK, W. D., WANG, S. S., WEINRICH, S. L., AVILION, A. A., CHIU, C. P., ADAMS, R. R., CHANG, E., ALLSOPP, R. C., & YU, J. (1995). The RNA component of human telomerase. *Science (New York, N.Y.)*, *269*(5228), 1236–1241. https://doi.org/10.1126/science.7544491

FERNANDES, C. A. H., MOREA, E. G. O., DOS SANTOS, G. A., DA SILVA, V. L., VIEIRA, M. R., VIVIESCAS, M. A., CHATAIN, J., VADEL, A., SAINTOMÉ, C., FONTES, M. R. M., & CANO, M. I. N. (2020). A multi-approach analysis highlights the relevance of RPA-1 as a telomere end-binding protein (TEBP) in *Leishmania amazonensis*. *Biochimica et biophysica acta. General subjects*, *1864*(7), 129607. https://doi.org/10.1016/j.bbagen.2020.129607

GALVIS OVALLOS, F., SILVA, R. A., SILVA, V. G. D., SÁBIO, P. B., & GALATI, E. A. B. (2020). Leishmanioses no Brasil: aspectos epidemiológicos, desafios e perspectivas. Atualidades em medicina tropical no Brasil: protozoários. Stricto Sensu Editora, 2020. p. 227–255.

GIARDINI, M. A., LIRA, C. B., CONTE, F. F., CAMILLO, L. R., DE SIQUEIRA NETO, J. L., RAMOS, C. H., & CANO, M. I. (2006). The putative telomerase reverse transcriptase

component of *Leishmania amazonensis*: gene cloning and characterization. *Parasitology research*, *98*(5), 447–454. https://doi.org/10.1007/s00436-005-0036-4

GIARDINI, M. A., SEGATTO, M., DA SILVA, M. S., NUNES, V. S., & CANO, M. I. (2014). Telomere and telomerase biology. *Progress in molecular biology and translational science*, *125*, 1–40. https://doi.org/10.1016/B978-0-12-397898-1.00001-3

GILSON, E., & GÉLI, V. (2007). How telomeres are replicated. *Nature reviews. Molecular cell biology*, *8*(10), 825–838. https://doi.org/10.1038/nrm2259

GREIDER, C. W., & BLACKBURN, E. H. (1989). A telomeric sequence in the RNA of Tetrahymena telomerase required for telomere repeat synthesis. *Nature*, *337*(6205), 331–337. https://doi.org/10.1038/337331a0

GRIFFITHS, A. J. F.; WESSLER, S. R.; CARROLL, S. B.; DOEBLEY, J. (2016)Introdução à genética. Editora Guanabara Koogan, 11ª edição.

GUPTA, S. K., KOLET, L., DONIGER, T., BISWAS, V. K., UNGER, R., TZFATI, Y., & MICHAELI, S. (2013). The Trypanosoma brucei telomerase RNA (TER) homologue binds core proteins of the C/D snoRNA family. *FEBS letters*, *587*(9), 1399–1404. https://doi.org/10.1016/j.febslet.2013.03.017

HUKEZALIE, K. R., & WONG, J. M. (2013). Structure-function relationship and biogenesis regulation of the human telomerase holoenzyme. *The FEBS journal*, *280*(14), 3194–3204. https://doi.org/10.1111/febs.12272

JACOBS, S. A., PODELL, E. R., & CECH, T. R. (2006). Crystal structure of the essential N-terminal domain of telomerase reverse transcriptase. *Nature structural & molecular biology*, *13*(3), 218–225. https://doi.org/10.1038/nsmb1054

JIANG, J., MIRACCO, E. J., HONG, K., ECKERT, B., CHAN, H., CASH, D. D., MIN, B., ZHOU, Z. H., COLLINS, K., & FEIGON, J. (2013). The architecture of Tetrahymena telomerase holoenzyme. *Nature*, *496*(7444), 187–192. https://doi.org/10.1038/nature12062

KARAMYSHEVA, Z. N., GUTIERREZ GUARNIZO, S. A., & KARAMYSHEV, A. L. (2020). Regulation of Translation in the Protozoan Parasite *Leishmania*. *International journal of molecular sciences*, *21*(8), 2981. https://doi.org/10.3390/ijms21082981

KERR S. F. (2000). Palaearctic origin of *Leishmania*. *Memorias do Instituto Oswaldo Cruz*, *95*(1), 75–80. https://doi.org/10.1590/s0074-02762000000100011

LAI, A. C., NGUYEN BA, A. N., & MOSES, A. M. (2012). Predicting kinase substrates using conservation of local motif density. *Bioinformatics (Oxford, England)*, *28*(7), 962–969. https://doi.org/10.1093/bioinformatics/bts060

LAINSON, R.; SHAW, J. J. (1987). Evolution, classification and geographical distribution. In: The leishmaniases in Biology and Medicine . Academic Press, v. 1p. 2–120.

LIN, J., LY, H., HUSSAIN, A., ABRAHAM, M., PEARL, S., TZFATI, Y., PARSLOW, T. G., & BLACKBURN, E. H. (2004). A universal telomerase RNA core structure includes structured motifs required for binding the telomerase reverse transcriptase protein. *Proceedings of the National Academy of Sciences of the United States of America*, *101*(41), 14713–14718. https://doi.org/10.1073/pnas.0405879101

LIRA, C. B., DE SIQUEIRA NETO, J. L., KHATER, L., CAGLIARI, T. C., PERONI, L. A., DOS REIS, J. R., RAMOS, C. H., & CANO, M. I. (2007). LaTBP1: a *Leishmania amazonensis* DNA-binding protein that associates in vivo with telomeres and GT-rich DNA using a Myb-like domain. *Archives of biochemistry and biophysics*, *465*(2), 399–409. https://doi.org/10.1016/j.abb.2007.06.020

LUE N. F. (2004). Adding to the ends: what makes telomerase processive and how important is it?. *BioEssays : news and reviews in molecular, cellular and developmental biology*, *26*(9), 955–962. https://doi.org/10.1002/bies.20093

LUKE, B., PANZA, A., REDON, S., IGLESIAS, N., LI, Z., & LINGNER, J. (2008). The Rat1p 5' to 3' exonuclease degrades telomeric repeat-containing RNA and promotes telomere

elongation in Saccharomyces cerevisiae. *Molecular cell*, 32(4), 465–477. https://doi.org/10.1016/j.molcel.2008.10.019

MARTÍNEZ, P., & BLASCO, M. A. (2015). Replicating through telomeres: a means to an end. *Trends in biochemical sciences*, *40*(9), 504–515. https://doi.org/10.1016/j.tibs.2015.06.003

MOREA, E. G. O., VIVIESCAS, M. A., FERNANDES, C. A. H., MATIOLI, F. F., LIRA, C. B. B., FERNANDEZ, M. F., MORAES, B. S., DA SILVA, M. S., STORTI, C. B., FONTES, M. R. M., & CANO, M. I. N. (2017). A calmodulin-like protein (LCALA) is a new Leishmania amazonensis candidate for telomere end-binding protein. *Biochimica et biophysica acta. General subjects*, *1861*(11 Pt A), 2583–2597. https://doi.org/10.1016/j.bbagen.2017.08.011

MOREA, E. G. O., VASCONCELOS, E. J. R., ALVES, C. S., GIORGIO, S., MYLER, P. J., LANGONI, H., AZZALIN, C. M., & CANO, M. I. N. (2021). Exploring TERRA during *Leishmania major* developmental cycle and continuous in vitro passages. *International journal of biological macromolecules*, *174*, 573–586. https://doi.org/10.1016/j.ijbiomac.2021.01.192

NASCIMENTO, A. F. S. C. DO; SANTOS, D. O. (2020). Leishmanioses como doenças negligenciadas: um panorama complexo. In: Atualidades em Medicina Tropical no Brasil: Protozoários. Stricto Sensu Editora, p. 214–226.

NETO, J. L., LIRA, C. B., GIARDINI, M. A., KHATER, L., PEREZ, A. M., PERONI, L. A., DOS REIS, J. R., FREITAS-JUNIOR, L. H., RAMOS, C. H., & CANO, M. I. (2007). *Leishmania* replication protein A-1 binds in vivo single-stranded telomeric DNA. *Biochemical and biophysical research communications*, *358*(2), 417–423. https://doi.org/10.1016/j.bbrc.2007.04.144

NEVES, D. P. (2016). Parasitologia Humana. Editora Atheneu, 13. Ed., São Paulo.

OHKI, R., & ISHIKAWA, F. (2004). Telomere-bound TRF1 and TRF2 stall the replication fork at telomeric repeats. *Nucleic acids research*, *32*(5), 1627–1637. https://doi.org/10.1093/nar/gkh309

OLOVNIKOV A. M. (1973). A theory of marginotomy. The incomplete copying of template margin in enzymic synthesis of polynucleotides and biological significance of the phenomenon. *Journal of theoretical biology*, *41*(1), 181–190. https://doi.org/10.1016/0022-5193(73)90198-7

ORGANIZACIÓN PANAMERICANA DE LA SALUD. (2020). Atlas interactivo de leishmaniasis en las Américas: aspectos clínicos y diagnósticos diferencialesOrganizacion Panamericana de la Salud. PALTEX..

PACE D. (2014). Leishmaniasis. *The Journal of infection*, *69 Suppl 1*, S10–S18. https://doi.org/10.1016/j.jinf.2014.07.016

PACHECO, R. S.; CARVALHO-COSTA, F. A. (2014). Diversidade Genética em Parasitos do Gênero *Leishmania*: uma abordagem molecular. In: Leishmanioses do continente americano. [s.l.] Editora FIOCRUZ, p. 29–38.

PODLEVSKY, J. D., & CHEN, J. J. (2016). Evolutionary perspectives of telomerase RNA structure and function. *RNA biology*, *13*(8), 720–732. https://doi.org/10.1080/15476286.2016.1205768

REIS-CUNHA, J. L.; VALDIVIA, H. O.; CASTANHEIRA, D. . Trypanosomatid Genome Organization and Ploidy. In: SILVA, M. S. DA; CANO, M. I. N. (Eds.). . Frontiers in Parasitology (Volume 1) Molecular and Cellular Biology of Pathogenic Trypanosomatids. [s.l: s.n.]. p. 43.

REITHINGER, R., DUJARDIN, J. C., LOUZIR, H., PIRMEZ, C., ALEXANDER, B., & BROOKER, S. (2007). Cutaneous leishmaniasis. *The Lancet. Infectious diseases*, *7*(9), 581–596. https://doi.org/10.1016/S1473-3099(07)70209-8

ROSS R. (1903). NOTE ON THE BODIES RECENTLY DESCRIBED BY LEISHMAN AND DONOVAN. *British medical journal*, *2*(2237), 1261–1262. https://doi.org/10.1136/bmj.2.2237.1261

SANDHU, R., SANFORD, S., BASU, S., PARK, M., PANDYA, U. M., LI, B., & CHAKRABARTI, K. (2013). A trans-spliced telomerase RNA dictates telomere synthesis in Trypanosoma brucei. *Cell research*, *23*(4), 537–551. https://doi.org/10.1038/cr.2013.35

SCHOEFTNER, S., & BLASCO, M. A. (2008). Developmentally regulated transcription of mammalian telomeres by DNA-dependent RNA polymerase II. *Nature cell biology*, 10(2), 228–236. https://doi.org/10.1038/ncb1685

SILVA, C. G.; SILVA, R. M. M.; DINIZ, V. A. CÔRTE-REAL, S. (2014). Ultraestrutura de Parasitos do Gênero *Leishmania*. In: Leishmanioses do continente americano. [s.l.] Editora FIOCRUZ,. p. 53–67.

SINGER, M. S., & GOTTSCHLING, D. E. (1994). TLC1: template RNA component of Saccharomyces cerevisiae telomerase. *Science (New York, N.Y.)*, *266*(5184), 404–409. https://doi.org/10.1126/science.7545955

STECK E. A. (1974). The leishmaniases. *Progress in drug research. Fortschritte der Arzneimittelforschung. Progres des recherches pharmaceutiques*, *18*, 289–351. https://doi.org/10.1007/978-3-0348-7087-0_22

THEIMER, C. A., & FEIGON, J. (2006). Structure and function of telomerase RNA. *Current opinion in structural biology*, *16*(3), 307–318. https://doi.org/10.1016/j.sbi.2006.05.005

VASCONCELOS, E. J., NUNES, V. S., DA SILVA, M. S., SEGATTO, M., MYLER, P. J., & CANO, M. I. (2014). The putative *Leishmania* telomerase RNA (LeishTER) undergoes trans-splicing and contains a conserved template sequence. *PloS one*, *9*(11), e112061. https://doi.org/10.1371/journal.pone.0112061

WATSON, J. D. (1972). Origin of Concatemeric T7DNA. Nature New Biology, v. 239, n. 94, p. 197–201, out. 1972.

WEBB, C. J., & ZAKIAN, V. A. (2016). Telomerase RNA is more than a DNA template. *RNA biology*, *13*(8), 683–689. https://doi.org/10.1080/15476286.2016.1191725

WHO (WORLD HEALTH ORGANIZATION). Leishmaniasis, Available at: https://apps.who.int/neglected_diseases/ntddata/leishmaniasis/leishmaniasis.html.

WU, P., TAKAI, H., & DE LANGE, T. (2012). Telomeric 3' overhangs derive from resection by Exo1 and Apollo and fill-in by POT1b-associated CST. *Cell*, *150*(1), 39–52. https://doi.org/10.1016/j.cell.2012.05.026

WU, R. A., UPTON, H. E., VOGAN, J. M., & COLLINS, K. (2017). Telomerase Mechanism of Telomere Synthesis. *Annual review of biochemistry*, *86*, 439–460. https://doi.org/10.1146/annurev-biochem-061516-045019

XU Y. (2011). Chemistry in human telomere biology: structure, function and targeting of telomere DNA/RNA. *Chemical Society reviews*, *40*(5), 2719–2740. https://doi.org/10.1039/c0cs00134a

YANG, C. P., CHEN, Y. B., MENG, F. L., & ZHOU, J. Q. (2006). Saccharomyces cerevisiae Est3p dimerizes in vitro and dimerization contributes to efficient telomere replication in vivo. *Nucleic acids research*, *34*(2), 407–416. https://doi.org/10.1093/nar/gkj445

ZAPPULLA, D. C., & CECH, T. R. (2006). RNA as a flexible scaffold for proteins: yeast telomerase and beyond. *Cold Spring Harbor symposia on quantitative biology*, *71*, 217–224. https://doi.org/10.1101/sqb.2006.71.011

ZHANG, Q., KIM, N. K., & FEIGON, J. (2011). Architecture of human telomerase RNA. *Proceedings of the National Academy of Sciences of the United States of America*, *108*(51), 20325–20332. https://doi.org/10.1073/pnas.1100279108

Apêndice 1

Artigo publicado em: **Frontiers in Cell and Developmental Biology**

frontiers in Cell and Developmental Biology

BRIEF RESEARCH REPORT
published: 28 October 2021
doi: 10.3389/fcell.2021.713415

Possible Involvement of Hsp90 in the Regulation of Telomere Length and Telomerase Activity During the *Leishmania amazonensis* Developmental Cycle and Population Proliferation

Beatriz C. D. de Oliveira[1†], Mark E. Shiburah[1†], Stepany C. Paiva[1†], Marina R. Vieira[1], Edna Gicela O. Morea[1], Marcelo Santos da Silva[1], Cristiane de Santis Alves[1], Marcela Segatto[2], Fernanda Gutierrez-Rodrigues[3], Júlio C. Borges[4], Rodrigo T. Calado[3] and Maria Isabel N. Cano[1*]

[1] Department of Chemical and Biological Sciences, Institute of Biosciences, São Paulo State University (UNESP), São Paulo, Brazil, [2] Faculdade Brazileira Multivix, Vitória, Brazil, [3] Hemocentro da Faculdade de Medicina de Ribeirão Preto, Universidade of São Paulo, São Paulo, Brazil, [4] São Carlos Institute of Chemistry, University of São Paulo, São Paulo, Brazil

OPEN ACCESS

Edited by:
Andrew Burgess,
Anzac Research Institute, Australia

Reviewed by:
Juliana Ide Aoki,
University of São Paulo, Brazil
Pedro José Alcolea,
Consejo Superior de Investigaciones Científicas (CSIC), Spain

***Correspondence:**
Maria Isabel N. Cano
maria.in.cano@unesp.br

[†]These authors have contributed equally to this work and share first authorship

Specialty section:
This article was submitted to Cell Growth and Division, a section of the journal Frontiers in Cell and Developmental Biology

Received: 22 May 2021
Accepted: 29 September 2021
Published: 28 October 2021

Citation:
de Oliveira BCD, Shiburah ME, Paiva SC, Vieira MR, Morea EGO, da Silva MS, Alves CS, Segatto M, Gutierrez-Rodrigues F, Borges JC, Calado RT and Cano MIN (2021) Possible Involvement of Hsp90 in the Regulation of Telomere Length and Telomerase Activity During the Leishmania amazonensis Developmental Cycle and Population Proliferation. Front. Cell Dev. Biol. 9:713415. doi: 10.3389/fcell.2021.713415

The *Leishmania* developmental cycle comprises three main life forms in two hosts, indicating that the parasite is continually challenged due to drastic environmental changes. The disruption of this cycle is critical for discovering new therapies to eradicate leishmaniasis, a neglected disease that affects millions worldwide. Telomeres, the physical ends of chromosomes, maintain genome stability and cell proliferation and are potential antiparasitic drug targets. Therefore, understanding how telomere length is regulated during parasite development is vital. Here, we show that telomeres form clusters spread in the nucleoplasm of the three parasite life forms. We also observed that amastigotes telomeres are shorter than metacyclic and procyclic promastigotes and that in parasites with continuous *in vitro* passages, telomere length increases over time. These observed differences in telomere length among parasite's life stages were not due to lack/inhibition of telomerase since enzyme activity was detected in all parasite life stages, although the catalysis was temperature-dependent. These data led us to test if, similar to other eukaryotes, parasite telomere length maintenance could be regulated by Hsp83, the ortholog of Hsp90 in trypanosomatids, and *Leishmania* (LHsp90). Parasites were then treated with the Hsp90 inhibitor 17AAG. The results showed that 17AAG disturbed parasite growth, induced accumulation into G2/M phases, and telomere shortening in a time-dependent manner. It has also inhibited procyclic promastigote's telomerase activity. Besides, LHsp90 interacts with the telomerase TERT component as shown by immunoprecipitation, strongly suggesting a new role for LHsp90 as a parasite telomerase component involved in controlling telomere length maintenance and parasite life span.

Keywords: *Leishmania* life forms, continuous *in vitro* passages, telomeres maintenance, telomerase ribonucleoprotein complex, LHsp90

Apêndice 2

Capítulo de livro publicado em: **Human Genome Structure, Function and Clinical Considerations (págs. 207-243)**

Chapter 7
Human Chromosome Telomeres

Florencia Barbé-Tuana, Lucas Kich Grun, Vinícius Pierdoná, Beatriz Cristina Dias de Oliveira, Stephany Cacete Paiva, Mark Ewusi Shiburah, Vítor Luiz da Silva, Edna Gicela Ortiz Morea, Verônica Silva Fontes, and Maria Isabel Nogueira Cano

7.1 Introduction

The discovery that telomeres, the terminal structures of eukaryotic chromosomes, have a role in controlling genomic stability and reflect an individual's life experiences adds an appeal for the study of these genomic sequences. Telomeres can work as mitotic clocks and sensors of individuals' general health.

Telomeres are ribonucleoprotein complexes ranging in size from 10,000 to 15,000 base pairs (bp) located at the end of linear chromosomes. They are formed by double-stranded non-coding repeated DNA sequences arranged in tandem,

F. Barbé-Tuana (✉)
Postgraduate Program in Cellular and Molecular Biology, School of Health, Sciences and Life, Pontifical Catholic University of Rio Grande do Sul (PUCRS), Porto Alegre, Rio Grande do Sul, Brazil

Laboratory of Immunobiology, School of Sciences, Life and Health, Pontifical Catholic University of Rio Grande do Sul – PUCRS, Porto Alegre, Brazil
e-mail: florencia.tuana@pucrs.br

L. K. Grun
Postgraduate Program in Pediatrics and Child Health, School of Medicine, Pontifical Catholic University of Rio Grande do Sul (PUCRS), Porto Alegre, Rio Grande do Sul, Brazil
e-mail: lucas.grun@pucrs.br

V. Pierdoná
Postgraduate Program: Biochemistry, Federal University of Rio Grande do Sul (UFRGS), Porto Alegre, Rio Grande do Sul, Brazil

B. C. D. de Oliveira · S. C. Paiva · M. E. Shiburah · V. L. da Silva · E. G. O. Morea · V. S. Fontes · M. I. N. Cano
Department of Chemical and Biological Sciences, Biosciences Institute, Sao Paulo State University, Botucatu, Brazil
e-mail: bcd.oliveira@unesp.br; edna.gicela-ortiz-morea@unesp.br; vs.fontes@unesp.br; maria.in.cano@unesp.br

L. A. Haddad (ed.), *Human Genome Structure, Function and Clinical Considerations*, https://doi.org/10.1007/978-3-030-73151-9_7

Apêndice 3

Artigo publicado em: **Cells**

cells

MDPI

Review

Cell Cycle, Telomeres, and Telomerase in *Leishmania* spp.: What Do We Know So Far?

Luiz H. C. Assis [1,†], Débora Andrade-Silva [1,†], Mark E. Shiburah [1], Beatriz C. D. de Oliveira [1], Stephany C. Paiva [1], Bryan E. Abuchery [2], Yete G. Ferri [2], Veronica S. Fontes [1], Leilane S. de Oliveira [1], Marcelo S. da Silva [2,*] and Maria Isabel N. Cano [1,*]

[1] Telomeres Laboratory, Department of Chemical and Biological Sciences, Biosciences Institute, São Paulo State University (UNESP), Botucatu 18618-689, Brazil; lhc.assis@unesp.br (L.H.C.A.); debora.dede@gmail.com (D.A.-S.); me.shiburah@unesp.br (M.E.S.); bcd.oliveira@unesp.br (B.C.D.d.O.); stephany.paiva@unesp.br (S.C.P.); vs.fontes@unesp.br (V.S.F.); leilane.oliveira@unesp.br (L.S.d.O.)

[2] DNA Replication and Repair Laboratory (DRRL), Department of Chemical and Biological Sciences, Biosciences Institute, São Paulo State University (UNESP), Botucatu 18618-689, Brazil; bryan.abuchery@unesp.br (B.E.A.); yete.gambarini@unesp.br (Y.G.F.)

* Correspondence: marcelo.santos-silva@unesp.br (M.S.d.S.); maria.in.cano@unesp.br (M.I.N.C.)

† Both authors contributed equally to the paper.

Abstract: Leishmaniases belong to the inglorious group of neglected tropical diseases, presenting different degrees of manifestations severity. It is caused by the transmission of more than 20 species of parasites of the *Leishmania* genus. Nevertheless, the disease remains on the priority list for developing new treatments, since it affects millions in a vast geographical area, especially low-income people. Molecular biology studies are pioneers in parasitic research with the aim of discovering potential targets for drug development. Among them are the telomeres, DNA–protein structures that play an important role in the long term in cell cycle/survival. Telomeres are the physical ends of eukaryotic chromosomes. Due to their multiple interactions with different proteins that confer a likewise complex dynamic, they have emerged as objects of interest in many medical studies, including studies on leishmaniases. This review aims to gather information and elucidate what we know about the phenomena behind *Leishmania* spp. telomere maintenance and how it impacts the parasite's cell cycle.

Keywords: *Leishmania* spp.; leishmaniases; cell cycle; telomeres; telomerase

Citation: Assis, L.H.C.; Andrade-Silva, D.; Shiburah, M.E.; de Oliveira, B.C.D.; Paiva, S.C.; Abuchery, B.E.; Ferri, Y.G.; Fontes, V.S.; de Oliveira, L.S.; da Silva, M.S.; et al. Cell Cycle, Telomeres, and Telomerase in *Leishmania* spp.: What Do We Know So Far? *Cells* **2021**, *10*, 3195. https://doi.org/10.3390/cells10113195

Academic Editor: Zhixiang Wang

Received: 16 October 2021
Accepted: 14 November 2021
Published: 16 November 2021

1. Introduction

Leishmaniases are among the poverty-related endemic diseases. They are well-known to cause a wide spectrum of clinical manifestations and their harsh incidences in East Africa, the Indian subcontinent, and Latin America, where approximately one million new diagnostics are expected yearly [1]. The disease is vector-induced and caused by more than twenty species of the *Leishmania* genus, protozoan parasites that belong to the Trypanosomatidae family [1]. The invertebrate host is a phlebotomine insect that is infected during a blood meal with amastigote forms. Inside the insect digestive system, amastigotes transform into procyclic promastigotes, which are noninfective but highly proliferative forms. Procyclics eventually migrate to the proboscis and differentiate into infective metacyclic promastigote forms [2,3]. The transmission to humans occurs when a preinfected insect (female phlebotomines) regurgitates during its blood meal infective but nonproliferative forms (metacyclic promastigotes) into the mammalian host skin. Afterward, metacyclics are phagocytosed by neutrophils or macrophages, and further inside the phagolysosomes, the parasites undergo a series of morphogenetic modifications, leading to the formation of amastigotes. The amastigotes then multiply and reach the bloodstream, causing the initiation of clinical manifestations. A new cycle of infection can occur when infected macrophages are ingested by other female phlebotomines (Figure 1).

Apêndice 4

Capítulo de livro publicado em: **Methods in Molecular Biology (págs. 127-135)**

Chapter 10

Synchronization of *Leishmania amazonensis* Cell Cycle Using Hydroxyurea

Beatriz C. D. de Oliveira, Luiz H. C. Assis, Mark E. Shiburah, Stephany C. Paiva, Veronica S. Fontes, Leilane S. de Oliveira, Vitor L. da Silva, Marcelo S. da Silva, and Maria Isabel N. Cano

Abstract

Leishmania spp. comprises a group of protozoan parasites that affect millions of people around the world. Understanding the main cell cycle-dependent events could provide an important route for developing specific therapies since some factors involved in cell cycle control may have low similarity relative to their homologs in mammals. Furthermore, accurate cell cycle-dependent analyses often require many cells, which can be achieved through cell cycle synchronization. Here, we described a useful method to synchronize procyclic promastigote forms of *Leishmania amazonensis* using hydroxyurea (HU) and the analysis of its DNA content profile. This approach can be extended to other trypanosomatids, such as *Trypanosoma cruzi* or *Trypanosoma brucei*, and provides an effective method for arresting more than 80% of cells at the G1/S phase transition.

Key words *Leishmania amazonensis*, Cell cycle synchronization, Hydroxyurea, DNA content profile

1 Introduction

Leishmania genus comprises more than 20 species of single-celled protozoan parasites, most of them showing human and veterinary medical importance. They are the causative agents of leishmaniasis, a neglected tropical disease with a large spectrum of clinical manifestations that affect millions worldwide [1, 2]. The parasite presents three main life forms in its developmental cycle: amastigotes (proliferative), procyclic promastigotes (proliferative), and metacyclic promastigotes (quiescent) [3, 4]. Procyclic and metacyclic promastigotes are both flagellates. They grow and suffer morphological transformations inside the gastric apparatus of the phlebotomine (insect vector). They can also be maintained in axenic cultures under controlled conditions, facilitating laboratory manipulation. Metacyclics are preadapted to infect the mammalian host.

Zhixiang Wang (ed.), *Cell-Cycle Synchronization: Methods and Protocols*, Methods in Molecular Biology, vol. 2579,
https://doi.org/10.1007/978-1-0716-2736-5_10,

Apêndice 5

Preprint publicado em: **BioRxiv** - doi: 10.1101/2023.11.10.566567v1.full

New Results

Follow this preprint

The impact of knocking out the *Leishmania major* telomerase RNA (*Leish*TER): from altered cell proliferation to decreased parasite infectivity

Beatriz Cristina Dias de Oliveira, Mark Ewusi Shiburah, Luiz Henrique de Castro Assis, Veronica Silva Fontes, Pedro Henrique Gallo-Francisco, Selma Giorgio, Marcos Meuser Batista, Maria Nazaré Correia Soeiro, Rubem Figueiredo Sadok Menna-Barreto, Juliana Ide Aoki, Adriano Cappellazzo Coelho, Maria Isabel Nogueira Cano

doi: https://doi.org/10.1101/2023.11.10.566567

Abstract

The telomerase RNA, TER, is an intrinsic component of the telomerase ribonucleoprotein complex. It contains the telomere template sequence copied by the enzyme during telomere elongation. This unique molecule shows divergent nucleotide sequences but a more conserved secondary structure containing domains involved with telomerase assembly and biogenesis. The present work aims to characterize the biological roles played by the *Leishmania* TER component (*Leish*TER) in parasite homeostasis. We generated double knockout (*Lm*TER$^{-/-}$) parasites, which showed a distinct growth pattern at early passages, characterized by lower density and an extended stationary phase compared to the control. Although this pattern normalized after multiple in vitro passages, ablation of *Leish*TER affected cell division and proliferation, with cells arrested at the G0/G1 phase. Progressive telomere shortening was also observed during continuous passages, along with a reduction in the expression of TERRA29. Complementation with the episomal expression of *Leish*TER did not restore telomere length to the control levels, corroborating preliminary results showing that the overexpression of TER has a dominant negative effect on parasite lifespan. *Lm*TER$^{-/-}$ also presented a higher percentage of gamma-H2A phosphorylation, likely due to stalled replication forks since no DNA damage was observed. Also, no plasma membrane modifications were detected, but pro-survival autophagic signals were present. Intriguingly, *Lm*TER$^{-/-}$ retained the ability to transform into metacyclic forms, although its in vitro infectivity and growth inside the host cell were compromised. Together, these results highlight the importance of TER in parasite lifespan and open a discussion about its potential as a drug target against *Leishmania*.

Apêndice 6

Preprint publicado em: **BioRxiv** - doi.org/10.1101/2023.11.10.566596

New Results

Follow this preprint

Ablation of telomerase reverse transcriptase in *Leishmania major* results in a senescent-like phenotype and loss of infectivity

Mark Ewusi Shiburah, Beatriz Cristina Dias de Oliveira, Habtye Bisetegn, Débora Andrade Silva, Luiz Henrique de Castro Assis, Rubem Menna Barreto, Marcos Meuser Batista, Maria de Nazaré Correia Soeiro, Benedito D. Menozzi, Helio Langoni, Juliana Ide Aoki, Adriano Capellazzo Coelho, Maria Isabel N. Cano

doi: https://doi.org/10.1101/2023.11.10.566596

Abstract | Full Text | Info/History | Metrics | Preview PDF

Abstract

The lack of efficient human vaccines and effective nontoxic drugs for leishmaniasis necessitates a search for new therapeutic targets. The telomere environment could provide potential targets against leishmaniasis. TERT, the telomerase reverse transcriptase component, has been on the radar for new therapeutic options against several diseases for more than two decades. In this study, we constructed a full deletion (*Lm*TERT-/-) and an ORF disruption (*Lm*N420) of the gene encoding the TERT component of *Leishmania major*. *Lm*TERT-/- and *Lm*N420 parasites showed replicative and proliferative defects, growth impairment, cell cycle alterations, increased DNA damage, and progressive telomere shortening. Blockage of parasite altruism and the presence of autophagosomes characteristic of a senescent-like phenotype were also detected. *Lm*TERT-/- and *Lm*N420 parasites caused either micro lesion development or no visible lesions in mouse footpads and reduced infectivity in macrophages. While our checks to see if telomere erosion had reached the *SCG* genes involved in lipophosphoglycan modification showed no changes, our proteomic assessment revealed a downregulation of a metacyclic-associated protein. Complementation of the knockout lineages using the WT *Lm*TERT restored some of the lost phenotypes. Therefore, we speculate that the pleiotropic effects of the loss of *Lm*TERT advance the case for using it as a drug target against the parasite.

Competing Interest Statement

The authors have declared no competing interest.